Economic Geology, v. 118, no. 1, pp. 177–208

Alkaline-Silicate REE-HFSE Systems

Charles D. Beard,[1,†,*] Kathryn M. Goodenough,[1] Anouk M. Borst,[2,3,4] Frances Wall,[5] Pete R. Siegfried,[5,6] Eimear A. Deady,[1] Claudia Pohl,[7] William Hutchison,[4] Adrian A. Finch,[4] Benjamin F. Walter,[8,9] Holly A.L. Elliott,[5,10] and Klaus Brauch[7]

[1]*British Geological Survey, The Lyell Centre, Research Avenue South, Edinburgh EH14 4BA, United Kingdom*

[2]*Department of Earth and Environmental Sciences, KU Leuven, Celestijnenlaan 200E, Heverlee 3001, Belgium*

[3]*Geodynamics and Mineral Resources Unit, Leuvensteenweg 13, Tervuren 3080, Belgium*

[4]*School of Earth and Environmental Sciences, University of St. Andrews, Bute Building, St. Andrews, Fife KY16 9TS, United Kingdom*

[5]*Camborne School of Mines and the Environment and Sustainability Institute, University of Exeter, Penryn Campus, Cornwall TR10 9FE, United Kingdom*

[6]*GeoAfrica Prospecting Services CC, P.O. Box 24218, Windhoek, Namibia*

[7]*Terratec Geophysical Services, Schillerstr. 3, Heitersheim 79423, Germany*

[8]*Karlsruhe Institute of Technology (KIT), Adenauerring 20b, Karlsruhe 76131, Germany*

[9]*Eberhard Karls University Tübingen, Wilhelmstrasse 56, Tübingen 72074, Germany*

[10]*College of Science and Engineering, University of Derby, Kedleston Road, Derby DE22 1GB, United Kingdom*

Abstract

Development of renewable energy infrastructure requires critical raw materials, such as the rare earth elements (REEs, including scandium) and niobium, and is driving expansion and diversification in their supply chains. Although alternative sources are being explored, the majority of the world's resources of these elements are found in alkaline-silicate rocks and carbonatites. These magmatic systems also represent major sources of fluorine and phosphorus. Exploration models for critical raw materials are comparatively less well developed than those for major and precious metals, such as iron, copper, and gold, where most of the mineral exploration industry continues to focus. The diversity of lithologic relationships and a complex nomenclature for many alkaline rock types represent further barriers to the exploration and exploitation of REE-high field strength element (HFSE) resources that will facilitate the green revolution. We used a global review of maps, cross sections, and geophysical, geochemical, and petrological observations from alkaline systems to inform our description of the alkaline-silicate REE + HFSE mineral system from continental scale (1,000s km) down to deposit scale (~1 km lateral). Continental-scale targeting criteria include a geodynamic trigger for low-degree mantle melting at high pressure and a mantle source enriched in REEs, volatile elements, and alkalies. At the province and district scales, targeting criteria relate to magmatic-system longevity and the conditions required for extensive fractional crystallization and the residual enrichment of the REEs and HFSEs. A compilation of maps and geophysical data were used to construct an interactive 3-D geologic model (25-km cube) that places mineralization within a depth and horizontal reference frame. It shows typical lithologic relationships surrounding orthomagmatic REE-Nb-Ta-Zr-Hf mineralization in layered agpaitic syenites, roof zone REE-Nb-Ta mineralization, and mineralization of REE-Nb-Zr associated with peralkaline granites and pegmatites. The resulting geologic model is presented together with recommended geophysical and geochemical approaches for exploration targeting, as well as mineral processing and environmental factors pertinent for the development of mineral resources hosted by alkaline-silicate magmatic systems.

Introduction

The global push to decarbonize energy production and transport is underpinning rapid growth in the demand for critical raw materials used in a range of new technologies and is driving expansion and diversification in their supply chains (Hodgkinson and Smith, 2018). The rare earth elements (REEs) are recognized as particularly critical due to their importance in the direct-drive generators of wind turbines and the motors of electric vehicles and the dominance of their supply chain by China (Cox and Kynicky, 2018; Goodenough et al., 2018; European Commission, 2020). Although alternative sources are being explored, the majority of global REE resources are found in alkaline-silicate rocks and carbonatites (Chakhmouradian and Wall, 2012). Alkaline-silicate igneous systems also host deposits of other critical raw materials, including the high field strength elements (HFSEs) such as niobium, zirconium, and hafnium, plus fluorine, phosphate, and scandium (Wall et al., 1999; Mitchell, 2015; Pirajno, 2015; Dostal, 2017; Williams-Jones and Vasyukova, 2018; Broom-Fendley et al., 2020). Demand for the REEs and other critical raw materials is increasing (Hund et al., 2020) and is not likely to be met by recycling alone for some decades (Alonso et al., 2012; Binnemans et al., 2013; Jowitt et al., 2018). Mining of known occurrences and discovery of new deposits will therefore be

†Corresponding author: e-mail, cdb53@cam.ac.uk
*Present address: Department of Earth Sciences, University of Cambridge, Downing Street, Cambridge, Cambridgeshire CB2 3EQ, United Kingdom

ISSN 0361-0128; doi:10.5382/econgeo.4956; 32 p.
Digital appendices are available in the online Supplements section.

Submitted: March 18, 2021 / Accepted: March 16, 2022

required to secure their future supply (Goodenough et al., 2018).

This article provides an overview of REE + HFSE mineral systems associated with alkaline-silicate magmatism and provides a guide for economic geologists who wish to develop their contained resources. The mineral exploration industry has historically focused, and continues to focus, on major and precious metals, such as iron, copper, and gold (Arndt et al., 2017), the mineral systems of which are better understood (e.g., Hedenquist et al., 2000; Barnes and Lightfoot, 2005; Sillitoe, 2010; McCuaig and Hronsky, 2014; Goldfarb and Groves, 2015; Hagemann et al., 2016). We present a critical review of the literature on alkaline-silicate magmatic systems, with geologic and exploration targeting factors pertinent for the development of critical raw material resources from their contained mineralization. This includes the complex mineralogy and geometallurgy of alkaline-silicate systems, which must be considered in the development of any exploration model, as well as the environmental and social issues that may be associated with rare element mining. Previous reviews have provided highly valuable summaries of alkaline-silicate systems and their associated mineral deposits (e.g., Verplanck et al., 2014; Dostal, 2016, 2017; Morgenstern et al., 2017; Banks et al., 2019; Woolley, 2019). We synthesize these and other observations into a generalized scale-dependent mineral systems model (e.g., Knox-Robinson and Wyborn, 1997; McCuaig et al., 2010; McCuaig and Hronsky, 2014), with recommendations on geophysical, geochemical, and geologic techniques to apply during exploration. Relevant to the continental scale (300–10,000 km), we discuss the temporal distribution of various mineralization types and the influence of tectonic setting. We then present province-scale controls (~300 km) pertaining to translithospheric structures that guide magma ascent, the persistence of magmatism, the importance of depth of emplacement, and the influence of country-rock lithology on mineralization potential and the formation of alteration aureoles. At the district scale (~25 km lateral) we present a schematic interactive 3-D model for an idealized alkaline-silicate system (App. 1). This model illustrates the key lithologic relationships and relative position of various classes of mineralization in alkaline-silicate REE + HFSE systems. Pop-up panels within this model show grade tonnage information and REE profiles for each deposit class, as well as information on ore mineralogy and processing technology status. In the manuscript we discuss associated targeting criteria for mineralization, relevant at the prospect and deposit scale.

Alkaline-Silicate Rocks

Volcanic and plutonic silicate rocks that have an excess of alkalies relative to aluminium ((Na + K)/Al > 1) on a molar basis and that therefore contain (real or normative) minerals with a similar excess of alkalies (such as alkali-rich amphibole or clinopyroxene) have been termed alkaline or peralkaline by various authors (Sørensen, 1974; Fitton and Upton, 1987; Le Maitre et al., 2005). The presence of feldspathoid minerals warrants classification as alkaline, whereas the term peralkaline is used exclusively for rocks that meet the above chemical definition. Peralkaline rocks are divided into miaskitic and agpaitic varieties—the former having the REEs + HFSEs largely hosted by the minerals zircon and titanite and the latter containing a wealth of complex Na-Ca-HFSE minerals, many of which contain structurally essential halogens (Marks and Markl, 2017). Extreme enrichments in alkalies can form hyperagpaitic assemblages, denoted by the presence of appreciable amounts of water-soluble minerals and the (partial) destabilization of alkali feldspar and feldspathoids (Marks and Markl, 2017). More broadly, the term alkaline-silicate refers to igneous systems that contain alkaline or peralkaline rocks, even if these systems are volumetrically dominated by metaluminous lithologies (Marks et al., 2011).

Alkaline-silicate complexes predominantly occur in continental tectonic settings and are found throughout the geologic record, from the Neoarchean to the present day (Woolley and Kjarsgaard, 2008; Figs. 1–3). Alkaline-silicate magmas have a mantle source, although the exact nature of that source varies between and within provinces (Bell and Simonetti, 2010; Hutchison et al., 2019, 2021). They are most commonly associated with lithospheric-scale extension, although some post-collisional alkaline magmatic provinces are associated with transcurrent tectonics (Hou et al., 2009; Banks et al., 2019; Goodenough et al., 2021). Alkaline-silicate complexes commonly occur in provinces, which are regional-scale features (10s to 100s km extent) comprising several individual igneous complexes. Each complex may include both alkaline-silicate rocks and carbonatites, with carbonatite-bearing systems typically associated with more oxidized upper mantle sources (Braunger et al., 2020). Many more alkaline-silicate occurrences are known when compared to carbonatites (>3,000 in compilation of Woolley, 2019, and other books in this series, see http://alkcarb.myrocks.info/ vs. >600 carbonatites; Walter et al., 2021). Carbonatites represent important sources of REEs and HFSEs and are described in detail elsewhere (Verplanck et al., 2016; Wang et al., 2020); here we focus on the alkaline-silicate components of these igneous systems.

Before focusing on the geology of alkaline-silicate systems, the sections below summarize engineering, social, and environmental factors that are best considered at an early stage of any exploration campaign. We then present the geology and associated exploration approaches for these mineral systems at a range of scales, gradually focusing in from continental to deposit scale.

Metallurgical Challenges and the Importance of REE Profiles

The diversity of minerals within alkaline-silicate deposits is much greater than that of most mined base metal or precious metal deposits. Consequently, mineralogy and metallurgy are important considerations during REE + HFSE exploration in alkaline-silicate systems. The mineralogical diversity results because these magmas typically contain dozens of elements at weight percent concentration and crystallize at low temperatures where complex solid solutions stabilized by entropy are thermodynamically unfavorable (Putnis, 1992). Rare earth minerals represent 233 (4%) of the 5,455 species approved by the International Mineralogical Association (Downs, 2006, rruff.info/ima); however, at the time of writing only four are processed commercially for the REEs (bastnäsite-Ce, monazite-Ce, loparite-Ce, xenotime-Y). Apatite associated with alkaline rocks has also been processed commercially for

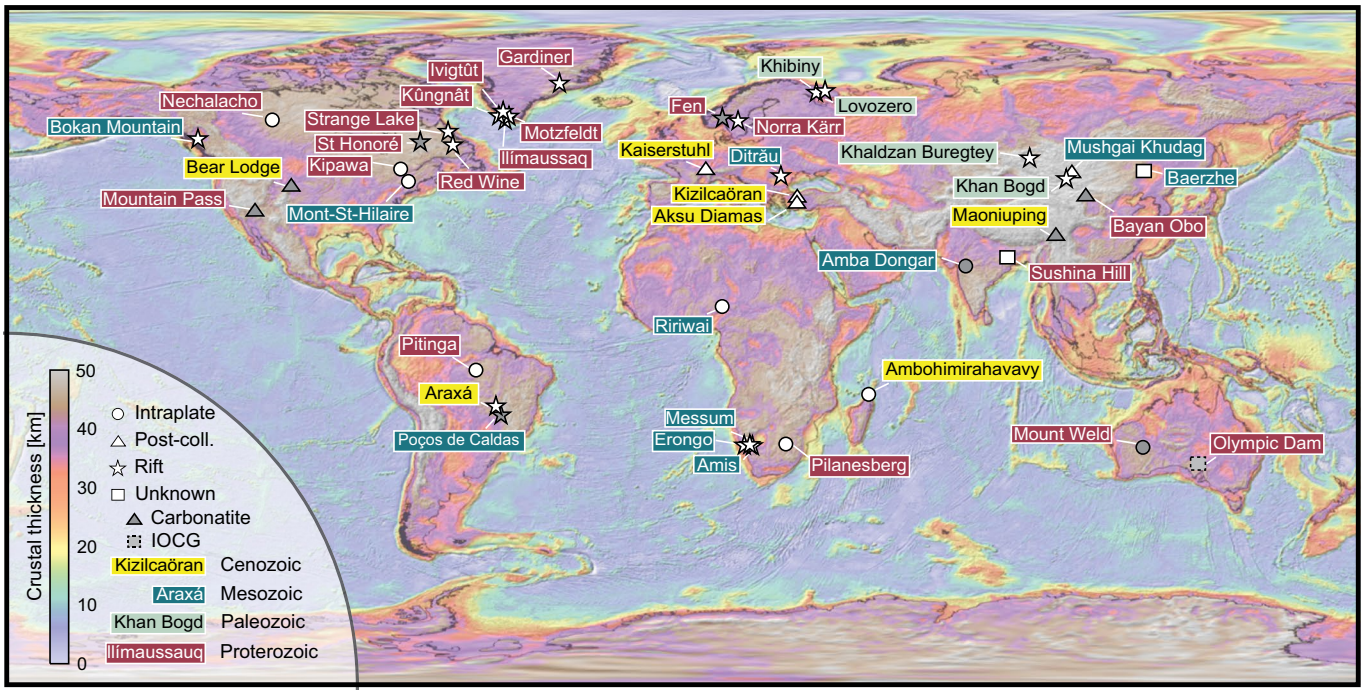

Fig. 1. A world map showing rare earth element-high field strength element (REE-HFSE) deposits and alkaline-silicate complexes mentioned in the main text. Alkaline-silicate complexes with and without carbonatite are shown in white, and systems containing major carbonatite-associated REE deposits are shown in gray. The crustal basement thickness map is an inversion of satellite gravity data (Alvey et al., 2018). IOCG = iron oxide copper-gold.

REEs (Jordens et al., 2013; Suli et al., 2017), and ion adsorption deposits, including those representing weathering products of alkaline-silicate rocks, currently supply the majority of the world's heavy REEs (HREEs; Bao and Zhao, 2008; Weng et al., 2015; Jowitt et al., 2017; Li et al., 2019). Since the REEs are usually dispersed in a number of phases that are not equally processable, grade tonnage diagrams cannot be used to directly assess the economic potential of a deposit. Metallurgical procedures for several other REE minerals are at pilot stage, including eudialyte, steenstrupine, and allanite (see App. 2; Davris et al., 2017; Stark et al., 2017; Voßenkaul et al., 2017; Battsengel et al., 2018; Kursun et al., 2019). Recovery rates and energy usage are improving rapidly as the pertinent metallurgical techniques mature (e.g., Wall et al., 2017; Demol et al., 2019; Marion et al., 2020). Other critical raw materials found in alkaline rocks are commercially extracted from a range of ore minerals, including pyrochlore (niobium), columbite (niobium, tantalum), apatite (phosphate), and zircon (zirconium, hafnium) (Gibson et al., 2015). In addition to mineralogy, the texture of the rocks influences the efficiency of beneficiation, with large grains able to be processed more easily than fine-scale intergrowths (e.g., Hagni, 1999; Neumann and Medeiros, 2015). The economics of REE deposits are further controlled by the relative abundance of elements, which are commonly expressed as a chondrite-normalized "REE pattern" (Chakhmouradian and Wall, 2012; Chakhmouradian and Zaitsev, 2012; Goodenough et al., 2018). Many companies report total rare earth oxide (TREO) grades, which offer an oversimplified view of the potential economics of a deposit. The HREEs are less abundant than light REEs (LREEs) but command a higher price (Binnemans et al., 2018; Goodenough et al., 2018; Anenburg, 2020, and associated web tool; lambdar.rses.anu.edu.au/alambdar). Neodymium, an LREE that is used in high-strength permanent magnets, is considered the most critical of the REEs for electric vehicle and wind turbine supply chains (Ballinger et al., 2020). Alkaline-silicate associated deposits tend to have flatter REE profiles than carbonatites, so are relatively enriched in the rarer and more valuable middle and heavy REEs (see pop-ups in 3-D model, App. 1).

As highlighted above, metallurgical factors have a major influence on project economics, as they control the potential yield of a commodity that might be liberated during ore processing, the reagent and energy requirements of this processing, and the expected market value of the extracted commodity. Considering metallurgy late in the exploration process risks the spending of significant effort to understand the geology of an uneconomic deposit. Workflows for the analysis of REE minerals and textural information prior to metallurgical test work can be gleaned using relatively inexpensive petrographic techniques, such as optical microscopy and chemical mapping via microanalytical methods (Grammatikopoulos et al., 2013; Smythe et al., 2013; Edahbi et al., 2018).

Environmental and Social Considerations

The most important environmental and social considerations associated with the mining of REE-HFSE deposits in alkaline rocks are different from those of many other ore deposits. Radioactivity is the most high-profile environmental concern (Chakhmouradian and Wall, 2012), whereas acid mine drainage, often a major environmental consideration in mining scenarios, is usually not a problem (Verplanck et al., 2014). There have been only a few published environmental studies of

mines in alkaline-silicate systems and also relatively few long-term studies of REEs and associated minor elements in the environment. As a result, there is a much smaller set of regulatory data to inform environmental and social considerations.

The risks posed by the radionuclides uranium and thorium require special consideration in all alkaline-silicate systems (Chakhmouradian and Wall, 2012). These elements occur in many deposits, either in the REE and Nb minerals or in other associated phases. When sequestered within REE ore minerals, these actinides are not separated from the REEs until the later stages of the beneficiation process, which can result in production of mine waste that is enriched in radionuclides. The issue here is not necessarily the danger of irradiation, but rather the burden and cost of radioactive waste management for the mining company or operator. Measures to address radioactivity will be greater at the processing plant than at the mine site. Although the concentrations of U and Th in alkaline rocks are highly variable, experience so far suggests that the issue is likely to be a social concern even where the actual environmental risk is negligible (Ali, 2014; Jamaludin and Lahiri-Dutt, 2017; Speiser et al., 2019). If addressed poorly during exploration, mining, and extraction activities, this problem can damage public trust and potentially halt operations indefinitely (Phua and Velu, 2012; Ali, 2014). Environmental and safety reporting should follow the well-documented standards developed by the uranium sector (see www.world-nuclear.org). Depending on the cultural tolerance and legislation regarding radiation from mining (Wall, 2013) there is a possibility for extraction of uranium as a by-product (Roberts and Hudson, 1983; Huston et al., 2016). This may increase the economic viability of deposits while simultaneously reducing the radioactivity of the waste products (see www.wise-uranium.org). Thorium poses a greater risk for projects than uranium due to its lower global demand and higher abundance. (Th is not included in British Geological Survey [Brown et al., 2019] or U.S. Geological Survey [2019] global resource compilations.) While some Th can be separated during beneficiation, the REEs and Nb, Ta, Zr minerals usually incorporate some Th into their lattices (e.g., monazite, REE fluorocarbonates, pyrochlore). As a result, the extraction of REEs from these minerals can pose a radiation risk (Phua and Velu, 2012; Wall, 2013).

In general, the toxicity of the REEs is thought to be low; however, few long-term data sets exist (Pagano et al., 2015). The REEs have been used in growth promoters and fertilizers in China and in a variety of medical applications, including drug delivery and magnetic resonance imaging. Health risks associated with prolonged exposure to Ce, and also other REEs, have been noted in some industrial and agricultural settings (see Rim et al., 2013; Wall, 2013). Cerium nanoparticles are toxic (García et al., 2011; Dahle and Arai, 2015), and although REEs have been used in catalytic converters for many cars, there are few environmental studies on this subject. The REEs have been measured in river water (Kulaksiz and Bau, 2011; Brito et al., 2018) but there are few environmental limits and regulations for them.

We recommend that the environmental impact of various production options be compared quantitatively with life cycle assessment (LCA) simulations (Wall et al., 2017; Pell et al., 2019, 2021). These can inform decisions about the impact of various project options—for example, the effect that various reagent source pathways have on emissions and on water use (e.g., $CO_2 \cdot$ eq per kg of commodity produced, particulate generation).

Continental-Scale Characteristics

Within the mineral systems concept (Knox-Robinson and Wyborn, 1997; McCuaig et al., 2010; McCuaig and Hronsky, 2014; Banks et al., 2019) a series of processes occur to mobilize and concentrate a commodity, depositing it downstream at a site of mineralization. At the continental scale (>1,000 km) the main processes that control the potential for ore formation are (1) a source of the commodity, (2) the generation of a medium to carry the commodity, and (3) a geodynamic event that can mobilize the commodity. To form a deposit, all components of a mineral system must be present; therefore, screening at the continental scale can help identify promising search areas at the province scale (~300 km). The mineral systems approach can be used to derisk projects before relatively more expensive and specialist exploration techniques are used at finer spatial scales (Banks et al., 2020). In the case of alkaline-silicate REE-HFSE systems and carbonatite-bearing systems, most of the commodity and its transporting medium (magma) are thought to originate from the mantle. The source composition is therefore influenced by global-scale (bio)geochemical cycles that have evolved throughout geologic time (White, 2015). The mobilization of REEs from the mantle is triggered by tectonic and mantle geodynamic perturbations that generate silicate melt and facilitate their ascent into the continental crust. At the continental and province scales, targeting factors are similar for alkaline-silicate and carbonatite systems, and the topics discussed in the following sections apply to carbonatites as well as to the alkaline-silicate systems that are the main focus of this article.

Alkaline-silicate rocks and carbonatites can be broadly divided into two associations: those in continental rift and intraplate settings and those formed in postcollisional settings (Figs. 1, 2). In the latter, magmatism is generally associated with a change in stress regime from compressional to transcurrent that postdates continental collision by millions to tens of millions of years (Goodenough et al., 2021). Alkaline magmatism also represents a minor but ubiquitous component of oceanic island systems (Fitton and Upton, 1987; Willbold and Stracke, 2006). No economic mineralization, other than construction materials, is known from alkaline-silicate systems from oceanic island settings (Woolley and Kjarsgaard, 2008; Woolley, 2019), perhaps because a thinner lithosphere does not afford the magmas sufficient opportunity to fractionate and residually enrich the incompatible REEs and HFSEs (cf. Wiesmaier et al., 2012). For this reason, the oceanic island setting will not be discussed further.

Screening at the continental scale aims to identify province-scale features that potentially contain REE + HFSE mineralization. Exploration indicators, as with many ore deposit types, are therefore country-scale geologic maps, crustal-scale cross sections, and an understanding of the geodynamic history of a region or craton. Continental-scale geochemical mapping of igneous rocks can also be used to delineate and extend known and favorable regions for mineralization. Such an approach has been applied to Archean nickel sulfide and gold systems

in Western Australia (McCuaig et al., 2010) where a restricted range of Nd isotope depleted mantle model ages of low-Ca granites map the edge of a paleocraton at time of their emplacement. This shows excellent spatial correlation with known nickel and gold mineral systems.

Tectonic settings and triggers for mantle melting

Alkaline-silicate systems are most commonly coincident with continental sutures and the margins of cratons (Burke et al., 2003; Pirajno, 2015; Humphreys-Williams and Zahirovic, 2021; Fig. 1). In continental rift and intraplate settings, alkaline-silicate melts are generated where the plate divergence rate is low (e.g., 12.4 mm yr^{-1}, Basin and Range, Bennett et al., 2003; 5–15 mm yr^{-1}, East African rift, Saria et al., 2014) or along the failed arm of rift triple junctions associated with thermochemical mantle plumes and continental breakup (Dewey and Burke, 1974; Bell and Simonetti, 2010; Ernst and Bell, 2010). In such settings, as seen in the modern East African rift (Mahood, 1984; Hutchison et al., 2016a; Rooney, 2020b), the East Greenland Tertiary province (Brooks and Nielsen, 1982), and the Mesoproterozoic Gardar rift of southwest Greenland (Upton et al., 2003; Upton, 2013) magmas tend to be sodic, rather than potassic, and commonly attain peralkaline compositions (Marks et al., 2011). Though several major mineralized alkaline-silicate and carbonatite systems are known from postcollisional settings, the academic community have thus far focused on the intraplate and rift-related systems, and the literature on postcollisional settings is therefore less comprehensive (Goodenough et al., 2021). Melt compositions in postcollisional settings tend to be potassic, and mantle melting here has been attributed to slab break-off, lithospheric delamination, and adiabatic decompression associated with orogenic collapse (Kay and Mahlburg Kay, 1993; Huw Davies and von Blanckenburg, 1995). In both rift and postcollisional settings, experimental evidence indicates that the alkali-rich, Si-poor nature of the primary silicate melts is best explained by low-degree partial melting of mantle beneath thick continental crust (Massuyeau et al., 2015; Schmidt and Weidendorfer, 2018; Figs. 1, 2). Such high-pressure melting further yields high concentrations of REEs, HFSEs, P, and CO_2 for a given source composition. Geophysical techniques such as seismic tomography, magnetotellurics, and satellite gravity mapping can be used to infer the present-day structure and thickness of the crust (Fig. 1), providing information on areas where high-pressure mantle melting might have recently occurred (Percival et al., 2006; Clowes, 2010; Alvey et al., 2018). For older terranes, crustal thickness can be inferred where the uplift and erosion history are known, for example via petrochronology and phase-equilibrium modeling of metamorphic assemblages associated with orogens (e.g., Weller et al., 2021).

In most continental rift and intraplate examples, the physical trigger for melting is likely to be a combination of adiabatic decompression associated with crustal thinning and, in some cases, plume-lithosphere interaction (Kieffer et al., 2004; Koptev et al., 2015; Rooney, 2017). Adiabatic decompression associated with crustal thinning can impart a subtle yet persistent influence on the upper mantle that is compatible with five to tens of million years' duration of activity of some alkaline provinces (e.g., East African rift; Macgregor, 2015). For alkaline-silicate and carbonatite complexes peripheral to and roughly contemporaneous with flood basalt volcanism, melt generation likely reflects the influence of a thermochemical mantle plume (Ebinger and Sleep, 1998; Ernst and Bell, 2010; Furman et al., 2016). In these intraplate occurrences, low-degree melting may reflect the destabilization of asthenospheric mantle rocks or metasomes in the subcontinental lithospheric mantle, perhaps via fluxing by deep-derived volatiles or via adiabatic decompression toward the edge of a plume head (Garcia et al., 1993; Haase et al., 2019). Alkaline-silicate and carbonatite systems associated with continental flood basalts tend to slightly predate (<10 m.y.) or overlap with the timing of these flood-volcanic events (Ernst, 2014).

Alkaline magmatism can also be associated with hotspot tracks—the tails of mantle plumes. At the Cretaceous Monteregian Hills province in Quebec, Canada, radiogenic Pb and primitive He isotope compositions indicate major contributions from a mature mantle plume source (Roulleau and Stevenson, 2013; Chen and Simonetti, 2015; Méjean et al., 2020). Recent U-Pb zircon geochronology supports the hotspot model, with age dates broadly consistent with the modeled

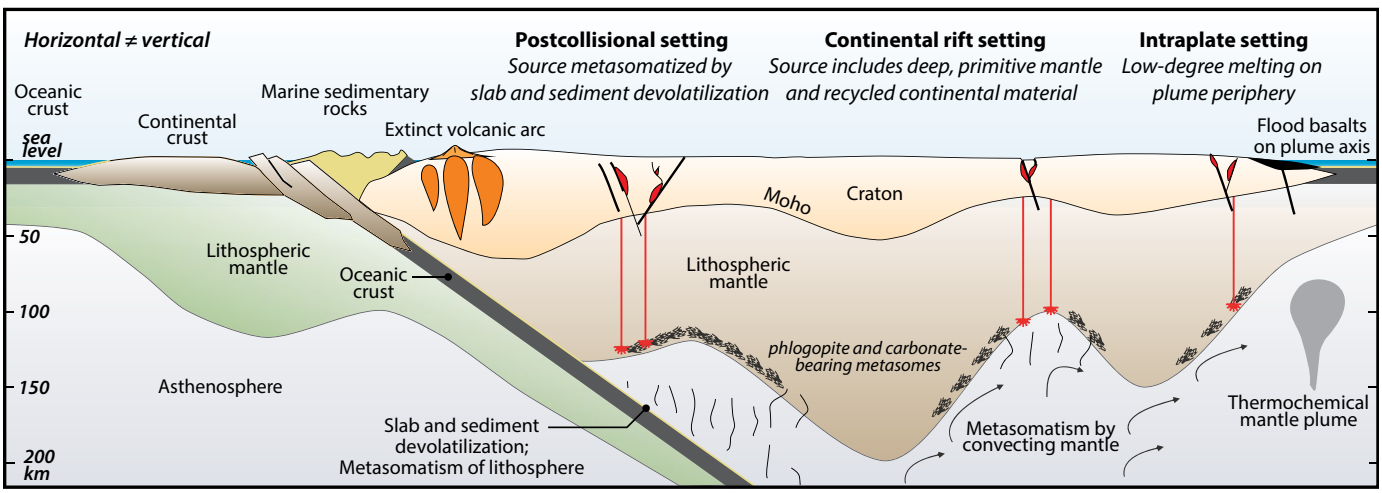

Fig. 2. A schematic cross section at continental scale showing the tectonic settings and melt sources inferred for postcollisional, continental rift, and intraplate alkaline-silicate magmatic systems. Vertical scale follows Condie (2016).

track of the Great Meteor hotspot (Kinney et al., 2021). However, there has been some debate as to whether plume impingement simply introduced material to the lithospheric mantle (cf. Aulbach et al., 2013), and low-degree melting was triggered later via structural reactivation of paleorifts during opening of the North Atlantic Ocean (Roulleau and Stevenson, 2013).

The influence of mantle melt source composition on mineralization potential

The xenolith cargo and high concentrations of incompatible elements in alkaline-silicate systems suggest they originate as low-degree partial melts of enriched sources in the lithospheric mantle (Kramm and Kogarko, 1994; Rosatelli et al., 2007; Pilet et al., 2008; Bartels et al., 2015; Foley and Fischer, 2017; Tappe et al., 2017; Fig. 2). Indeed, melting experiments indicate that minor CO_2 and H_2O in the mantle source strongly reduce the silica activity of the produced melts and can depress the peridotite solidus (Massuyeau et al., 2015). Extensive differentiation of these primary melts is required to enrich REEs + HFSEs to economically interesting concentrations (Marks and Markl, 2017).

Direct links between source composition and mineralization potential have not been proven conclusively; however, there is an increasing body of evidence for a link between source composition and mineralization (e.g., Pilet et al., 2008; Hutchison et al., 2019, 2021). The probability of forming a deposit is likely to be elevated where the underlying mantle is enriched in the metals of interest. Sources may also favor mineralization if they can contribute a cocktail of volatiles that promotes the residual enrichment of metals during crystal fractionation in a crustal magmatic system (e.g., fluorine; Guzmics et al., 2012, 2019; Aseri et al., 2015; Beard et al., 2020). Such sources may result from the metasomatism of the lithospheric mantle by fluids or melts derived from subduction of REE-rich marine sediments, including those containing abundant organic phosphorite material or Fe-Mn oxide crusts that accumulate at low rates of sedimentation (Plank, 2013). Marine shale and clay also contain elevated concentrations of REEs and fluorine relative to primitive mantle (4–70 and 30–52× primitive mantle, respectively; Barth et al., 2000; John et al., 2011). In most arcs, the degree of melting is too great, and primitive melts are not associated with notable enrichment of REEs, HFSEs, or alkalies (Elliott et al., 1997; Spandler and Pirard, 2013). Low-degree melting is therefore paramount because the same sediment packages are being subducted below many arc volcanic systems today. Metals and volatile elements may also be introduced to the cratonic lithosphere via the impingement of thermochemical mantle plumes (Aulbach et al., 2013) or via carbonate metasomatism associated with subduction (Tappe et al., 2017).

Xenolith assemblages and geochemical evidence indicate that rift-related alkaline-silicate systems tap sources that contain phlogopite, magnetite, amphibole, apatite, and carbonate minerals and are mostly garnet or spinel lherzolites (Upton and Emeleus, 1987; Köhler et al., 2009; Melluso et al., 2016; Marks and Markl, 2017). Note that melt generation above the garnet stability field may be a factor in the relative enrichment of HREEs, as garnet in the mantle restite would retain the HREEs during melting (Adam and Green, 2006; Bartels et al., 2015). Primitive volcanic rocks and dikes associated with alkaline-silicate systems suggest that their primary melts are usually reduced alkali-basalt to basanite (feldspar-bearing), or nephelinite in composition (feldspar-free), and are rarely melilititic (Elburg and Cawthorn, 2017; Marks and Markl, 2017; Braunger et al., 2020).

The radiogenic $^{143}Nd/^{144}Nd$ and $^{176}Hf/^{177}Hf$ isotope systems provide direct information about the source of the metals of interest, rather than a proxy as most geochemical tools do. Many rift-related and intraplate alkaline-silicate rocks have Nd-Hf isotope compositions that overlap with those of high-μ (HIMU) oceanic island basalts (Bell and Simonetti, 2010), indicating that their melt source is mantle dominated and contains a recycled oceanic crust component (Chauvel et al., 1992). Some alkaline-silicate systems, especially in postcollisional settings, have compositions that extend toward enriched mantle 2 and enriched mantle 1 (EM-2 and EM-1) oceanic island basalt compositions (Goodenough et al., 2021), reflecting contributions from continental crustal sources (Willbold and Stracke, 2010). Here, continental material is either introduced to magmas through assimilation during ascent or more likely via incorporation into the mantle source, for example via subduction of sedimentary rocks.

Radiogenic Ar, Xe, and He isotope compositions from intraplate alkaline-silicate rocks and associated carbonatites in Canada, Brazil, and Russia indicate contributions from primordial, deep-seated mantle sources (Sasada et al., 1997; Tolstikhin et al., 2002). The heavy nitrogen isotope composition of alkaline-silicate rocks from the Kola Peninsula further indicates contributions from deep-seated sources, either from recycled oceanic crust or generated via metal-silicate partitioning of nitrogen during formation of our planetary core (Dauphas and Marty, 1999). The $\delta^{11}B$ isotope composition of carbonatites and their associated alkaline-silicate rocks has become progressively heavier since the Archean (Hulett et al., 2016), consistent with subduction recycling of sedimentary material into their mantle source regions (Smith et al., 2018). Sulfur ($\delta^{34}S$) isotope compositions are consistent with $\delta^{11}B$, showing both positive and negative values that extend beyond the range of typical upper mantle melts (mid-ocean ridge basalt; MORB), indicating contributions from recycled surface sources in the lithospheric mantle or in plumes (Hutchison et al., 2019, 2020).

Alkaline-silicate magmas in postcollisional settings tend to be potassic and miaskitic, with common enrichments of LREEs, barium, strontium, and fluorine (Goodenough et al., 2021). The potassic nature and high Rb/Sr of many postcollisional alkaline magmas indicate contributions from a phlogopite-bearing mantle source that has been metasomatized by subduction-related fluids (Couzinié et al., 2016; Tappe et al., 2017; Braunger et al., 2020). Devolatilization reactions in subducting slabs release a host of incompatible elements and can induce metasomatism of the base of the lithosphere (Kerrick and Connelly, 2001; Spandler and Pirard, 2013; Schmidt and Poli, 2014). The negative primitive mantle-normalized Nb-Ta anomalies of postcollisional alkaline rocks (e.g., Liu et al., 2015) are similar to those reported from arc tholeiites and may result from the presence of residual rutile in the slab and the low solubility of Nb-Ta–bearing minerals in subduction zone fluids (Baier et al., 2008; Marschall et al., 2013). The

higher proportion of carbonatite relative to silicate rocks in postcollisional settings may reflect contributions from sources relatively enriched in carbonate (Massuyeau et al., 2015).

The key points for exploration are that mineralized alkaline-silicate rocks are predominantly products of low-degree, high-pressure melting of mantle rocks (crustal thickness ≥40 km; Fig. 1) and that the mantle is the dominant source of their REE and HFSE payload. Intraplate and rift occurrences tend to tap deep, plume-influenced sources containing a mixture of recycled oceanic crust and primordial mantle material. Post-collisional complexes have more continental-like geochemical characteristics, potentially reflecting contributions from mantle with more recent subduction-related metasomatism. While source composition is likely to influence mineralization potential, a direct link has yet to be proven.

The temporal distribution of mineralization

Because the composition and dynamics of the Earth's crust and mantle have evolved through geologic time, so has the potential for REE + HFSE mineralization (Fig. 3). As stated above, the controls on REE-HFSE mineralization at the continental scale are similar for alkaline-silicate and carbonatite systems; therefore, statements made in this section apply to both. The oldest known alkaline-silicate and carbonatite systems formed in the Neoarchean and are preserved in cratonic areas of Canada, Finland, and Greenland (Larsen and Rex, 1992; Rukhlov and Bell, 2010; O'Brien et al., 2015; Marks and Markl, 2017). From the Paleoproterozoic onward, alkaline-silicate and carbonatite magmatism is preserved on all continents and has been episodic, with peaks of activity associated with continental rifting and the existence of supercontinents (Rukhlov and Bell, 2010; Woolley and Bailey, 2012; Cawood and Hawkesworth, 2015; Tappe et al., 2017; Fig. 3a).

Resource tonnage data as a function of age reveal several major pulses of REE mineralization (Smith et al., 2016; Fig. 3b). The earliest two are associated with relatively small discrete deposits (3.3 and 4.2 Mt TREO) that formed during the Paleoproterozoic in intraplate settings. Through the Mesoproterozoic, the thickness of juvenile continental crust increased to >35 km (Dhuime et al., 2015), and major REE deposits were formed on multiple paleocontinents. These include iron oxide copper-gold–related REE mineralization at Olympic Dam, Australia (6.6 Mt TREO; Oreskes and Einaudi, 1990), a major portion of the mineralization at the Bayan Obo deposit, China (30.8 Mt TREO; Song et al., 2018), the Sulphide Queen deposit at Mountain Pass, USA (1.6 Mt TREO; Castor, 2008), and the Kvanefjeld and Kringlerne deposits of the Ilímaussaq Complex, Greenland (11.1 and 28.0 Mt TREO; Upton, 2013).

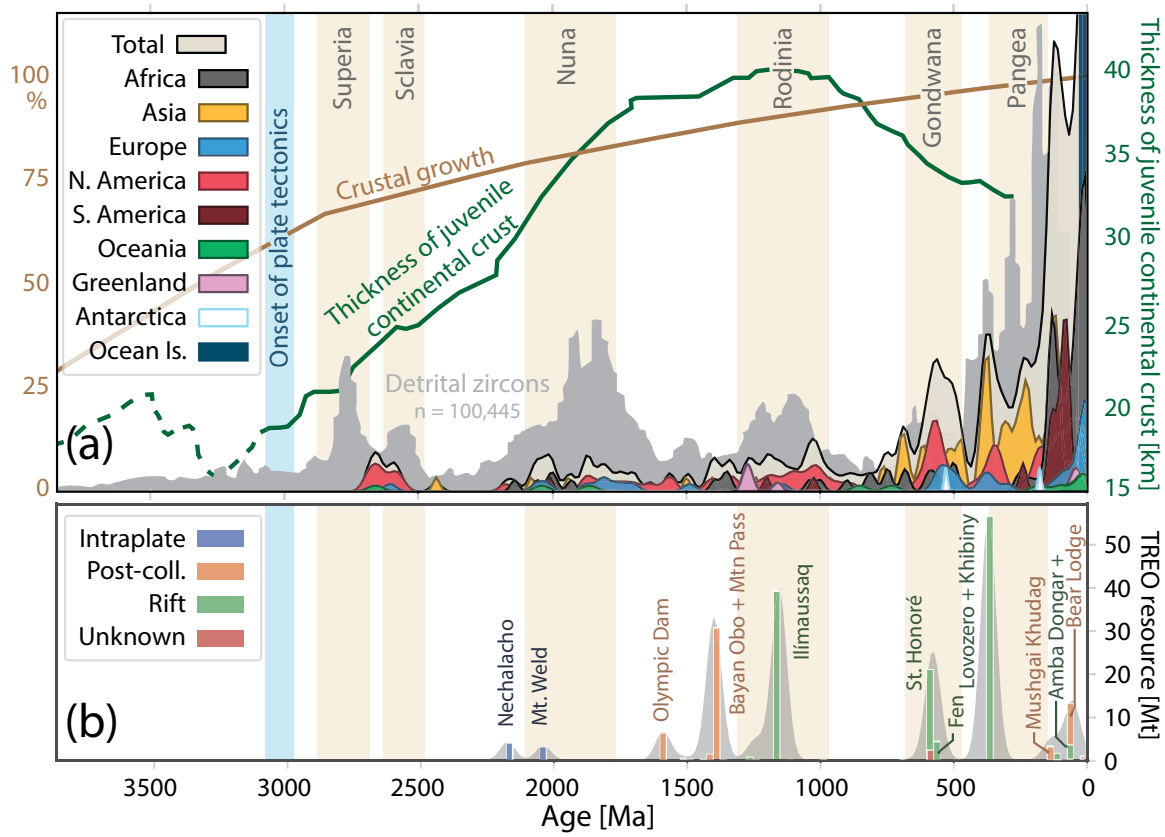

Fig. 3. Age distribution diagram for alkaline-silicate and carbonatite systems. (a) Kernel density curves for occurrences based on data from Woolley and Kjarsgaard (2008) and Marks and Markl (2017) (n = 377). Vertical bars indicate the existence of supercontinents after Cawood and Hawkesworth (2015). Global detrital zircon abundances after Voice et al. (2011) are a proxy for the rate of growth of the continental crust (cf. Arndt and Davaille, 2013). The volume percentage of continental crustal growth is after Dhuime et al. (2012), and the emergence of plate tectonics and thickness of juvenile continental crust are after Dhuime et al. (2015). (b) Histogram of total rare earth oxide (TREO) resources (measured + inferred, n = 107), with bin width set at 25 m.y. Resource data are also shown in a grade-tonnage diagram in Figure 7.

The sum total of Mesoproterozoic-age REE mineral systems represents ~30% of current global REE resources by tonnage (Smith et al., 2016). The Proterozoic saw the assembly of two supercontinents named Nuna (Columbia) and Rodinia (Fig. 3a) and their subsequent breakup by the emplacement of the Keweenawan (1115–1085 Ma) and Mackenzie (1267 Ma) large igneous provinces (Ernst and Bleeker, 2010) and the Gardar alkaline province (1325–1144 Ma; Upton, 2013; Stockmann et al., 2018). This period was also notable for the development of extensive base and precious metal mineralization (Huston et al., 2010). The late Proterozoic saw emplacement of the St Honoré alkaline-silicate and carbonatite complex, Canada, with mantle melting likely triggered by movement on the St. Laurence rift and opening of the Iapetus Ocean (O'Brien and van der Pluijm, 2012; Tremblay et al., 2013; Néron et al., 2018).

In the Paleozoic, rifting and alkaline magmatism developed across the Baltic Shield of northern Europe (Goodenough et al., 2016). The world's largest alkaline complexes, Khibiny and Lovozero, were emplaced as part of the Kola alkaline province in Russia, an area that shows repeated alkaline magmatism throughout the Proterozoic (Downes et al., 2005; Kalashnikov et al., 2016a).

A somewhat smaller pulse of REE mineralization is preserved from the most recent 200 m.y. (Smith et al., 2016). This REE resource peak is small, considering the abundance of alkaline-silicate and carbonatite systems known from the same time period (Fig. 3). It is dominated by deposits with a comparatively shallow depth of emplacement (e.g., Mianning-Dechang belt, China, Hou et al., 2009; Liu and Hou 2017; Chilwa province, Malawi; Broom-Fendley et al., 2017; Baerzhe, China, Wu et al., 2021).

The apparent lack of REE mineralization in the Archean might have resulted from high mantle temperatures and consequently greater degrees of partial melting relative to more recent times (Herzberg et al., 2010; Weller et al., 2019). Thin, nascent continental crust (Dhuime et al., 2015), or potentially a vertical tectonic regime (Bédard et al., 2013), was apparently not conducive to alkaline magmatism or REE mineralization.

The largest known REE deposits formed in the Proterozoic and Paleozoic and likely reflect an availability of enriched mantle source material, with a geodynamic environment conducive to persistent or repeated generation of high-pressure, low-degree mantle melting over long geologic timescales. The advent of plate tectonics began the subduction recycling of continentally derived sediments into the mantle (Delavault et al., 2016), locally enriching REEs and other incompatible elements relative to primitive mantle (e.g., Willbold and Stracke, 2010). In the Proterozoic, the thickness of juvenile continental crust increased from ~20 to 35 km (Fig. 3), as recorded by a compilation of Nd isotope model ages, Si contents, and Rb/Sr ratios (Dhuime et al., 2015). A thicker lid of continental crust would have promoted higher-pressure mantle melting, with experimental data indicating that the resultant melts would have been Si poor and alkali rich (Massuyeau et al., 2015). In some alkaline-silicate REE-HFSE systems, reactivation of continental sutures may be important for mineralization. Indeed, nearly 90% of deformed alkaline rocks and carbonatites on the African continent occur within known or inferred Proterozoic suture zones, and isotopic evidence suggests that melting of these deformed rocks may contribute to later magmatism (Burke et al., 2003; Rooney, 2020b). Multiple periods of reactivation are recorded in REE ores of the giant Bayan Obo carbonatite deposit where Sm-Nd ages of mineralization span 1.0 b.y. (e.g., Song et al., 2018).

The mechanisms responsible for the small peak of the Mesozoic to Cenozoic (≤200 Ma) REE tonnage remain to be determined. The reduced tonnage could reflect mineralization of REEs at depths not yet explored. Indeed, the influence of confining pressure on mineralization potential in alkaline-silicate systems is not currently well constrained (see "Volcanic connections and the depth of emplacement" section below). Additionally, a shift in the dominant tectonic style may have reduced the potential for REE mineralization. The temporal reduction in global REE tonnage correlates with a shift from Mesoproterozoic, single-lid-like tectonics, as recorded by abundant A-type granites and anorthosites, toward a Cenozoic subduction-dominated tectonic style, as indicated by the presence of ophiolites and blueschists (Stern, 2020).

In summary, the continental-scale features that may indicate the likelihood of alkaline-silicate associated REE-HFSE mineralization include the following: (1) a tectonic history that resulted in the metasomatic enrichment of the mantle, e.g., at suture zones between cratonic blocks, and (2) a trigger for low-degree mantle melting, e.g., an episode of continental rifting, a thermochemical mantle plume, or a hotspot track. Country-wide geochemical, geophysical, and geologic mapping data sets will typically provide information to guide exploration at the continental scale.

Clusters and Alignments of Deposits at the Province Scale

Once promising province-scale (~300 km) search regions have been identified, these may be mapped in finer detail, searching for promising districts at the scale of individual intrusive or volcanic systems (~25 km; Fig. 4). Province-scale exploration should map crustal-scale structures that can focus magma ascent from the mantle (Black et al., 1985; Hutton, 1988; Petford et al., 2000; Magee et al., 2018). Within alkaline-silicate and carbonatite provinces, magmas have been focused toward intersections of crustal lineaments (Sørensen, 1970; Acocella et al., 2003; Pirajno, 2010; Decrée et al., 2015; Robertson et al., 2016; Banks et al., 2019), and intrusions may be nested to the point that they overlap (e.g., Gardar province, Greenland; Fig. 4b; Upton, 2013; Finch et al., 2019) or alternatively may be strung out along crustal lineaments (e.g., Monteregian Hills, Canada, Eby, 1987; Damaraland alkaline province, Namibia; Fig. 4c; Marsh, 1973; Miller, 2008).

In continental rift settings, intrusions are commonly located within a 60- to 100-km-wide zone bounded by and containing translithospheric faults that may show transcurrent and vertical offset (Sørensen, 1970). In the Gardar province, Greenland, the largest intrusive bodies (Igdlerfigsalik, Ilímaussaq, Nunarsuit, Motzfeldt) straddle these long-lived faults and are crosscut by them (Upton, 2013; Finch et al., 2019). The importance of fault-bounded zones for magma focusing is also apparent in the Chilwa province, Malawi (Garson, 1965; Nyalugwe et al., 2019) and the modern East African rift (Bastow et al., 2008). Many continental rifts are asymmetric (Brune et al., 2014), with a lower plate characterized by

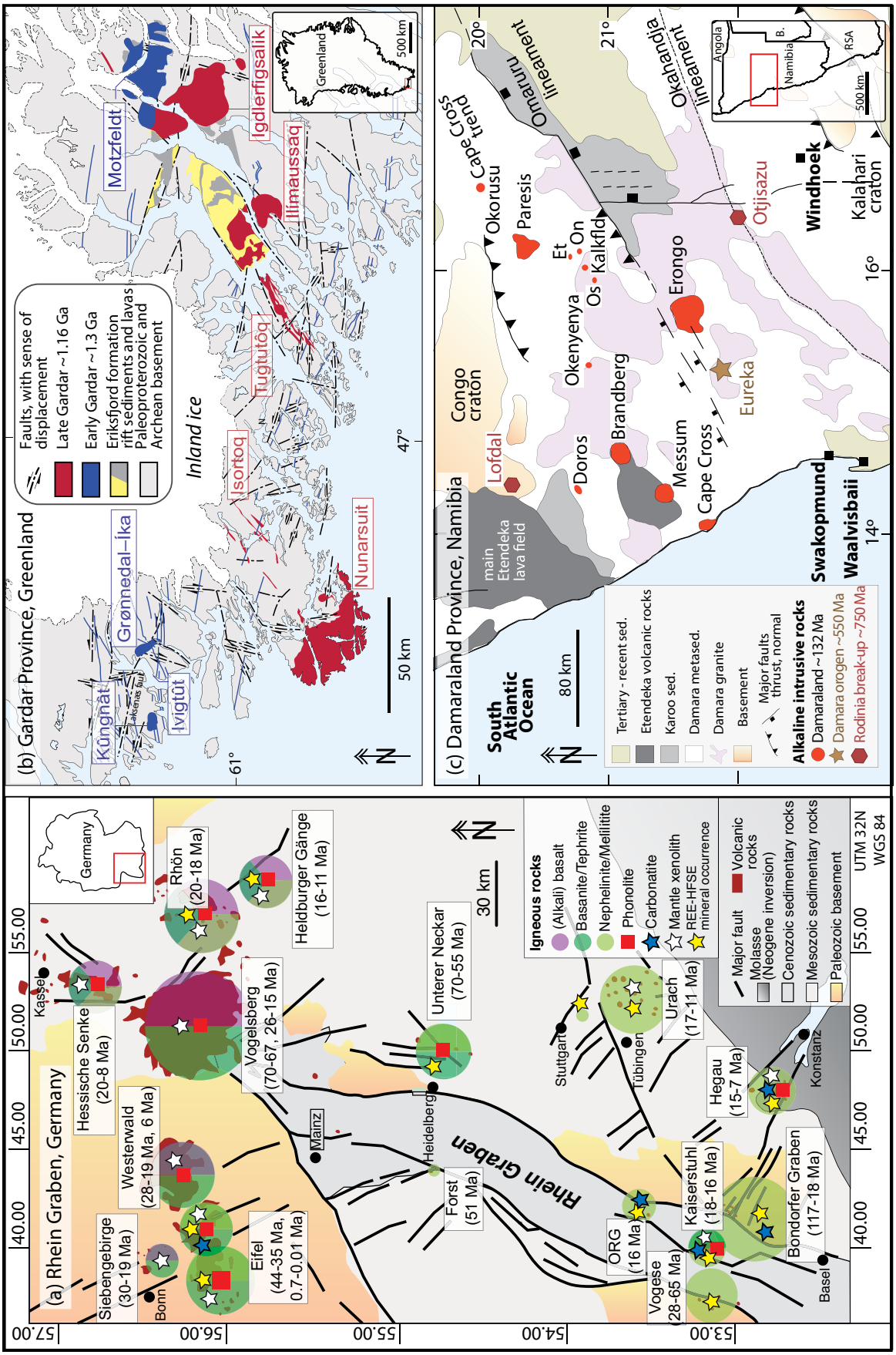

Fig. 4. Province-scale maps of alkaline-silicate rare earth element-high field strength element (REE-HFSE) systems showing major crustal structures that control the location of intrusive and volcanic complexes at the district scale (~25 km). (a) The Variscan-Miocene Rhine Graben system in southwest Germany after Banks et al. (2019), emplaced in a postcollisional setting. (b) The Mesoproterozoic Gardar province in southwest Greenland after Sørensen (2006) and Upton (2013), emplaced in a continental rift setting. Here, large, inferred NE-SW–trending structures follow fjords that are parallel to the Ketilidian margin. The Paatusoq Complex (not shown, east of the Greenland ice cap) is situated on the intersection of major east-west faults and Jokum's shear, a major terrain boundary. (c) The Cretaceous Damaraland province of Namibia, associated with the Etenedeka-Paraná large igneous province and the opening of the South Atlantic Ocean, after Brown et al. (2014). The Cape Cross trend follows an inferred, rift-perpendicular structure that runs parallel to the Omaruru lineament. Note that scale varies among the three maps.

marked thinning and extension and an upper plate, commonly with steeper normal faults and alkalic magmatism (Şengör and Natal'in, 2001; Lund, 2008). While the effect of rift asymmetry on REE-HFSE mineralization potential has not been examined in detail, the greater thickness of the upper plate and lower degree of mantle melting beneath it probably favor REE-HFSE mineralization on the upper margin of asymmetric rift systems.

In postcollisional alkaline-silicate and carbonatite provinces, the intrusions are commonly aligned along crustal-scale transcurrent shear zones (Hutton and Reavy, 1992; e.g., Mianning-Dechang belt, China, Hou et al., 2009; Kaiserstuhl and related Miocene complexes, southwest Germany, Banks et al., 2019). These structures trace relict, potentially ephemeral, permeability through which mantle melts traversed thickened continental crust (Sylvester, 1989; Bonin, 2004).

Magnetic surveys represent an effective tool for mapping structural lineaments that represent potential crustal permeability (Riedel et al., 2013). Additionally, they are effective in the search for intrusive systems under cover, of particular exploration interest in partially covered provinces that host proven mineralization. To resolve features on the scale of individual intrusive or volcanic systems (~25 km) a maximum flight line spacing of 400 m should be used. At this scale of investigation, surveys must be conducted using airborne techniques and are typically implemented by governments or international development organizations (e.g., World Bank Mining Governance and Growth Support project; Nyalugwe et al., 2019). Magnetometers are most often flown together with gamma-ray spectrometers.

Gamma-ray spectrometry is used to determine the U, Th, and K concentration in rocks and soils. This technique is typically sensitive to a penetration depth of 30 cm (Shives, 2015) and has been used to map lithologies and to identify potential zones of mineralization (e.g., McCafferty et al., 2014). Uranium and thorium can be associated with, or contained within, REE-bearing minerals, and gamma-ray spectrometry can therefore be used as an indirect indicator of REE mineralization (Steenfelt, 1991; Bedini and Rasmussen, 2018). One should note, however, that Th and especially U are mobile during low-temperature alteration (Timofeev et al., 2018; Nisbet et al., 2019); therefore, use of gamma-ray spectrometry alone may miss U-Th–poor, REE-HFSE–rich portions of a deposit (Finch et al., 2019), the very parts that would produce the lowest fraction of radioactive by-product (see "Environmental and social considerations" section). It is therefore crucial to use mineralogical information when interpreting radiometric measurements at the district and especially the deposit scale.

District-Scale Characteristics

The district scale focuses on individual intrusive and volcanic complexes that typically spread over 10–40 km in lateral extent (Fig. 5). These complexes tend to comprise several stages of magmatism, only some of which may be associated with REE-HFSE mineralization. We used the spatial relationship between lithologies, structural features, and the location of various types of REE-HFSE mineralization to build an interactive 3-D geologic model for an idealized system at the district scale (25-km cube, Fig. 6; 3-D geomodel in App. 1). The 3-D model is based primarily on observations from the HiTech AlkCarb project's natural laboratories, particularly intrusions of the Gardar province in Greenland and the Damaraland province in Namibia. We have also drawn on literature for many other alkaline complexes (Fig. 5). Below, we discuss the geologic observations used to construct the model. These include the typical relationship between intrusive units, the impacts of volcanism and depth of emplacement, the processes by which wall rocks can influence mineralization, and characteristics of the alteration aureole surrounding intrusive systems. Additional details on the construction of the 3-D model are in Appendix 1.

Within the mineral system framework (Knox-Robinson and Wyborn, 1997; McCuaig and Hronsky, 2014; Banks et al., 2019), focused transport, concentration, and trapping of the commodity are the processes that are critical at the district scale. The preservation of mineralization is of additional concern, especially in rapidly eroding regions with steep topography.

Exploration at the district scale introduces higher-resolution airborne magnetic and radiometric surveys. The typical line spacing for such surveys is 70 to 100 m in order to resolve distinct volcanic and intrusive phases within the system (Brauch et al., 2018). Geochemical proxies in soil, stream sediment, or surface grab samples may also be used to vector toward mineralization (Steenfelt, 2012; see "Wall-rock influences and fenite alteration halos" section). Such techniques have been applied effectively in diamond and porphyry Cu exploration projects globally (e.g., Schulze, 2003; Grütter et al., 2004; Sillitoe, 2010; Williamson et al., 2016). Hyperspectral imaging techniques are under development and have the potential to directly map the REE content of mineralized rocks exposed at surface (Boesche et al., 2015; Neave et al., 2016; Bedini and Rasmussen, 2018; Möller and Williams-Jones, 2018; Booysen et al., 2020). Such techniques will be best applied in arid environments, such as hot deserts and the Arctic.

Plutonic relationships, magmatic system evolution, and the timescales of alkaline magmatism

A variety of intrusion morphologies are known from continental rift settings (Fig. 5). Large, layered silica-undersaturated examples (diam 18–40 km; blue, brown in 3-D geomodel) include the Devonian Lovozero and Khibiny Complexes in Russia (Kalashnikov et al., 2016a), the Mesoproterozoic Ilímaussaq Complex in southwest Greenland (Ferguson, 1964; Larsen and Sorensen, 1987; Marks and Markl, 2015; Borst et al., 2018), and the Mesoproterozoic Pilanesberg Complex in South Africa (Andersen et al., 2017; Elburg and Cawthorn, 2017). Typically smaller silica-saturated examples (diam 0.3–6 km; dark pink in 3-D geomodel) include the Mesoproterozoic Strange Lake Complex in Canada (Vasyukova and Williams-Jones, 2019a), the Cretaceous Baerzhe Complex in China (Wu et al., 2021), and the Cretaceous Brandberg-Amis Complex in Namibia (Schmitt et al., 2002). Subvolcanic levels (2–5 km) of these alkaline-silicate magmatic systems can host REE mineralization, commonly with higher HREE/LREE than carbonatite REE deposits, as well as zirconium, niobium, tantalum, uranium, and thorium (Dostal, 2017; Goodenough et al., 2018).

Mineralized alkaline-silicate magmatic systems are commonly polyphase, their intrusions preserving a general

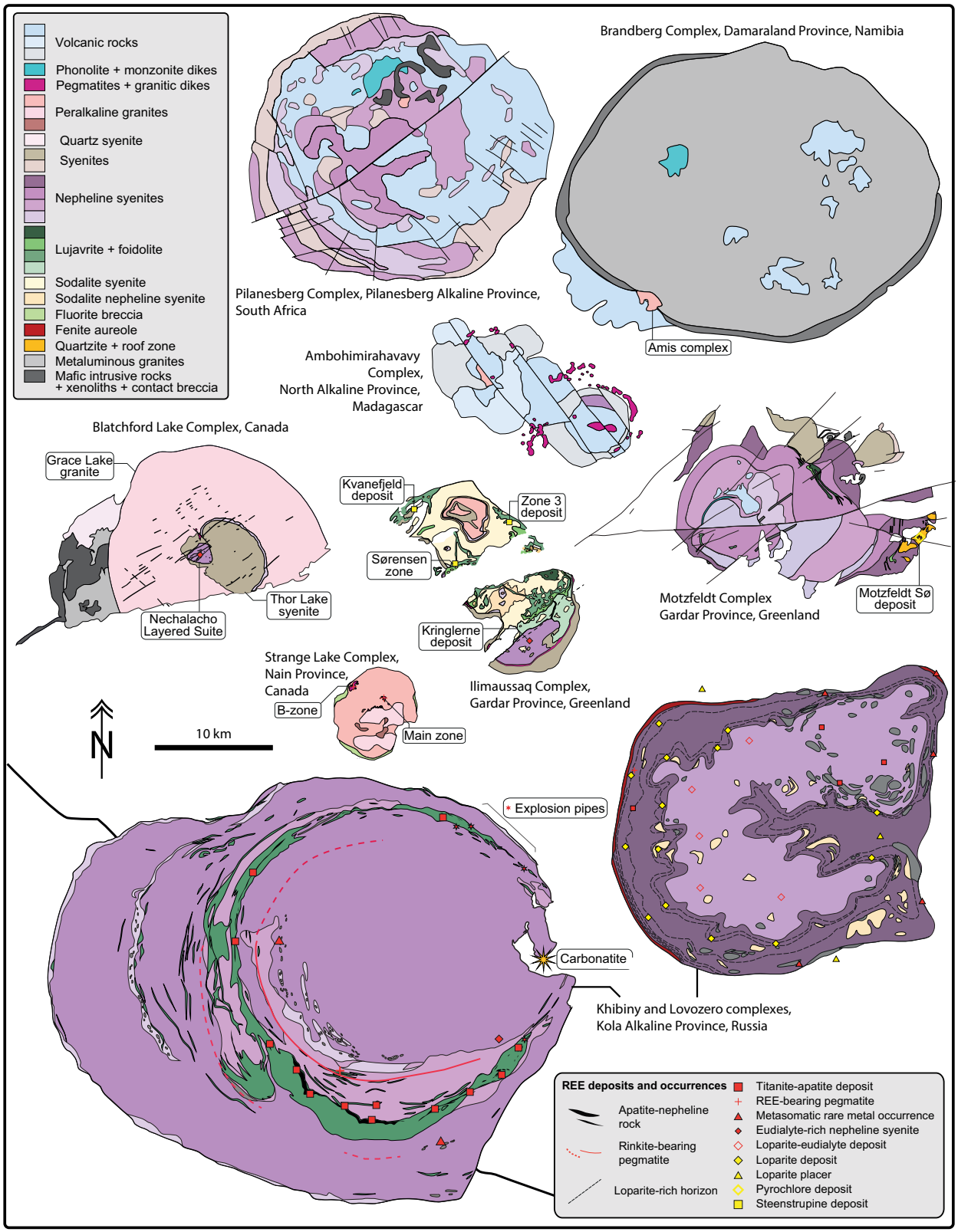

Fig. 5. A compilation of district-scale geologic maps from alkali silicate systems associated with rare earth element-high field strength element (REE-HFSE) mineralization. Scale is consistent between maps. Pilanesberg after Cawthorn (2015), Brandberg after Schmitt et al. (2000), Ambohimirahavavy after Estrade et al. (2019), Blatchford Lake after Möller and Williams-Jones (2016a), Ilímaussaq after Upton (2013), Motzfeldt after Finch et al. (2019), Strange Lake after Siegel et al. (2018), and Khibiny and Lovozero after Kalashnikov et al. (2016a). Multiple colors per lithology reflect divisions between similar units in the original maps.

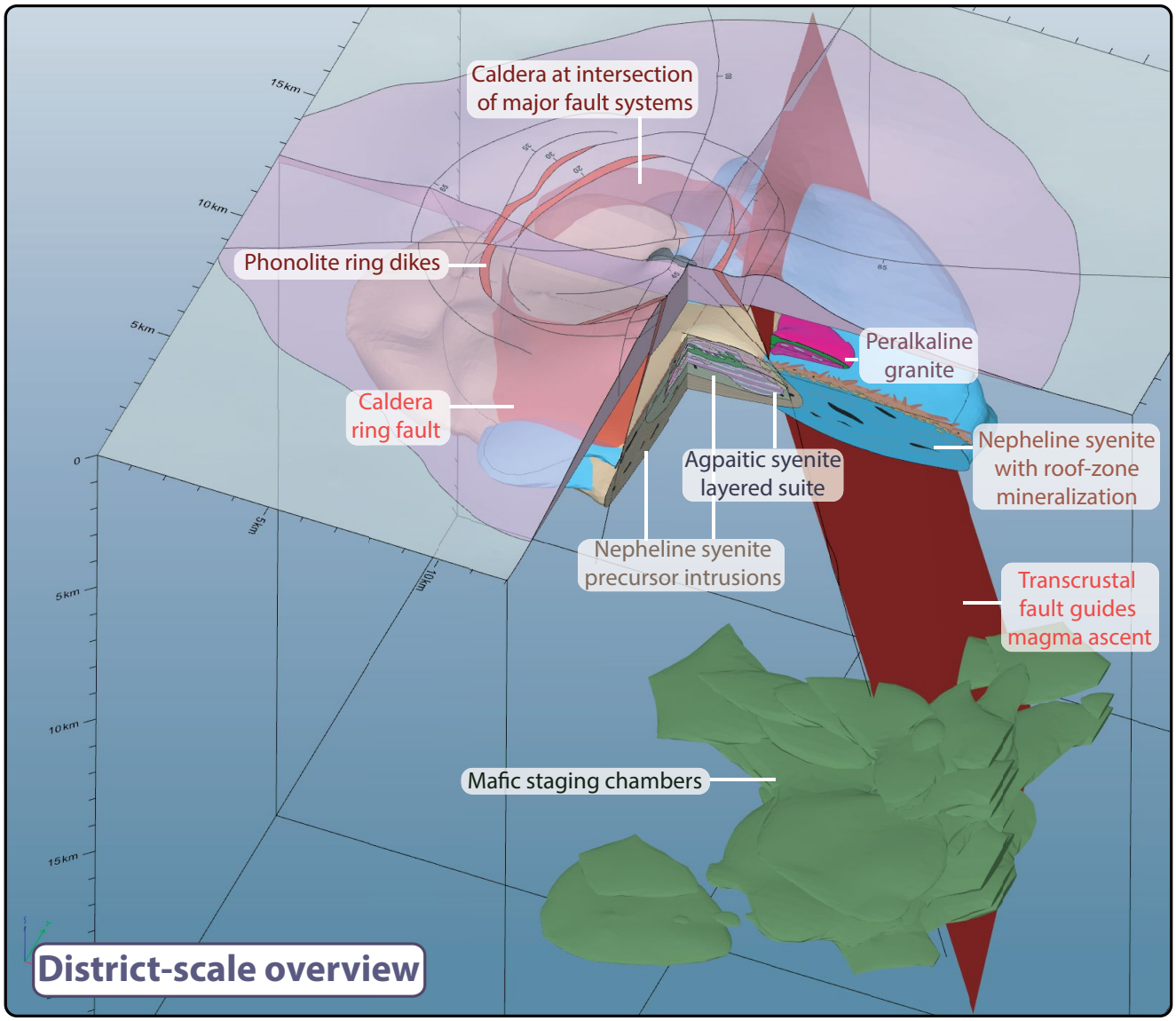

Fig. 6. Overview of the 3-D alkaline-silicate geomodel showing a surface caldera (geometry after Coumans and Stix, 2016) and a series of mafic staging chambers (green) that are inferred from gravity and magnetotelluric surveys (Blundell, 1978; Samrock et al., 2018). Many alkaline-silicate complexes occur on intersections of major fault systems, and magma ascent is thought to be guided by transcrustal fault systems (Banks et al., 2019). At a depth of ~2–3 km is a nested system of intrusions (blue, brown, pale pink). These have undergone a variety of levels of fractionation and of assimilation of country rocks (black, yellow), resulting in the formation of several types of rare earth element-high field strength element (REE-HFSE) mineralization. Detailed views of the mineralization are in Figures 8 and 9. The interactive 3-D model is in Appendix 1.

decrease in silica with time (e.g., Messum, Namibia, Harris et al., 1999; Erongo, Namibia, Trumbull et al., 2003; Blatchford Lake Complex, Canada, Mumford et al., 2014; Möller and Williams-Jones, 2016a; Fig. 5). This is expressed as a succession of intrusive phases that may include granites or quartz syenites toward the exterior, with later nepheline syenites toward the center. The alkali content of polyphase systems displays a similar general increase with time, tracking an increase in the degree of fractional crystallization relative to a primary mantle melt (e.g., Ilímaussaq, Greenland, Marks and Markl, 2015; Motzfeldt, Greenland, Jones, 1984; Finch et al., 2019). It is expressed as a succession from alkali gabbro, through miaskitic toward agpaitic syenite compositions. The most evolved agpaitic units (purple in the 3-D geomodel) range in size from small sill-like bodies within an otherwise miaskitic intrusive suite (Motzfeldt, Jones, 1984) to layered intrusive bodies that represent the volumetrically dominant lithology (e.g., Lovozero, Khibiny, Kalashnikov et al., 2016a). In particularly large silica-undersaturated systems, carbonatite may occur as minor late plugs or dikes emplaced into the cores or margins of alkaline-silicate intrusions (Fig. 5) (Kalashnikov et al., 2016a).

The systematics of the silica content of alkaline-silicate magmatic systems can be explained using an analogy from continental flood basalt systems (Cox and Hawkesworth, 1985; Arndt et al., 1993; Beard et al., 2017). The first phase

of a magmatic system is intruded into fresh country rocks that may contain minerals stable only at low temperature. Intrusion of this magma establishes a strong chemical potential gradient, and the most mobile components of the country rock are destabilized and assimilated into the magmatic plumbing system. As the magmatic system becomes established, altered country rocks, crystal mushes, and related igneous rocks create a physicochemical barrier between the silicate melt and the fresh country rocks, resulting in a decrease in crustal assimilation with time (Harris et al., 1999; Riishuus et al., 2008). This effect is captured in the 3-D geomodel via systematic changes to the character of intrusive phases: the first and outermost intrusive phase (blue in Fig. 6; based on Motzfeldt Sø and Grace Lake granite, Blatchford Lake Complex, Fig. 5) is characterized by common xenoliths and a silica-saturated roof zone (orange, see "Silicate roof zone deposits" section below), formed via extensive interaction between the silica-undersaturated intrusive body and its silica-rich country rocks. Later intrusive phases emplaced toward the center of the complex show a progressive decrease in silica content, brought about by a decrease in interaction between their melts and the country rocks (Precursor intrusion i, ii; pale brown, pale green in Fig. 6; e.g., Thor Lake syenite, Blatchford Lake Complex, Fig. 5). This intrusive sequence is characterized by an inward decrease in the number of xenoliths and an increase in autoliths.

Producing the extreme alkali enrichments seen in agpaitic systems requires high fractions of crystallization relative to a primary melt composition derived from mantle (>90%; Spandler and Morris, 2016). Direct fractionation of a single package of mantle-derived liquid provides a simple mechanism by which to explain the formation of peralkaline igneous rocks (Ablay et al., 1998). However, recent trace element and radiogenic isotope measurements from pyroclastic volcanic deposits suggest that rejuvenation of magmatic systems partially remelts early formed cumulates or associated igneous rocks to produce silicate melts with more evolved compositions (Wiesmaier et al., 2012; Wolff et al., 2020). A progressive remelting and crystal fractionation model is further supported by the common occurrence of autoliths in layered alkaline intrusions (e.g., Upton, 2013). Whether crystal fractionation results in residual enrichment of the REEs and HFSEs is a delicate balance controlled largely by melt composition and by the mineralogy of the crystallizing assemblage. Dry crystallization (low α_{H_2O}) produces a mineral assemblage rich in alkali feldspar and poor in clinopyroxene and amphibole (Giehl et al., 2013), which effectively enriches REEs in the residual melts (Beard et al., 2019). The high fluorine content of some mineralized alkaline systems (Andersen et al., 2010; Vasyukova and Williams-Jones, 2016) may further promote residual enrichment as it decreases the activity of REEs in the melt, reducing their uptake into minerals (Beard et al., 2020), and depresses HFSE mineral solubility (Marr et al., 1998; Aseri et al., 2015). Other minor elements, such as chlorine (Marr et al., 1998) and sulfur (Zheng et al., 2021), may also play important roles in the behavior of REEs and HFSEs in alkaline magmatic systems, but their influence is not yet well characterized. In the 3-D geomodel, the degree of fractionation increases inward between intrusive phases, culminating with an agpaitic layered intrusion (purple; e.g., Nechalacho Layered Suite, Blatchford Lake Complex, and Ilímaussaq Complex; Fig. 5).

Detailed geochronological studies indicate that polyphase alkaline-silicate magmatic systems are emplaced over geologically short timescales (<3 m.y., sometimes within the uncertainty of modern U-Pb techniques; Ilímaussaq Complex and Nechalacho Layered Suite; Krumrei et al., 2006; Möller and Williams-Jones, 2016b; Borst et al., 2019). By contrast, some mineralized silica-saturated systems appear to be monogenetic or dominantly emplaced in a single pulse (e.g., Ivigtût, Baerzhe, Strange Lake; Goodenough et al., 2000; Yang et al., 2014; Siegel et al., 2018). Short, inferred timescales represent minima, as they may result from overprinting of earlier magmatism or from only shallow levels of exposure where the complexity of the precursor feeder system is not represented at surface and is hence unrecognized.

To allow for the extensive fractionation required to form agpaitic compositions, the ascent rate of alkaline-silicate magmas must be sufficiently slow (and probably persistent). The rapid melt ascent associated with the formation of monogenetic diatreme breccia pipes, a common feature of alkaline magmatic provinces, appears to be incompatible with REE-HFSE mineralization (2.5–60 m/s; Spera, 1984). These pipes, however, can pre- and postdate mineralization (e.g., Genge et al., 1995; Woolley, 2003; Humphreys et al., 2010), their permeability representing a potential trap for later hydrothermal mineralization (e.g., Dalucao, China; Liu and Hou, 2017). The processes that result in some alkaline-silicate systems being apparently short-lived while others remain intermittently active for millions of years are not yet well understood.

The presence of highly evolved peralkaline magmas and the complexity of growth zoning patterns in their autocryst and antecryst cargo indicate the crucial role for mafic staging chambers in the crust (Larsen, 1976; Bédard et al., 1988). Such magmatic bodies (dark green in 3-D geomodel and Fig. 6) have been inferred at a depth of >14 km below the modern East African rift via magnetotelluric techniques (Samrock et al., 2018) and are consistent with a positive Bouguer gravity anomaly in the Gardar province, Greenland (Blundell, 1978).

In postcollisional systems, common rock types include sheeted syenitic, phonolitic, and trachytic intrusions and carbonatite dikes, with REE, F, and Ba mineralization hosted in stockworks, breccia pipes, carbonatite dikes, and carbohydrothermal veins (e.g., Hou et al., 2009; Guo and Liu, 2019; Goodenough et al., 2021). Carbonatite is commonly more abundant than in continental rift systems, but alkaline-silicate rocks are usually still volumetrically dominant. A comprehensive description of the types of mineralization is not within the scope of this review.

Volcanic connections and the depth of emplacement

Linking alkaline-silicate volcanism to mineralization in the underlying plutonic systems has proved challenging, as exposure of mineralization tends to occur where volcanic sequences have been largely eroded. Extensive volcanism is thought to be incompatible with mineralization, as the associated volatile release may dissipate the commodity into the environment (cf. Sillitoe, 2010). However, minor, late eruptions—for example, of lamprophyre or carbonatite diatremes—have the potential to carry mineralized rocks to surface and offer a window into

the magmatic system at depth (e.g., Monte Vulture, Italy, Beccaluva et al., 2002; Teide, Tenerife, Wiesmaier et al., 2012).

The East African rift has been considered as a potential active analogue for the Mesoproterozoic Gardar province, Greenland (Macdonald and Upton, 1993; Macdonald et al., 2014). Cenozoic volcanoes of the East African rift are characterized by major pyroclastic eruptions (>10 km^3) of evolved peralkaline rhyolite, smaller effusive eruptions (<10 km^3), and the development of caldera structures (Macdonald et al., 2014; Hutchison et al., 2016b; Rooney 2020a; see 3-D geomodel). Calderas are typically associated with the development of ring faults and associated intrusions (Cole et al., 2005; Coumans and Stix, 2016), which in turn can be recognized in many alkaline igneous complexes, including those from the Gardar province (Macdonald et al., 2014). Furthermore, caldera structures may represent foci for permeability and mineralization.

The Ambohimirahavavy Complex in Madagascar (Fig. 5) represents an emplacement depth of <2 km and comprises a syenitic ring intrusion surrounding a central mass of volcaniclastic rocks, indicating the presence of a now partially eroded caldera (Estrade et al., 2014a). At the margins of the ring intrusion, REE- and HFSE-rich peralkaline granitic dikes are exposed, demonstrating that mineralization had developed in the underlying magma chamber (Estrade et al., 2014b). However, the volcaniclastic rocks preserved in the complex show no hint of mineralization. The Poços de Caldas Alkaline Complex in Brazil (Schorscher and Shea, 1992) and Pilanesberg Complex in South Africa (Cawthorn, 2015; Andersen et al., 2017; Elburg and Cawthorn, 2017) also represent eroded caldera systems, with late agpaitic nepheline syenites intruding the volcanic succession (Fig. 5). Pyroclastic ejecta from alkaline-silicate and carbonatite volcanoes may also contain REE minerals, but to attain economic grades and tonnages these minerals must be concentrated by sedimentary processes to form placer deposits, as reported at Aksu Diamas in Turkey (Deady et al., 2019).

In the 3-D geomodel (App. 1), the surface-level lithologies are based on the Ambohimirahavavy Complex, Madagascar (Estrade et al., 2019). The caldera fault system is based on analogue sandbox experiments (Coumans and Stix, 2016).

In the absence of volcanic rocks, depth of emplacement is difficult to constrain for alkaline-silicate systems, because of a dearth of calibrated mineral equilibrium barometers (Putirka, 2008; Masotta et al., 2013). Depth of emplacement may, however, influence mineralization potential because higher-pressure systems may more effectively retain dissolved volatiles. This is because pressure influences (1) the mineralogy of the crystallizing assemblage (Pilet et al., 2010; Iacovino et al., 2016; Romano et al., 2018) and, thus, the effectiveness of residual enrichment of REEs and HFSEs (Beard et al., 2019), (2) melt structure and phase equilibria associated with immiscibility of melts and fluid phases (Veksler, 2004; Massuyeau et al., 2015), and (3) the tendency for brittle fractures to form in country rocks (Brantut et al., 2013), which in turn influences the effectiveness of wall-rock assimilation and metasomatism, as well as the potential for volcanism or the venting of volatiles.

On passive or rifted continental margins, overburden at the time of emplacement has been used to estimate emplacement depth, especially in ultrabasic and carbonatitic systems (Frolov, 1971; Epshteyn and Kaban'kov, 1984). Map compilations from these studies suggest that intrusion geometry may represent a qualitative indicator of pressure because of the greater plasticity of crust at depth and, thus, a greater tendency for emplacement structures to be circular in plan view (Frolov, 1971). Additionally, paleodepth constraints have been made using the intersections of fluid inclusion isochores (Konnerup-Madsen and Rose-Hansen, 1984; Krumrei et al., 2007; Vasyukova et al., 2016; Walter et al., 2021), phase equilibria (Möller and Williams-Jones, 2016a), and mineral geobarometers from adjacent and contemporaneous intrusive units (Mumford, 2013). Typical inferred emplacement depths for mineralized alkaline-silicate systems are 3–5 km, as shown in the interactive 3-D geologic model (Fig. 6; App. 1).

Wall-rock influences and fenite alteration halos

Mineralized alkaline-silicate rocks are hosted by a variety of igneous, metamorphic, and sedimentary lithologies, giving the initial impression that country-rock type does not play an influential role in mineralization. In some classes of alkaline-silicate-associated deposits, this is probably true, whereas for others, host lithology may play an important role in mineralization—for example, in roof zone deposits (see "Silicate roof zone deposits" section below).

The retention of magmatic volatiles is important for maintaining a depolymerized melt structure and thus delaying the crystallization of common HFSE phases, such as zircon (e.g., Boehnke et al., 2013) that can terminate residual enrichment of the REEs and HFSEs. Consequently, fine-grained host rocks that are impermeable and lack structures to facilitate fluid escape (Walter et al., 2018) or that react readily with magmatic fluids to seal off permeability may increase the potential for focused mineralization (e.g., Fe-rich country rocks; Elliott et al., 2018).

Country-rock assimilation can trigger saturation of crystal phases in the melt that either harbour or reject the REEs or HFSEs, affecting both the relative and absolute abundance of metals in the residual melt (e.g., Giebel et al., 2019). Via this mechanism, reactions with country rock represent a metal-trapping mechanism as they can abruptly decrease the metal carrying capacity of melt and fluid phases by triggering saturation of REE-HFSE minerals ("Silicate roof zone deposits" section below; Motzfeldt Sø, Finch et al., 2019). Indeed, assimilation of silica-rich lithologies may be the origin of oversaturated alkaline rocks in general (e.g., Eby, 1984; Stevenson et al., 1997; Harris et al., 1999; Marks and Markl, 2001). Interaction between alkaline-silicate melt and country rocks can alternatively trap rare metal mineralization in a reaction zone, as seen in skarn-hosted deposits at the Ambohimirahavavy Complex, Madagascar (Estrade et al., 2015). Where fluid or melt phases escape the main intrusion, the REE tenor can be dispersed into the country rock, as seen at the Illerfissalik Complex, Gardar province (Sokół et al., 2022). This contrasts with world-class agpaitic layered syenite REE-HFSE mineralization at the neighboring Ilímaussaq intrusion (Borst et al., 2016).

In the 3-D interactive geomodel (App. 1), the blue alkaline intrusive phase highlights the interaction between alkaline magmatic systems and their country rocks. It is based

dominantly on features observed in the Motzfeldt Complex, Gardar province, Greenland (e.g., Finch et al., 2019) where the upper intrusive margin is a laterally continuous and structurally complex roof zone, generated via the reaction between alkaline-silicate melt and the country rocks that overlie the intrusion. Xenoliths of silica-rich Eriksfjord formation sandstones (yellow) have rounded shapes and appear to have reacted readily with the alkaline-silicate magmas. By contrast, basalt xenoliths (black) preserve angular forms and appear to have been relatively unreactive with the magma. Xenoliths up to kilometer scale are found throughout the main intrusive body of several systems in the Gardar province (Upton et al., 2003; Upton, 2013; Finch et al., 2019).

Alteration halos in wall rocks have been used during exploration for some classes of mineralization associated with magmatic systems, such as porphyry Cu deposits (Sillitoe, 2010). These aureoles can have a large footprint relative to the mineralization itself, and systematic variations in alteration mineralogy and composition can aid in the targeting of deposits. The alkali metasomatic aureoles that surround alkaline-silicate and carbonatite intrusions are termed "fenite." Because fenite composition is controlled by protolith mineralogy, fluid composition, pressure, and temperature, it has potential for use as a vectoring tool during exploration (Elliott et al., 2018; Broom-Fendley et al., 2021). The extent of fenite is additionally controlled by country-rock permeability. Fenitization is typically less pronounced around alkaline-silicate systems than around carbonatite bodies (usually <100 m vs. 1–2 km; Ferguson, 1964; Al Ani and Sarapää, 2009; Arzamastsev et al., 2011). Fenites that formed at depth are typically sodium dominated, containing conspicuous green veins of sodic clinopyroxene and amphibole that crosscut rocks dominated by alkali feldspar (Elliott et al., 2018). Fenites formed in shallower settings or more proximal to intrusive bodies tend to be potassium dominated and brecciated, containing abundant K-feldspar (~90%), with albite and minor assemblages of apatite, clinopyroxene, and rutile (Elliott et al., 2018). The potassium enrichment in fenite can be mapped by radiometric surveys and used as a vector toward mineralization (Simandl, 2015; Simandl and Paradis, 2018). Because fenite aureoles are formed via fluid expulsion from a parental intrusion, their extent, mineralogy, and geochemistry record information about the metal tenor of the parent intrusion (Dowman et al., 2017; Broom-Fendley et al., 2021). This effect is not yet characterized to a sufficient level for widespread use in exploration.

As country-rock lithology and structure influence the type of deposits that may have formed and the extent of reaction halos, the exploration approach at the district scale will need to be adjusted depending on the geology into which the alkaline-silicate system was emplaced.

Prospect and Deposit-Scale Characteristics

The critical raw material deposits associated with alkaline-silicate systems occur either within igneous layered cumulates (orthomagmatic type) or within the upper margins of intrusive bodies where the magmatic system has interacted with country rocks (silicate roof zone type, peralkaline granite type). Alkaline-silicate intrusions containing mineralization are typically circular to oval in plan view (4–650 km^2; Fig. 5). The largest intrusions may be composites of several smaller bodies. Glacial erosion, exploration drilling, and geophysical surveys have revealed the 3-D structure of several REE-HFSE–mineralized alkaline-silicate systems, indicating the thickness, horizontal extent, and structural controls on mineralization (Upton, 2013; Kalashnikov et al., 2016a). These have been used to build the 3-D geomodel presented here (Fig. 6; App. 1).

At the prospect (~5 km) scale, ground geophysical methods offer insight into the 3-D structure of the subsurface in order to target with drilling campaigns promising geologic features at the deposit scale. These surveys include magnetic, gravity, seismic, resistivity, induced polarization, and audio magnetotelluric (AMT) techniques. None of these image REE mineralization directly, because associated unmineralized igneous rocks usually have similar petrophysical properties. However, these techniques can constrain the thickness of volcanic units and the morphology of intrusive bodies, especially where their properties contrast strongly with their host rocks (e.g., Brauch et al., 2018). Recent developments in joint 3-D inversion of gravity and magnetic data were used to map a nepheline monzogabbro pipe in the Kaiserstuhl alkaline silicate and carbonatite complex in Germany (www.terratec-geoservices.com; dos Santos et al., 2019).

At the deposit scale, exploration campaigns typically use a variety of core logging techniques and handheld devices. The data acquired by industry-standard downhole logging probes allow for automated discrimination of lithology and potentially of mineralized zones. These probes typically measure (1) spectral gamma as an indicator for uranium, thorium, and potassium concentrations (2) magnetic susceptibility to indicate the presence of ferromagnetic minerals, and (3) resistivity and chargeability as indicators for the presence of clay minerals, which are key to understanding the geometry of REE-HFSE deposits in weathered alkaline-silicate rocks. Since it is not possible to measure REE concentration directly with standard geophysical probes, it is necessary to correlate borehole logging results with handheld X-ray fluorescence measurements carried out on the core. Some recent borehole logging instruments allow for direct measurements of the REE content (e.g., oreLOG by UIT Dresden, Germany; Märten et al., 2015). However, these probes are not yet standard equipment in the exploration industry. Petrographic investigations are recommended because modal mineralogy and species mineralogy are crucial for understanding the deposit metallurgy and therefore economic potential (see "Metallurgical Challenges and the Importance of REE Profiles" section). The association of Th radiometric anomalies with REE mineralization as observed in numerous exploration projects worldwide plays a key role in this case (e.g., Tukiainen et al., 1984).

Orthomagmatic deposits in layered agpaitic syenite suites

Agpaitic syenite systems that host orthomagmatic mineralization represent the most evolved and alkali-rich melt compositions known on this planet (Marks and Markl, 2017) and contain some of the largest known REE deposits (Fig. 7; Goodenough et al., 2016; Smith et al., 2016). Several intrusions dominated by silica-undersaturated agpaitic rocks and exceeding 10 km in diameter are known: Ilímaussaq, Greenland (8 × 18 km; Marks and Markl, 2015; Borst et al., 2018),

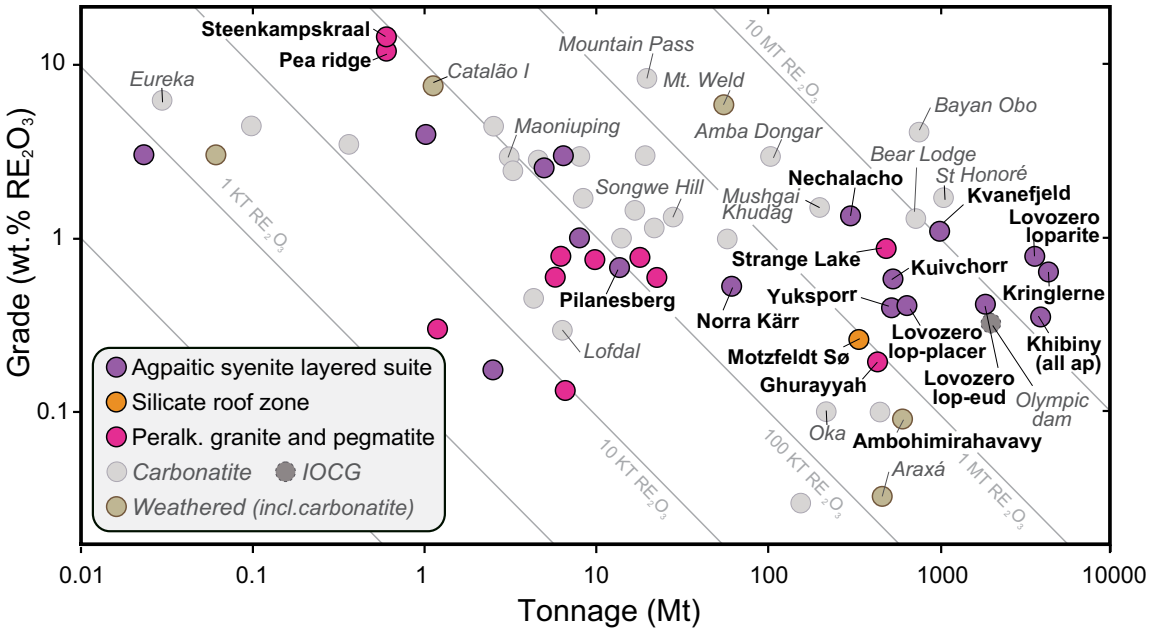

Fig. 7. Total RE_2O_3 grade (total rare earth oxide; TREO) versus tonnage diagram showing a global set of deposits. Diagonal gray lines indicate rare earth element (REE) tenor. Alkaline-silicate–associated REE deposits occupy a similar range of grade-tonnage space to carbonatite-associated REE deposits. Deposits in agpaitic syenite layered suites extend to greater REE tenor than most granite, pegmatite, or silicate roof zone deposits. Data from Woolley and Kjarsgaard (2008), Smith et al. (2016), and various company reports. The classification of deposits is based on the text in the "Prospect and Deposit-Scale Characteristics" section. A compilation of Joint Ore Reserves Committee (JORC) and NI 43-101 code-compliant resource estimates is in Appendix 3. Abbreviations: ap = apatite, eud = eudialyte, IOCG = iron oxide copper-gold, lop = loparite.

Khibiny and Lovozero, Russia (both ~40 km; Kalashnikov et al., 2016a), and Pilanesberg, South Africa (25 km; Cawthorn, 2015). These are layered intrusions consisting mainly of feldspathoid syenites and include early sodalite-rich roof rocks that are interpreted as flotation cumulates (Krumrei et al., 2007; Fig. 8; 3-D geomodel). Their stratified floor sequences are rich in sodic clinopyroxene, sodic amphibole, and ferrous fluorine-rich biotite. Late carbonatite is known from only a few examples (e.g., Gardiner, Khibiny) but is volumetrically minor compared with the silicate rocks (Kalashnikov et al., 2016a; Marks and Markl, 2017). Polyphase intrusive complexes that contain minor agpaitic units about 2 km in outcrop diameter are much more abundant (Mt. St. Hilaire, Poços de Caldas, Nechalacho, Motzfeldt, Norra Kärr; Fig. 5); therefore, these are what the 3-D interactive model is based on (Fig. 8; App. 1). Note that the subsurface extent of agpaitic units can be larger (e.g., Nechalacho; Möller and Williams-Jones, 2016a) but has only been drill defined in a few systems. The agpaitic portions of these polyphase systems may include igneous stratification similar to that described above (Möller and Williams-Jones, 2016a), and several contain Joint Ore Reserves Committee (JORC) or NI 43-101 code-compliant REE-HFSE resources (Fig. 7; App. 3). The majority of agpaitic rock occurrences are as minor late dikes and pegmatites within composite magmatic systems or as discontinuous blebs in otherwise miaskitic intrusions (Marks and Markl, 2017). Few, if any, of these constitute deposits of economic significance.

In orthomagmatic deposits, the ore minerals are located (1) within rhythmic cumulate layering in the floor sequence (Ilímaussaq, Khibiny, Lovozero; Sørensen, 1969; Kalashnikov et al., 2016a; Hunt et al., 2017; Borst et al., 2018; Mikhailova et al., 2019; Fig. 8) or (2) in late crosscutting dikes or sill-like magmatic bodies (Ilímaussaq, Motzfeldt, Poços de Caldas; Jones, 1984; Ulbrich et al., 2005; Ratschbacher et al., 2015). The former appear to span entire intrusive systems (plan view 4–650 km^2) up to a thickness of several hundred meters (Larsen and Sorensen, 1987; Féménias et al., 2005; Upton, 2013; Kalashnikov et al., 2016b). Mineralization occurs as complex Na-HFSE-silicate and Na-HFSE-oxide minerals such as eudialyte, steenstrupine-(Ce), loparite, and pyrochlore and tends to be HREE rich relative to most carbonatite-hosted deposits (e.g., at Ilímaussaq, Khibiny, Lovozero, Nechalacho, Motzfeldt; Sørensen, 1969; Bohse et al., 1971; Tukiainen, 1988; Sørensen, 1992; Möller and Williams-Jones, 2016a; Marks and Markl, 2017). Eight code-compliant resources have an average size of 750 Mt at 1.3 % TREO, the largest being the Kringlerne deposit in the Ilímaussaq Complex, Greenland (Fig. 7; pop-outs in 3-D geomodel).

Cumulate deposits of apatite and titanite are also known from peralkaline syenite intrusive systems and have been mined for phosphate and titanium (e.g., Kovdor, Khibiny; Kalashnikov et al., 2016b; Gerasimova et al., 2018; Kogarko, 2018). Although scandium is sensu stricto an REE, scandium deposits known from layered peralkaline systems are spatially separate from other REE deposits. This is because scandium is highly compatible in the M1 site of clinopyroxene (Beard et al., 2019) and is therefore concentrated early on in mafic cumulates (e.g., at Crater Lake, prev. Misery Lake, Canada; Williams-Jones and Vasyukova, 2018). Potentially economic scandium enrichments are also known from weathered carbonatites and granitic pegmatites (Siegfried et al., 2018).

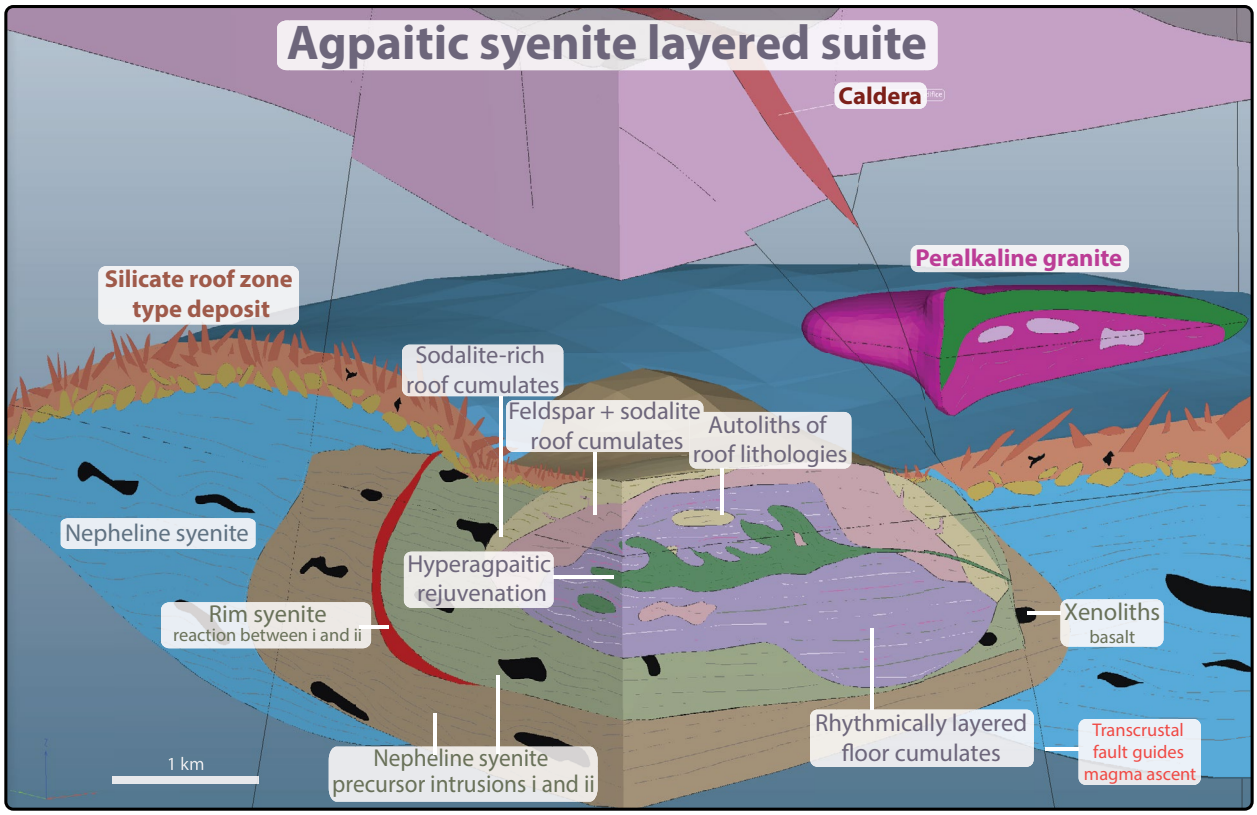

Fig. 8. A detailed view of the 3-D geologic model showing the internal structure of an agpaitic layered suite. Orthomagmatic rare earth element-high field strength element (REE-HFSE) mineralization is in rhythmically layered floor cumulates and in hyperagpaitic rejuvenations. Where present, precursor phases of the intrusion tend to record a general inward decrease in SiO_2 and increase in molar (Na + K)/Al (blue, brown, olive). These track decreasing levels of crustal contamination and increasing fractionation. A fine-grained rim syenite may occur on the boundary between intrusive phases (red; cf. Mumford et al., 2014). Detailed views of the silicate roof zone and peralkaline granite are in Figures 9 and 10. The interactive 3-D model is in Appendix 1.

Orthomagmatic deposits of REEs and HFSEs are also known from late hyperagpaitic magmatic bodies that crosscut alkaline-silicate intrusive systems (Fig. 8; 3-D geomodel). At the Ilímaussaq Complex, Greenland, exposure on the walls of fjords reveals that the late-stage lujavrite intrusions may have unzipped floor and roof cumulate layering and splayed both up- and down-section through a preexisting layered suite (combined thickness of 320 m; Ratschbacher et al., 2015). Similar features are reported at the Lovozero Complex, Russia, as the murmanite-lovozerite–bearing porphyritic malignites (Mikhailova et al., 2019). Both deposits are the products of evolved residual melts formed by crystal fractionation that may have pooled under the roof of deeper intrusive bodies or under kilometer-scale xenoliths or may have infiltrated units overlying the main intrusion (Sørensen et al., 2006; Ratschbacher et al., 2015). The largest known example of a crosscutting hyperalkaline REE-HFSE deposit is at Kvanefjeld in the Ilímaussaq intrusion, Greenland, with 437 Mt at 1.1% TREO (Greenland Minerals Ltd., 2015; Fig 7). At Kvanefjeld, steenstrupine-(Ce) is the dominant REE-U-Th mineral of economic interest (Khomyakov and Sørensen, 2001; Sørensen and Larsen, 2001; Sørensen et al., 2011; Andersen and Friis, 2014; see pop-up in 3-D geomodel).

The mineralization in layered peralkaline syenite systems may be preserved as fresh, unaltered igneous minerals but is commonly overprinted or completely obliterated, occurring as complex pseudomorph assemblages of alteration minerals (Feng and Samson, 2015; Borst et al., 2016; Möller and Williams-Jones, 2017; van de Ven et al., 2019). These assemblages might not influence overall ore grades, but finely intergrown secondary phases might be challenging to process and extract with a commercial-scale metallurgical process optimized for eudialyte alone (Zakharov et al., 2011), although work is ongoing to develop beneficiation workflows (Stark et al., 2017; Vaccarezza and Anderson, 2020). This overprinting by autometasomatism occurs due to the flushing of residual Na-rich aqueous fluids, melts, and in some cases magmatic hydrocarbons through the cumulate pile during late stages of crystallization (Markl et al., 2001; Mitchell and Liferovich, 2006; Salvi and Williams-Jones, 2006; Marks and Markl, 2015; Borst et al., 2016). Retrograde solubility of some REE-HFSE phases further promotes breakdown and metal remobilization during cooling (e.g., Aja et al., 1995; Timofeev et al., 2015). Late-stage melts and fluids may therefore (partially) remobilize orthomagmatic mineralization, carrying the metals upward through the crystal pile (van de Ven et al., 2019). If residual melt and fluid phases are retained to low temperatures (<200°C), then the intrusion may also retain its metal budget largely in situ (van de Ven et al., 2019).

Several metamorphosed examples of orthomagmatic peralkaline syenite deposits are known (Norra Kärr, Red Wine, Kipawa, and Sushina Complexes; Chakrabarty et al., 2016, 2018; Atanasova et al., 2017; Sjöqvist et al., 2017). The main REE mineral of interest in all these cases is eudialyte. However, there has been only limited study on the effect of metamorphism on REE minerals and the potential remobilization of REE that such conditions might trigger (Sjöqvist et al., 2020).

Mining of orthomagmatic deposits in agpaitic syenite layered suites has occurred in only a few cases because of metallurgical challenges posed by their complex REE-HFSE mineralogy (pop-up in 3-D geomodel, App. 1). In the Khibiny Complex in Russia, HREE-rich rinkite pegmatites at the Yuksporr Lovshorrite deposit were mined for REEs, Nb and Ti between 1934 and 1939, and apatite mines are currently in production (e.g., Kalashnikov et al., 2016a). The only operating Nb production in an alkali silicate system is the Karnasurt mine in nepheline syenites of the Lovozero Complex, Kola Peninsula, Russia. Here loparite, a perovskite group mineral, is targeted for Ti, Nb, Ta, and REEs (Mitchell, 2015; Kalashnikov et al., 2016a).

Silicate roof zone deposits

Silicate roof zone type deposits occur in the upper portions of layered alkaline-silicate systems and occasionally underneath large xenoliths or autoliths within layered suites (Sørensen, 1992; Sørensen et al., 2011; Fig. 9). In the former case, roof zones may be continuous across the lateral extent of plutons (up to ~10 km) with a thickness of several hundred meters (Stephenson and Upton, 1982; Upton et al., 2013). The metasomatic reaction of residual melts and fluids with the roof and country rocks forms complex networks of crosscutting lenses and sills as well as late-stage veins and pegmatites (Müller-Lorch et al., 2007). These late-magmatic pegmatites and veins are often enriched in a variety of elements (e.g., Li, Be, U, Th, REEs, Ti, Nb, Ta, Zr, and Zn; Bailey et al., 2001).

Roof zones represent the reaction products of metalliferous residual fluids and melts with roof rocks, which include both igneous roof cumulates and country rocks. They are defined by strong thermal and chemical gradients (Huppert and Sparks, 1988), including redox; thus, ascending melts and fluids that enter the roof undergo abrupt changes in metal carrying capacity, in some cases causing saturation of minerals that can trap a mobile commodity. Deposits in roof zones are less well studied than the orthomagmatic type, and key questions for future work relate to their internal structure, the mechanisms of mineralization, and the physical and chemical relationship between roof zones and their underlying alkaline-silicate plutons. Roof zone mineralization is known from alkaline granitic rocks (Bushveld Complex, Bailie and Robb, 2004; Mutele et al., 2017) and syenite complexes associated with continental rifting (Gardar province, Finch et al., 2019; Ditrău Complex, Romania, Honour et al., 2018; Kola Peninsula, Russia, Kalashnikov et al., 2016a). The Grace Lake granite of the Blatchford Lake Complex, Canada, may represent

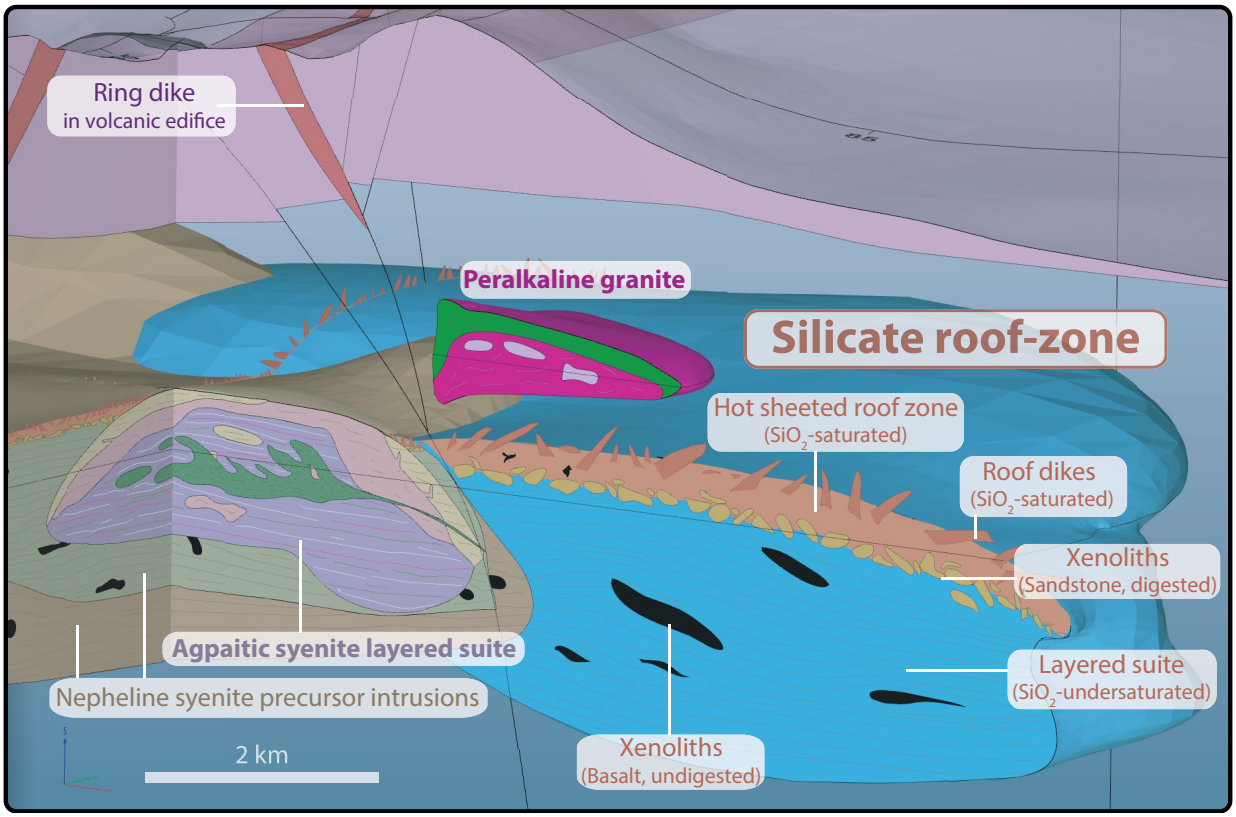

Fig. 9. A detailed view of a roof zone type deposit in the 3-D alkaline-silicate geomodel (overview in Fig. 6). This deposit class represents extensive interaction between alkaline-silicate magmas and their country rocks; this hybridization likely representing the trigger for mineralization. The interactive 3-D model is in Appendix 1.

a similar, but unmineralized, setting (Mumford, 2013; Mumford et al., 2014). In the case of the syenite complexes, the roof zone is characterized primarily by mineralization of Nb-Ta-Zr rather than of the REEs.

The best-studied example of a mineralized roof zone is that at Motzfeldt Sø, Greenland (Finch et al., 2019), where xenolith populations suggest preferential digestion of quartz arenite (yellow, Fig. 9; App. 1) relative to basaltic country rocks (black), resulting in generation of Si-F–rich hybrid melts. The Nb-Ta mineralization at Motzfeldt is hosted high in the roof by a series of discontinuous sheets of pyrochlore microsyenite, notably without chilled margins (Tukiainen et al., 1984; Tukiainen, 1988; Finch et al., 2019). Their contained pyrochlore preserves oscillatory concentric zonation of Nb and Ta, a record of polyphase crystal growth (McCreath et al., 2013). These pyrochlore grains may have been remobilized upward through the roof zone by several episodes of magma overturning or replenishment (Tukiainen, 1988). Pyrochlore from this type of system typically contains high concentrations of U and Th. However, postmagmatic hydrothermal alteration can increase the U-Th concentration of pyrochlore without strongly affecting HFSE concentrations (McCreath et al., 2012; Finch et al., 2019). For this reason, airborne gamma radiometric mapping, commonly used in exploration campaigns, may reveal regions rich in U and Th that do not necessarily correlate spatially with the Nb-Ta mineralization most favorable for beneficiation (Tukiainen et al., 1984; Finch et al., 2019). Motzfeldt Sø is the only roof zone type deposit with a code-compliant resource estimate, inferred to be 340 Mt at 120 ppm Ta_2O_5, 1,850 ppm Nb_2O_5, 4,600 ppm ZrO_2, and 2,600 ppm TREO (Ram Resources 2012; Fig. 7; pop-up in 3-D geomodel, App. 1).

Mineralization associated with peralkaline granites and pegmatites

Rare earth element-HFSE mineralization is also associated with peralkaline (A-type) granite magmatism (Fig. 10; 3-D geomodel). This type of deposit has recently been reviewed by Vasyukova and Williams-Jones (2020). The majority of REE-HFSE mineralization described here is in the upper parts of intrusions and associated with hydrothermal alteration and pegmatite formation (Vasyukova and Williams-Jones, 2019a).

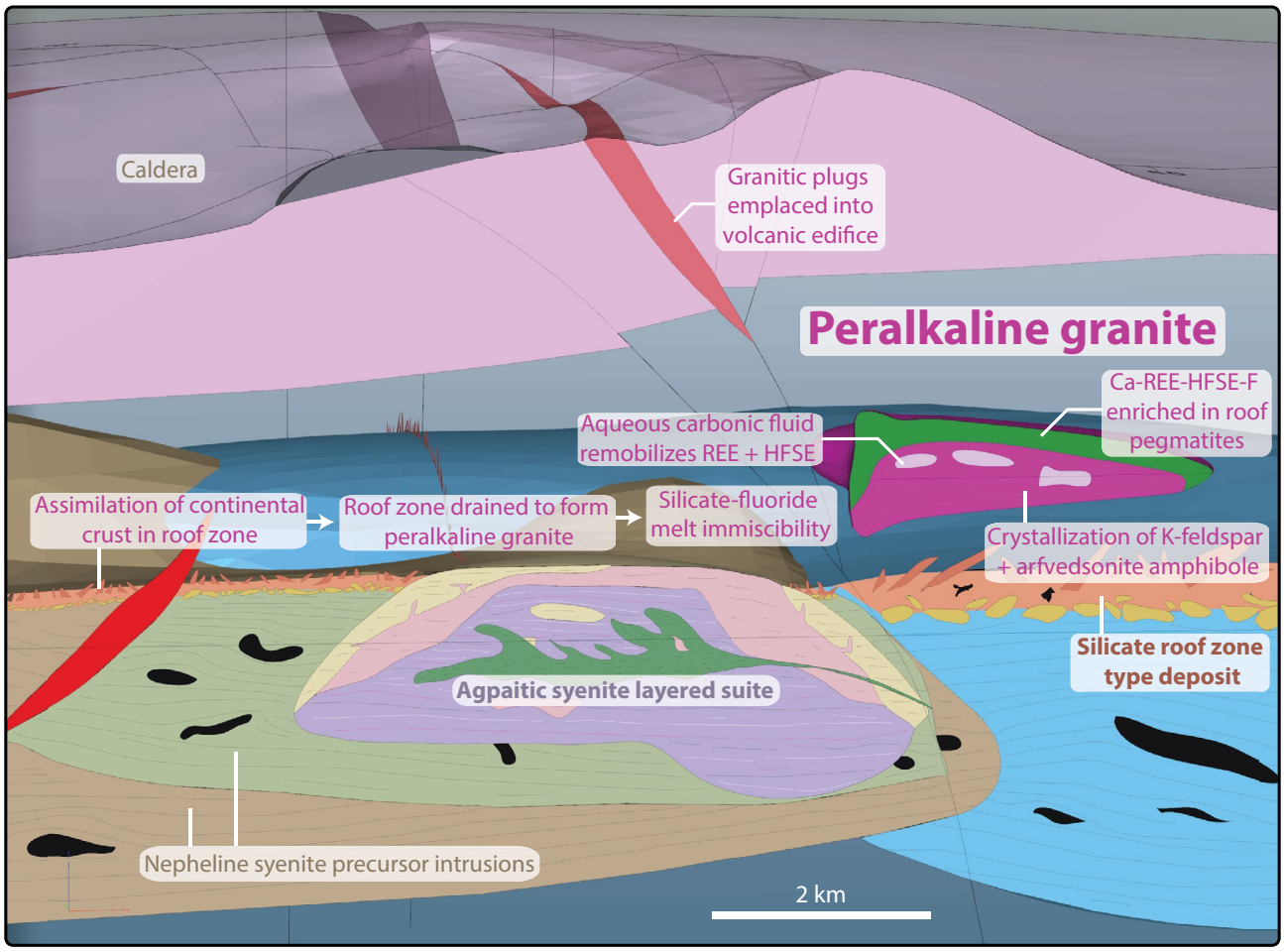

Fig. 10. A detailed view of the internal structure of a mineralized peralkaline granite intrusive body. Mineralization associated with peralkaline granites tends to be spatially associated with the roof where salt (ionic) melts and volatile-rich fluids accumulate. Granitic magmas may also be emplaced as plugs and dikes in the volcanic edifice, peripheral to major silica-undersaturated intrusive bodies (Estrade et al., 2014b). The interactive 3-D model is in Appendix 1. REE-HFSE = rare earth element-high field strength element.

Some of these systems have agpaitic compositions. The host granite intrusions may be monogenetic or polygenetic and are typically hundreds of meters to several kilometers in diameter (Fig. 5). They may also occur as plugs or dikes external to a major silica-undersaturated center (Ambohimirahavavy Complex, Estrade et al., 2014b; T zone, Nechalacho, Möller and Williams-Jones, 2016a). The fluorite-rich breccias that commonly define the margins of these granites suggest fluorine-rich melt compositions (Vasyukova and Williams-Jones, 2014, 2016). Compositional similarities with silicate roof zone deposits (see "Silicate roof zone deposits" section) suggest that A-type granites may be roof zones that were later mobilized through the crust (Fig. 10). REE-Zr-Nb mineralized pegmatites are typically tens of centimeters to tens of meters thick and occur in the upper part (cupola) of these granitic intrusions. Mineralization reflects the combined effects of early immiscible fluoride melts and late hydrothermal fluids (Vasyukova and Williams-Jones, 2019a). The anomalous enrichments of these roof pegmatites in fluorine, calcium, and the REEs are consistent with crystallization of a (REE-) fluoride melt phase (Veksler et al., 2012; Yang and van Hinsberg, 2019), as well as subsequent and extensive late-stage hydrothermal alteration (Salvi and Williams-Jones, 1996; Gysi and Williams-Jones, 2013). The Strange Lake granite, Canada, is presently the best-characterized example of this class of mineralization (Salvi and Williams-Jones, 2006; Siegel et al., 2018; Vasyukova and Williams-Jones, 2019b). REE-HFSE–mineralized pegmatites are additionally known from the Ambohimirahavavy and Manongarivo Complexes, Madagascar (Estrade et al., 2014a, b); the Amis Complex, Namibia (Schmitt et al., 2002; Bernard et al., 2020); Baerzhe, China (Qiu et al., 2019; Wu et al., 2021); Bokan Mountain, Alaska, USA (Dostal et al., 2014); the Evisa Complex, Corsica (Bernard et al., 2020); and Khaldzan Buregtey and Khan Bogd, Mongolia (Kovalenko et al., 1995; Kynicky et al., 2011). An extremely fluorine rich example that lacks REE-HFSE mineralization is the Ivigtût alkaline granite in the Gardar province, Greenland, where the (probably unique) 150-m-wide cryolite deposit within the granite was formed from a fluoride-rich, carbonate-rich fluid or melt (Goodenough et al., 2000; Köhler et al., 2008). Ivigtût has been mined out because cryolite from this deposit was a key ingredient for the smelting of aluminium in the 19th century (Berry, 2012).

Although many peralkaline granitic systems show significant enrichment in the REEs and HFSEs, virtually none have been exploited. This may be due, in part, to their complex mineralogy (Jaroni et al., 2019; Pell et al., 2021; pop-out in 3-D geomodel; "Metallurgical Challenges and the Importance of REE Profiles" section above). The REEs and HFSEs are typically hosted by multiple phases including zircon, elpidite, gittinsite, armstrongite, monazite-Ce, xenotime-Y, allanite-Ce, gadolinite-Y, columbite-tantalite, pyrochlore, bastnäsite-Ce, and REE fluorcarbonate minerals, such as fluocerite-(Ce), gagarinite-(Y), and fluorite-fluocerites (Gysi and Williams-Jones, 2013). Few of these minerals have proven workflows for commercial beneficiation (see "Metallurgical Challenges and the Importance of REE Profiles" section), but various key parameters such as their flotation properties and acid bake chemistry have been determined (Demol et al., 2019; Kursun et al., 2019). Variations in ore mineralogy and texture within individual deposits represent significant geometallurgical challenges.

The largest REE-HFSE deposits in peralkaline granitic systems have TREO resources about an order of magnitude smaller than their orthomagmatic silica-undersaturated cousins, with similar TREO grades (~1 wt %; Fig. 7). Strange Lake, Canada, has the largest REE resource with 278 Mt at 0.93% total rare earths (TRE; indicated) and 214 Mt at 0.85% TRE (inferred) for a total of 5.1 Mt TREO (Quest Rare Minerals Ltd., 2017).

There are several localities, such as the Erongo Complex in Namibia, Pitinga in Brazil, and the Nigerian younger granites (e.g., Ririwai Complex), where peralkaline granitic complexes may be associated with tin-tungsten mineralization in roof zone pegmatites and marginal facies (Lenharo et al., 2003; Kinnaird et al., 2016). Such mineralization is more characteristic of S-type granites and likely indicates the importance of crustal contamination in these plutons (Costi et al., 2009; Pirajno, 2015; Falster et al., 2018).

The Impact of Weathering

Weathering may extend hundreds of meters from the ground surface and can cause significant changes to both the geochemistry and mineralogy of alkaline-silicate complexes. In rare examples, such as at Tomtor in Russia (Lazareva et al., 2015) and Poços de Caldas in Brazil (Schorscher and Shea, 1992), the REE-HFSE grades have been enhanced by surface weathering as easily weathered components of the igneous rocks have been broken down and removed. At Poços de Caldas, lateritic and allitic weathering of phonolites and nepheline syenites with magmatic hydrothermal U-Th-REE enrichments further elevated metal concentrations and formed the recently mined Osamu Utsumi U-Zr-REE-Th deposit and the Morro do Ferro U-Th deposit (Schorscher and Shea, 1992; Takehara et al., 2016). However, in most cases, weathering breaks down REE minerals, which may then be dispersed into the surface environment, sequestered by secondary REE minerals, some of which are not yet easily processed (e.g., florencite-Ce, Barros De Oliveira and Liguori Imbernon, 1998; Wall and Zaitsev, 2004), or adsorbed in their ionic form onto mineral surfaces, especially clays. The latter process can generate ion adsorption deposits (IADs) from which the REEs are relatively easily recovered.

Global production of HREEs is dominated by IADs from southern China (~80%; Weng et al., 2015; Jowitt et al., 2017). These Chinese deposits formed in the weathering profile of a variety of types of granite (Bao and Zhao, 2008; Sanematsu and Watanabe, 2016), and similar weathering processes control the formation of IADs on syenites and pegmatites elsewhere (Estrade et al., 2019; Borst et al., 2020). IAD ore grades are relatively low (a few 100 to 1,000s of ppm of REE) compared to hard-rock alkaline-silicate and carbonatite deposits, but extraction can be economically viable through in situ or heap leaching of the clay-adsorbed REE fraction (Moldoveanu and Papangelakis, 2016).

The main factors that determine the mobilization and redistribution of the REEs in IADs are the REE mineralogy of the bedrock and the soil pH (Bao and Zhao, 2008; Li et al., 2020). During weathering, a portion of the REEs is released from minerals in the bedrock and adsorbed to clays and other

secondary phases in the regolith (Yang et al., 2013; Sanematsu and Watanabe, 2016; Estrade et al., 2019; Li et al., 2019; Borst et al., 2020).

Weathering of precursors with high REE grades and easily weathered REE phases produce higher-grade IAD deposits. For example, the Zudong deposit in southern China formed on a granite containing synchysite-Y (Li, et al., 2017, 2019, 2021; Xu et al., 2017), and the Ambohimirahavavy Complex in Madagascar formed on peralkaline granite, nepheline syenite, and pegmatite dikes containing eudialyte, apatite, and REE-fluorcarbonates (Estrade et al., 2019; Borst et al., 2020). Lower leachable REE grades have been reported where protoliths contained more resistant REE-bearing phases such as zircon, pyrochlore, monazite, and xenotime (Estrade et al., 2019). At the Bankeng deposit, China, the HREEs that liberated to groundwater by weathering were transported downslope, and where soil pH increases due to water-regolith interaction, they were efficiently fixed by adsorption to clays (Li et al., 2020). LREEs at Bankeng are richest upslope, possibly due to the presence of relatively resistant and LREE-rich monazite-Ce and apatite in the granite bedrock. Other factors that play a role in IAD formation are climate, topography, vegetation, and hydrological factors, such as seasonal variations to the depth of the water table (Yang et al., 2019; Li et al., 2020).

The thickness of the oxidation and weathering zones in IAD-type deposits can be mapped via induced polarization geophysical techniques (Brauch et al., 2018). The formation of clay minerals lowers the resistivity of the rocks relative to their igneous precursors. Their chargeability is also reduced during the oxidation and weathering of sulfide minerals (where present). Various IAD-type deposits are currently under exploration in South America, Africa, and Southeast Asia (Sanematsu and Watanabe, 2016).

Summary and Outlook

Alkaline-silicate–associated REE-HFSE deposits are a relatively understudied ore deposit type that is increasing in importance as global energy and transport infrastructures shift toward renewables. In the last two decades, the magmatic-hydrothermal evolution of these systems and their links to continental-scale geodynamic processes have been clarified. Recent developments in exploration have seen the successful delineation of substantial new REE resources within alkaline silicate rocks. However, mineralogy and mineral processing remain major hurdles to getting alkaline-silicate–associated deposits into production. Numerous pilot studies are underway and aim to develop beneficiation pathways for the diverse family of REE-HFSE ore minerals. As is the case for all mining projects, public trust must be earned early in the exploration process and maintained if commercial extraction is to take place. Special considerations must be made for the risks posed by radionuclides, which are likely to be a social concern even in cases where the actual environmental risk is negligible.

The current state of geologic understanding of alkaline-silicate systems allows for exploration programs to use a combination of geophysical and geochemical tools to progressively reduce the scale of search areas, following a mineral systems approach. Mineralization is known from continental rift, postcollisional, and intraplate (e.g., plume) tectonic settings. At the continental scale, the key targeting criteria are (1) a trigger for low-degree, ideally persistent, mantle melting, (2) melting at high pressure, for example, under thick continental crust ($\geq$ 40 km) at craton margins, and (3) a mantle source that is enriched in the commodity and a suitable cocktail of alkalies and volatiles to promote extensive fractional crystallization—for example, mantle that was metasomatized by subduction. Also note that (4) All mineralization identified thus far postdates the Archean, as high mantle potential temperatures early in Earth history do not appear to be associated with significant alkaline magmatism. Province-scale exploration should identify and map crustal-scale structures that could have focused magma ascent from the mantle. In continental rifts, the largest intrusive centers straddle long-lived fault systems and are crosscut by them. In postcollisional settings, intrusions are commonly aligned along crustal-scale transcurrent shear zones. At the district scale, exploration should target long-lived or repeatedly reactivated intrusive systems, as these have the greatest potential for the extensive fractional crystallization required for residual enrichments of the REEs and HFSEs. Volcanism does not appear to exclude the possibility of mineralization. However, the retention of magmatic volatiles is important for maintaining a depolymerized melt structure required for extended fractional crystallization. Highly reactive, low-permeability wall rocks are therefore key to the sealing-in of REE-HFSE–rich residual melts and fluid phases, thus preventing dispersal of the commodities into the wider environment. An interactive 3-D model presented at district scale shows the typical relationship between lithologies and places alkaline-associated mineralization within a horizontal and depth reference frame. This includes orthomagmatic mineralization in layered agpaitic syenites, silicate roof zone type deposits, and mineralization associated with peralkaline granites and pegmatites.

There is still much to learn. Outstanding questions highlighted by this work include the following:

1. What are the fundamental mantle and crustal factors that determine whether continental rifts or collisional belts are endowed with rich and extensive alkaline-silicate REE-HFSE mineral systems (e.g., Kola and Gardar provinces), smaller and more temporally limited systems (Mianning-Dechang belt), or none at all (mid-continent rift)?
2. Can the systematics of province-scale crustal structures be used as a robust predictor for the main focus of mineralization? What role, if any, does rift asymmetry play?
3. What are the effects of depth (pressure) of crystal fractionation on the residual enrichment of the REEs + HFSEs in transcrustal alkaline-silicate magmatic systems? Is there an important role for country-rock assimilation?
4. What are the processes that result in some alkaline-silicate systems being apparently short-lived, while others remain intermittently active, potentially for millions of years, preserving multiple stages of magma intrusion or volcanism?
5. What is the relationship between depth of emplacement and mineralization in alkaline-silicate intrusions? What influence does depth have on the extent of autometasomatism and on the retention of the metal budget within the intrusion versus that expelled into country rocks?

6. What is the relationship between fenite metasomatic aureoles and their parent intrusive bodies? Can the extent, mineralogy, or geochemistry of fenite alteration be used to indicate metal tenor in the parent intrusion?

Effective study of these and other problems will require integration of diverse approaches. These include the geochemical and mineralogical studies that have thus far been a major focus in alkaline systems, as well as experimental work on the thermodynamics of alkaline magmas, fluids, and metal transport mechanisms, field-based geochemical and geophysical studies, and the assembly and interrogation of global-scale geochemical and geophysical databases. Better and more detailed documentation of geologic relationships is required at all scales, but especially related to structure on the regional to district scale. The acquisition of this spatial data will allow for better targeting of laboratory studies and will hopefully clarify both the evolutionary histories of alkaline-silicate REE-HFSE systems and the fundamental controls on the formation of large and high-grade mineralization.

Acknowledgments

This research was supported by the HiTech AlkCarb project, funded through the European Union Horizon 2020 research and innovation program (689909). We thank the consortium members and expert councillors who imparted a wealth of knowledge through engaging debates and vigorous discussions, in particular Graham Banks, Michael Marks, Alan Woolley, Wei Chen, Janine Kavanagh, Anne McCaffrey, Paul Nex, Martin P. Smith, and Philip Verplanck. We also thank our hosts at field sites visited during the project, particularly Sam Broom-Fendley, Branko Corner, and Scott Swinden. Calum Ritchie is thanked for constructing the 3-D PDF geologic model. The manuscript has further benefited from discussions with Eva Marquis, Volker Möller, Nicholas Arndt, and Sebastian Tappe. We thank Olga Vasyukova, Stefano Salvi, Iain Samson, and Pierre Josso for their clear and insightful reviews, and the *Economic Geology* associate editor, AE "Willy" Williams-Jones. CDB, KMG, and EAD publish with the permission of the executive director of the British Geological Survey.

REFERENCES

Ablay, G.J., Carroll, M.R., Palmer, M.R., Martí, J., and Sparks, R.S.J., 1998, Basanite-phonolite lineages of the Teide-Pico Viejo Volcanic Complex, Tenerife, Canary Islands: Journal of Petrology, v. 39, p. 905–936, doi: 10.1093/petroj/39.5.905.

Acocella, V., Korme, T., Salvini, F., and Funiciello, R., 2003, Elliptic calderas in the Ethiopian rift: Control of pre-existing structures: Journal of Volcanology and Geothermal Research, v. 119, p. 189–203, doi: 10.1016/s0377-0273(02)00342-6.

Adam, J., and Green, T., 2006, Trace element partitioning between mica and amphibole-bearing garnet lherzolite and hydrous basanitic melt: 1. Experimental results and the investigation of controls on partitioning behaviour: Contributions to Mineralogy and Petrology, v. 152, p. 1–17, doi: 10.1007/s00410-006-0085-4.

Aja, S.U., Wood, S.A., and Williams-Jones, A.E., 1995, The aqueous geochemistry of Zr and the solubility of some Zr-bearing minerals: Applied Geochemistry, doi: 10.1016/0883-2927(95)00026-7.

Al Ani, T., and Sarapää, O., 2009, Rare earth elements and their mineral phases in Jammi carbonatite veins and fenites on the south side of Sokli Carbonatite Complex, NE Finland: Geological Survey of Finland, Report M19, 30 p., http://tupa.gtk.fi/raportti/arkisto/m19_4723_2009_34.pdf.

Ali, S.H., 2014, Social and environmental impact of the rare earth industries: Resources, v. 3, p. 123–134, doi: 10.3390/resources3010123.

Alonso, E., Sherman, A.M., Wallington, T.J., Everson, M.P., Field, F.R., Roth, R., and Kirchain, R.E., 2012, Evaluating rare earth element availability: A case with revolutionary demand from clean technologies: Environmental Science and Technology, v. 46, p. 3406–3414, doi: 10.1021/es203518d.

Alvey, A., Roberts, A., and Kusznir, N., 2018, What is the thickness of Earth's crust?: Geoscientist, v. 28, p. 10–15, doi: 10.1144/geosci2018-003.

Andersen, T., and Friis, H., 2014, The transition from agpaitic to hyperagpaitic magmatic crystallization in the Ilímaussaq Alkaline Complex, South Greenland: Journal of Petrology, v. 56, p. 1343–1364, doi: 10.1093/petrology/egv039.

Andersen, T., Erambert, M., Larsen, A.O., and Selbekk, R.S., 2010, Petrology of nepheline syenite pegmatites in the Oslo rift, Norway: Zirconium silicate mineral assemblages as indicators of alkalinity and volatile fugacity in mildly agpaitic magma: Journal of Petrology, v. 51, p. 2303–2325, doi: 10.1093/petrology/egq058.

Andersen, T., Elburg, M., and Erambert, M., 2017, The miaskitic-to-agpaitic transition in peralkaline nepheline syenite (white foyaite) from the Pilanesberg Complex, South Africa: Chemical Geology, v. 455, p. 166–181, doi: 10.1016/j.chemgeo.2016.08.020.

Anenburg, M., 2020, Rare earth mineral diversity controlled by REE pattern shapes: Mineralogical Magazine, v. 84, p. 629–639, doi: 10.1180/mgm.2020.70.

Arndt, N., and Davaille, A., 2013, Episodic Earth evolution: Tectonophysics, v. 609, p. 661–674, doi: 10.1016/j.tecto.2013.07.002.

Arndt, N.T., Czamanske, G.K., Wooden, J.L., and Fedorenko, V.A., 1993, Mantle and crustal contributions to continental flood volcanism: Tectonophysics, v. 223, p. 39–52, doi: 10.1016/0040-1951(93)90156-E.

Arndt, N.T., Fontboté, L., Hedenquist, J.W., Kesler, S.E., Thompson, J.F., and Wood, D.G., 2017, Future global mineral resources: Geochemical Perspectives, v. 6, p. 1–171, doi: 10.7185/geochempersp.6.1.

Arzamastsev, A.A., Arzamastseva, L.V., and Zaraiskii, G.P., 2011, Contact interaction of agpaitic magmas with basement gneisses: An example of the Khibina and Lovozero Massifs: Petrology, v. 19, p. 109–133, doi: 10.1134/s0869591111020032.

Aseri, A.A., Linnen, R.L., Che, X.D., Thibault, Y., and Holtz, F., 2015, Effects of fluorine on the solubilities of Nb, Ta, Zr and Hf minerals in highly fluxed water-saturated haplogranitic melts: Ore Geology Reviews, v. 64, p. 736–746, doi: 10.1016/j.oregeorev.2014.02.014.

Atanasova, P., Marks, M.A.W., Heinig, T., Krause, J., Gutzmer, J., and Markl, G., 2017, Distinguishing magmatic and metamorphic processes in peralkaline rocks of the Norra Kärr Complex (southern Sweden) using textural and compositional variations of clinopyroxene and eudialyte group minerals: Journal of Petrology, v. 58, p. 361–384, doi: 10.1093/petrology/egx019.

Aulbach, S., Griffin, W.L., Pearson, N.J., and O'Reilly, S.Y., 2013, Nature and timing of metasomatism in the stratified mantle lithosphere beneath the central Slave craton (Canada): Chemical Geology, v. 352, p. 153–169, doi: 10.1016/j.chemgeo.2013.05.037.

Baier, J., Audétat, A., and Keppler, H., 2008, The origin of the negative niobium tantalum anomaly in subduction zone magmas: Earth and Planetary Science Letters, v. 267, p. 290–300, doi: 10.1016/j.epsl.2007.11.032.

Bailey, J.C., Gwozdz, R., Rose-Hansen, J., and Sørensen, H., 2001, Geochemical overview of the Ilímaussaq Alkaline Complex, South Greenland: Geology of Greenland Survey, Bulletin 190, p. 35–53.

Bailie, R., and Robb, L., 2004, Polymetallic mineralization in the granites of the Bushveld Complex—examples from the central southeastern lobe: South African Journal of Geology, v. 107, p. 633–652, doi: 10.2113/gssajg.107.4.633.

Ballinger, B., Schmeda-Lopez, D., Kefford, B., Parkinson, B., Stringer, M., Greig, C., and Smart, S., 2020, The vulnerability of electric-vehicle and wind turbine supply chains to the supply of rare-earth elements in a 2-degree scenario: Sustainable Production and Consumption, v. 22, p. 68–76, doi: 10.1016/j.spc.2020.02.005.

Banks, G.J., Walter, B.F., Marks, M.A.W., and Siegfried, P.R., 2019, A workflow to define, map and name a carbonatite- or alkaline igneous-associated REE-HFSE mineral system: A case study from SW Germany: Minerals, v. 9, article 28, doi: 10.3390/min9020097.

Banks, G.J., Olsen, S.D., and Gusak, A., 2020, A method to evaluate REEHFSE mineralised provinces by value creation potential, and an example of application: Gardar REE-HFSE province, Greenland: Geoscience Frontiers, v. 11, p. 2141–2156, doi: 10.1016/j.gsf.2020.05.019.

Bao, Z., and Zhao, Z., 2008, Geochemistry of mineralization with exchangeable REY in the weathering crusts of granitic rocks in South China: Ore Geology Reviews, v. 33, p. 519–535, doi: 10.1016/j.oregeorev.2007.03.005.

Barnes, S.J., and Lightfoot, P.C., 2005, Formation of magmatic nickel-sulfide ore deposits and processes affecting their copper and platinum-group element contents: Economic Geology 100th Anniversary Volume, p. 179–213, doi: 10.5382/AV100.08.

Barros De Oliveira, S.M., and Liguori Imbernon, R.A., 1998, Weathering alteration and related REE concentration in the Catalao I Carbonatite Complex, central Brazil: Journal of South American Earth Sciences, v. 11, p. 379–388, doi: 10.1016/S0895-9811(98)00024-8.

Bartels, A., Nielsen, T.F.D., Lee, S.R., and Upton, B.G.J., 2015, Petrological and geochemical characteristics of Mesoproterozoic dyke swarms in the Gardar province, South Greenland: Evidence for a major subcontinental lithospheric mantle component in the generation of the magmas: Mineralogical Magazine, v. 79, p. 909–939, doi: 10.1180/minmag.2015.079.4.04.

Barth, M.G., McDonough, W.F., and Rudnick, R.L., 2000, Tracking the budget of Nb and Ta in the continental crust: Chemical Geology, v. 165, p. 197–213, doi: 10.1016/S0009-2541(99)00173-4.

Bastow, I.D., Nyblade, A.A., Stuart, G.W., Rooney, T.O., and Benoit, M.H., 2008, Upper mantle seismic structure beneath the Ethiopian hot spot: Rifting at the edge of the African low-velocity anomaly: Geochemistry, Geophysics, Geosystems, v. 9, Q12022, doi: 10.1029/2008GC002107.

Battsengel, A., Batnasan, A., Narankhuu, A., Haga, K., Watanabe, Y., and Shibayama, A., 2018, Recovery of light and heavy rare earth elements from apatite ore using sulphuric acid leaching, solvent extraction and precipitation: Hydrometallurgy, v. 179, p. 100–109, doi: 10.1016/j.hydromet.2018.05.024.

Beard, C.D., Scoates, J.S., Weis, D., Bédard, J.H., and Dell'Oro, T.A., 2017, Geochemistry and origin of the Neoproterozoic Natkusiak flood basalts and related Franklin sills, Victoria Island, Arctic Canada: Journal of Petrology, v. 58, p. 2191–2220, doi: 10.1093/petrology/egy004.

Beard, C.D., van Hinsberg, V.J., Stix, J., and Wilke, M., 2019, Clinopyroxene/melt trace element partitioning in sodic alkaline magmas: Journal of Petrology, v. 60, p. 1797–1823, doi: 10.1093/petrology/egz052.

Beard, C.D., van Hinsberg, V.J., Stix, J., and Wilke, M., 2020, The effect of fluorine on clinopyroxene/melt trace-element partitioning: Contributions to Mineralogy and Petrology, v. 5, doi: 10.1007/s00410-020-1672-5.

Beccaluva, L., Coltorti, M., Di Girolamo, P., Melluso, L., Milani, L., Morra, V., and Siena, F., 2002, Petrogenesis and evolution of Mt. Vulture alkaline volcanism (southern Italy): Mineralogy and Petrology, v. 74, p. 277–297, doi: 10.1007/s007100200007.

Bédard, J.H., Francis, D.M., and Ludden, J., 1988, Petrology and pyroxene chemistry of Monteregian dykes: The origin of concentric zoning and green cores in clinopyroxenes from alkali basalts and lamprophyres: Canadian Journal of Earth Sciences, v. 25, p. 2041–2058, doi: 10.1139/e88-190.

Bédard, J.H., Harris, L.B., and Thurston, P.C., 2013, The hunting of the snArc: Precambrian Research, v. 229, p. 20–48, doi: 10.1016/j.precamres.2012.04.001.

Bedini, E., and Rasmussen, T.M., 2018, Use of airborne hyperspectral and gamma-ray spectroscopy data for mineral exploration at the Sarfartoq Carbonatite Complex, southern West Greenland: Geosciences Journal, v. 22, p. 641–651, doi: 10.1007/s12303-017-0078-5.

Bell, K., and Simonetti, A., 2010, Source of parental melts to carbonatites—critical isotopic constraints: Mineralogy and Petrology, v. 98, p. 77–89, doi: 10.1007/s00710-009-0059-0.

Bennett, R.A., Wernicke, B.P., Niemi, N.A., Friedrich, A.M., and Davis, J.L., 2003, Contemporary strain rates in the northern Basin and Range province from GPS data: Tectonics, v. 22, doi: 10.1029/2001TC001355.

Bernard, C., Estrade, G., Salvi, S., Béziat, D., and Smith, M., 2020, Alkali pyroxenes and amphiboles: A window on rare earth elements and other high field strength elements behavior through the magmatic-hydrothermal transition of peralkaline granitic systems: Contributions to Mineralogy and Petrology, v. 175, p. 1–27, doi: 10.1007/s00410-020-01723-y.

Berry, D.A., 2012, Cryolite, the Canadian aluminium industry and the American occupation of Greenland during the Second World War: The Polar Journal, v. 2, p. 219–235, doi: 10.1080/2154896x.2012.735037.

Binnemans, K., Jones, P.T., Blanpain, B., Van Gerven, T., Yang, Y., Walton, A., and Buchert, M., 2013, Recycling of rare earths: A critical review: Journal of Cleaner Production, v. 51, p. 1–22, doi: 10.1016/j.jclepro.2012.12.037.

Binnemans, K., Jones, P.T., Müller, T., and Yurramendi, L., 2018, Rare earths and the balance problem: How to deal with changing markets?: Journal of Sustainable Metallurgy, v. 4, p. 126–146, doi: 10.1007/s40831-018-0162-8.

Black, R., Lameyre, J., and Bonin, B., 1985, The structural setting of alkaline complexes: Journal of African Earth Sciences (1983), v. 3, p. 5–16, doi: 10.1016/0899-5362(85)90019-3.

Blundell, D.J., 1978, A gravity survey across the Gardar igneous province, SW Greenland: Journal of the Geological Society, v. 135, p. 545–554.

Boehnke, P., Watson, E.B., Trail, D., Harrison, T.M., and Schmitt, A.K., 2013, Zircon saturation re-revisited: Chemical Geology, v. 351, p. 324–334, doi: 10.1016/j.chemgeo.2013.05.028.

Boesche, N.K., Rogass, C., Lubitz, C., Brell, M., Herrmann, S., Mielke, C., Tonn, S., Appelt, O., Altenberger, U., and Kaufmann, H., 2015, Hyperspectral REE (rare earth element) mapping of outcrops—applications for neodymium detection: Remote Sensing, v. 7, p. 5160–5186, doi: 10.3390/rs70505160.

Bohse, H., Brooks, C., and Kunzendorf, H., 1971, Field observations on the kakortokites of the Ilimaussaq intrusion, South Greenland, including mapping and analyses by portable X-ray fluorescence equipment for zirconium and niobium: Grønlands Geologiske Undersøgelse, Rapport 38, 43 p., https://web.archive.org/web/20210605000436id_/https://geusbulletin.org/index.php/rapggu/article/download/7278/13148.

Bonin, B., 2004, Do coeval mafic and felsic magmas in post-collisional to within-plate regimes necessarily imply two contrasting, mantle and crustal, sources? A review: Lithos, v. 78, p. 1–24, doi: doi.org/10.1016/j.lithos.2004.04.042.

Booysen, R., Jackisch, R., Lorenz, S., Zimmermann, R., Kirsch, M., Nex, P.A., and Gloaguen, R., 2020, Detection of REEs with lightweight UAV based hyperspectral imaging: Scientific Reports, v. 10, p. 0–12, doi: 10.1038/s41598-020-74422-0.

Borst, A.M., Friis, H., Andersen, T., Nielsen, T.F.D., Waight, T.E., and Smit, M.A., 2016, Zirconosilicates in the kakortokites of the Ilímaussaq Complex, South Greenland: Implications for fluid evolution and high-field-strength and rare-earth element mineralization in agpaitic systems: Mineralogical Magazine, v. 80, p. 5–30, doi: 10.1180/minmag.2016.080.046.

Borst, A.M., Friis, H., Nielsen, T.F., and Waight, T.E., 2018, Bulk and mush melt evolution in agpaitic intrusions: Insights from compositional zoning in eudialyte, Ilímaussaq Complex, South Greenland: Journal of Petrology, v. 59, p. 589–612, doi: 10.1093/petrology/egy038.

Borst, A.M., Waight, T., Finch, A., Storey, M., and Roux, P.L., 2019, Dating agpaitic rocks: A multi-system (U/Pb, Sm/Nd, Rb/Sr and $^{40}Ar/^{39}Ar$) isotopic study of layered nepheline syenites from the Ilímaussaq Complex, Greenland: Lithos, v. 324–325, p. 74–88, doi: 10.1016/j.lithos.2018.10.037.

Borst, A.M., Smith, M.P., Finch, A.A., Estrade, G., Villanova-de Benavent, C., Nason, P., Marquis, E., Horsburgh, N.J., Goodenough, K.M., Xu, C., Kynický, J., and Geraki, K., 2020, Adsorption of rare earth elements in regolith-hosted clay deposits: Nature Communications, v. 11, p. 1–15, doi: 10.1038/s41467-020-17801-5.

Brantut, N., Heap, M.J., Meredith, P.G., and Baud, P., 2013, Time-dependent cracking and brittle creep in crustal rocks: A review: Journal of Structural Geology, v. 52, p. 17–43, doi: 10.1016/j.jsg.2013.03.007.

Brauch, K., Pohl, C., Symons, G., and Tauchnitz, M., 2018, Paper on instrument tests and best practice for carbonatites and alkaline rocks: Deliverable D4.2 for the HiTech AlkCarb project, Terratec Geophysical Services, Heitersheim, Germany, 478 p., doi: 10.13140/RG.2.2.18235.08487.

Braunger, S., Marks, M.A., Wenzel, T., Chmyz, L., Guitarrari Azzone, R., and Markl, G., 2020, Do carbonatites and alkaline rocks reflect variable redox conditions in their upper mantle source?: Earth and Planetary Science Letters, v. 533, article 116041, doi: 10.1016/j.epsl.2019.116041.

Brito, P., Prego, R., Mil-Homens, M., Caçador, I., and Caetano, M., 2018, Sources and distribution of yttrium and rare earth elements in surface sediments from Tagus estuary, Portugal: Science of the Total Environment, v. 621, p. 317–325, doi: 10.1016/j.scitotenv.2017.11.245.

Brooks, C.K., and Nielsen, T.F.D., 1982, The E Greenland continental margin: A transition between oceanic and continental magmatism: Journal of the Geological Society, London, v. 139, p. 265–275, doi: 10.1144/gsjgs.139.3.0265.

Broom-Fendley, S., Brady, A.E., Horstwood, M.S., Woolley, A.R., Mtegha, J., Wall, F., Dawes, W., and Gunn, G., 2017, Geology, geochemistry and geochronology of the Songwe Hill carbonatite, Malawi: Journal of African Earth Sciences, v. 134, p. 10–23, doi: 10.1016/j.jafrearsci.2017.05.020.

Broom-Fendley, S., Siegfried, P.R., Wall, F., O'Neill, M., Brooker, R.A., Fallon, E.K., Pickles, J.R., and Banks, D.A., 2020, The origin and composition of carbonatite-derived carbonate-bearing fluorapatite deposits: Mineralium Deposita, v. 56, p. 863–884, doi: 10.1007/s00126-020-01010-7.

Broom-Fendley, S., Elliott, H.A., Beard, C.D., Wall, F., Armitage, P.E., Brady, A.E., Deady, E., and Dawes, W., 2021, Enrichment of heavy REE

and Th in carbonatite-derived fenite breccia: Geological Magazine, doi: 10.1017/S0016756821000601.

Brown, R., Summerfield, M., Gleadow, A., Gallagher, K., Carter, A., Beucher, R., and Wildman, M., 2014, Intracontinental deformation in southern Africa during the Late Cretaceous: Journal of African Earth Sciences, v. 100, p. 20–41, doi: 10.1016/j.jafrearsci.2014.05.014.

Brown, T., Idoine, N., Raycraft, E., Hobbs, S., Shaw, R., Everett, P., Kresse, C., Deady, E., and Bide, T., 2019, World mineral production 2013–17: British Geological Survey, Technical Report, doi: 10.1002/anie.201605417.

Brune, S., Heine, C., Pérez-Gussinyé, M., and Sobolev, S.V., 2014, Rift migration explains continental margin asymmetry and crustal hyperextension: Nature Communications, v. 5, article 4014, doi: 10.1038/ncomms5014.

Burke, K., Ashwal, L.D., and Webb, S.J., 2003, New way to map old sutures using deformed alkaline rocks and carbonatites: Geology, v. 31, p. 391–394, doi: 10.1130/0091-7613(2003)031<0391:NWTMOS>2.0.CO;2.

Castor, S.B., 2008, The Mountain Pass rare-earth carbonatite and associated ultrapotassic rocks, California: The Canadian Mineralogist, v. 46, p. 779–806, doi: 10.3749/canmin.46.4.779.

Cawood, P.A., and Hawkesworth, C.J., 2015, Temporal relations between mineral deposits and global tectonic cycles: Geological Society, London, Special Publication 393, p. 9–21, doi: 10.1144/SP393.1.

Cawthorn, R.G., 2015, The geometry and emplacement of the Pilanesberg Complex, South Africa: Geological Magazine, v. 152, p. 802–812, doi: 10.1017/S0016756814000764.

Chakhmouradian, A.R., and Wall, F., 2012, Rare earth elements: Minerals, mines, magnets (and more): Elements, v. 8, p. 333–340, doi: 10.2113/gselements.8.5.333.

Chakhmouradian, A.R., and Zaitsev, A.N., 2012, Rare earth mineralization in igneous rocks: Sources and processes: Elements, v. 8, p. 347–353, doi: 10.2113/gselements.8.5.347.

Chakrabarty, A., Mitchell, R.H., Ren, M., Saha, P.K., Pal, S., Pruseth, K.L., and Sen, A.K., 2016, Magmatic, hydrothermal and subsolidus evolution of the agpaitic nepheline syenites of the Sushina Hill Complex, India: Implications for the metamorphism of peralkaline syenites: Mineralogical Magazine, v. 80, p. 1161–1193, doi: 10.1180/minmag.2016.080.057.

Chakrabarty, A., Mitchell, R.H., Ren, M., Pal, S., Pal, S., and Sen, A.K., 2018, Nb-Zr-REE re-mobilization and implications for transitional agpaitic rock formation: Insights from the Sushina Hill Complex, India: Journal of Petrology, v. 59, p. 1899–1938, doi: 10.1093/petrology/egy084.

Chauvel, C., Hofmann, A.W., and Vidal, P., 1992, HIMU-EM: The French Polynesian connection: Earth and Planetary Science Letters, v. 110, p. 99–119.

Chen, W., and Simonetti, A., 2015, Isotopic (Pb, Sr, Nd, C, O) evidence for plume-related sampling of an ancient, depleted mantle reservoir: Lithos, v. 216–217, p. 81–92, doi: 10.1016/j.lithos.2014.11.024.

Clowes, R.M., 2010, Initiation, development, and benefits of Lithoprobe—shaping the direction of Earth science research in Canada and beyond: Canadian Journal of Earth Sciences, v. 47, p. 291–314, doi: 10.1139/E09-074.

Cole, J.W., Milner, D.M., and Spinks, K.D., 2005, Calderas and caldera structures: A review: Earth-Science Reviews, v. 69, p. 1–26, doi: 10.1016/j.earscirev.2004.06.004.

Condie, K.C., 2016, The mantle, *in* Earth an as evolving planetary system, 3rd ed.: Elsevier, p. 89–133, doi: 10.1016/B978-0-12-803689-1.00004-3.

Costi, H.T., Dall'Agnol, R., Pichavant, M., and Rämö, O.T., 2009, The peralkaline tin-mineralized madeira cryolite albite-rich granite of Pitinga, Amazonian craton, Brazil: Petrography, mineralogy and crystallization processes: The Canadian Mineralogist, v. 47, p. 1301–1327, doi: 10.3749/canmin.47.6.1301.

Coumans, J.P., and Stix, J., 2016, Caldera collapse at near-ridge seamounts: An experimental investigation: Bulletin of Volcanology, v. 78, p. 70, doi: 10.1007/s00445-016-1065-9.

Couzinié, S., Laurent, O., Moyen, J.F., Zeh, A., Bouilhol, P., and Villaros, A., 2016, Post-collisional magmatism: Crustal growth not identified by zircon Hf-O isotopes: Earth and Planetary Science Letters, v. 456, p. 182–195, doi: 10.1016/j.epsl.2016.09.033.

Cox, C., and Kynicky, J., 2018, The rapid evolution of speculative investment in the REE market before, during, and after the rare earth crisis of 2010–2012: The Extractive Industries and Society, v. 5, p. 8–17, doi: 10.1016/j.exis.2017.09.002.

Cox, K.G., and Hawkesworth, C.J., 1985, Geochemical stratigraphy of the Deccan Traps at Mahabaleshwar, Western Ghats, India, with implications for open system magmatic processes: Journal of Petrology, v. 26, p. 355–377, doi: 10.1093/petrology/26.2.355.

Dahle, J.T., and Arai, Y., 2015, Environmental geochemistry of cerium: Applications and toxicology of cerium oxide nanoparticles: International Journal of Environmental Research and Public Health, v. 12, no. 2, p. 1253–1278, doi: 10.3390/ijerph120201253.

Dauphas, N., and Marty, B., 1999, Heavy nitrogen in carbonatites of the Kola Peninsula: A possible signature of the deep mantle: Science, v. 286, p. 2488–2490.

Davris, P., Stopic, S., Balomenos, E., Panias, D., Paspaliaris, I., and Friedrich, B., 2017, Leaching of rare earth elements from eudialyte concentrate by suppressing silica gel formation: Minerals Engineering, v. 108, p. 115–122, doi: 10.1016/j.mineng.2016.12.011.

Deady, E., Lacinska, A., Goodenough, K., Shaw, R., and Roberts, N., 2019, Volcanic-derived placers as a potential resource of rare earth elements: The Aksu Diamas case study, Turkey: Minerals, v. 9, article 208, doi: 10.3390/min9040208.

Decrée, S., Boulvais, P., Cobert, C., Baele, J.M., Midende, G., Gardien, V., Tack, L., Nimpagaritse, G., and Demaiffe, D., 2015, Structurally controlled hydrothermal alteration in the syntectonic Neoproterozoic Upper Ruvubu Alkaline Plutonic Complex (Burundi): Implications for REE and HFSE mobilities: Precambrian Research, v. 269, p. 281–295, doi: 10.1016/j.precamres.2015.08.016.

Delavault, H., Chauvel, C., Thomassot, E., Devey, C.W., and Dazas, B., 2016, Sulfur and lead isotopic evidence of relic Archean sediments in the Pitcairn mantle plume: Proceedings of the National Academy of Sciences, v. 113, p. 12952–12956, doi: 10.1073/pnas.1523805113.

Demol, J., Ho, E., Soldenhoff, K., and Senanayake, G., 2019, The sulfuric acid bake and leach route for processing of rare earth ores and concentrates: A review: Hydrometallurgy, v. 188, p. 123–139, doi: 10.1016/j.hydromet.2019.05.015.

Dewey, J.F., and Burke, K., 1974, Hot spots and collisional breakup: Implications for collisional orogeny: Geology, v. 2, p. 57–60, doi: 10.1130/0091-7613(1974)2<57:HSACBI>2.0.CO;2.

Dhuime, B., Hawkesworth, C.J., Cawood, P.A., and Storey, C.D., 2012, A change in the geodynamics of continental growth 3 billion years ago: Science, v. 335, p. 1334–1336, doi: 10.1126/science.1216066.

Dhuime, B., Wuestefeld, A., and Hawkesworth, C.J., 2015, Emergence of modern continental crust about 3 billion years ago: Nature Geoscience, v. 8, p. 552–555, doi: 10.1038/ngeo2466.

dos Santos, R.P.Z., Mantovani, M.S.M., and Marangoni, Y.R., 2019, Geophysical modeling of Serra Negra and Salitre I, II and III alkaline-carbonatite complexes based on their gravimetric and magnetic signatures: International Congress of the Brazilian Geophysical Society, 16th, Rio de Janiero, 2019, Proceedings, p. 6.

Dostal, J., 2016, Rare metal deposits associated with alkaline/peralkaline igneous rocks: Reviews in Economic Geology, v. 18, p. 33–54, doi: 10.5382/Rev.18.02.

——2017, Rare earth element deposits of alkaline igneous rocks: Resources, v. 6, p. 1–12, doi: 10.3390/resources6030034.

Dostal, J., Kontak, D.J., and Karl, S.M., 2014, The Early Jurassic Bokan Mountain peralkaline granitic complex (southeastern Alaska): Geochemistry, petrogenesis and rare-metal mineralization: Lithos, v. 202–203, p. 395–412, doi: 10.1016/j.lithos.2014.06.005.

Dowman, E., Wall, F., Treloar, P.J., Rankin, A.H., and Corkhill, C., 2017, Rare earth mobility as a result of multiple phases of fluid activity in fenite around the Chilwa Island carbonatite, Malawi: Mineralogical Magazine, v. 81, p. 1367–1395, doi: 10.1180/minmag.2017.081.007.

Downes, H., Balaganskaya, E., Beard, A., Liferovich, R., and Demaiffe, D., 2005, Petrogenetic processes in the ultramafic, alkaline and carbonatitic magmatism in the Kola alkaline province: A review: Lithos, v. 85, p. 48–75, doi: 10.1016/j.lithos.2005.03.020.

Downs, R.T., 2006, The RRUFF project: An integrated study of the chemistry, crystallography, Raman and infrared spectros copy of minerals: General Meeting of the International Mineralogical Association, 19th, Kobe, Japan, 2006, Program and Abstracts.

Ebinger, C.J., and Sleep, N.H., 1998, Cenozoic magmatism throughout east Africa resulting from impact of a single plume: Nature, v. 395, p. 788–791.

Eby, G.N., 1984, Monteregian Hills I. Petrography, major and trace element geochemistry, and strontium isotopic chemistry of the western intrusions: Mounts Royal, St. Bruno, and Johnson: Journal of Petrology, v. 25, p. 421–452, doi: 10.1093/petrology/25.2.421.

——1987, The Monteregian Hills and White Mountain alkaline igneous provinces, eastern North America: Geological Society, London, Special Publication 30, p. 433–447, doi: 10.1144/GSL.SP.1987.030.01.21.

Edahbi, M., Benzaazoua, M., Plante, B., Doire, S., and Kormos, L., 2018, Mineralogical characterization using QEMSCAN® and leaching potential study of REE within silicate ores: A case study of the Matamec project, Québec, Canada: Journal of Geochemical Exploration, v. 185, p. 64–73, doi: 10.1016/j.gexplo.2017.11.007.

Elburg, M.A., and Cawthorn, R.G., 2017, Source and evolution of the alkaline Pilanesberg Complex, South Africa: Chemical Geology, v. 455, p. 148–165, doi: 10.1016/j.chemgeo.2016.10.007.

Elliott, H.A., Wall, F., Chakhmouradian, A.R., Siegfried, P.R., Dahlgren, S., Weatherley, S., Finch, A.A., Marks, M.A., Dowman, E., and Deady, E., 2018, Fenites associated with carbonatite complexes: A review: Ore Geology Reviews, v. 93, p. 38–59, doi: 10.1016/j.oregeorev.2017.12.003.

Elliott, T., Plank, T., Zindler, A., White, W., and Bourdon, B., 1997, Element transport from slab to volcanic front at the Mariana arc: Journal of Geophysical Research: Solid Earth, v. 102, p. 14,991–15,019, doi: 10.1029/97JB00788.

Epshteyn, Y.M., and Kaban'kov, V.Y., 1984, The depth of emplacement and mineral potential of ultramafic, ijolite, and carbonatite plutons: International Geology Review: v. 26, p. 1402–1415, doi: 10.1080/00206818409466660.

Ernst, R.E., 2014, Large igneous provinces: Cambridge University Press, 667 p.

Ernst, R.E., and Bell, K., 2010, Large igneous provinces (LIPs) and carbonatites: Mineralogy and Petrology, v. 98, p. 55–76, doi: 10.1007/s00710-009-0074-1.

Ernst, R.E., and Bleeker, W., 2010, Large igneous provinces (LIPs), giant dyke swarms, and mantle plumes: Significance for breakup events within Canada and adjacent regions from 2.5 Ga to the present: Canadian Journal of Earth Sciences, v. 47, p. 695–739, doi: 10.1139/E10-025.

Estrade, G., Béziat, D., Salvi, S., Tiepolo, M., Paquette, J.L.L., and Rakotovao, S., 2014a, Unusual evolution of silica-under- and -oversaturated alkaline rocks in the Cenozoic Ambohimirahavavy Complex (Madagascar): Mineralogical and geochemical evidence: Lithos, v. 206, p. 361–383, doi: 10.1016/j.lithos.2014.08.008.

Estrade, G., Salvi, S., Béziat, D., Rakotovao, S., and Rakotondrazafy, R., 2014b, REE and HFSE mineralization in peralkaline granites of the Ambohimirahavavy Alkaline Complex, Ampasindava peninsula, Madagascar: Journal of African Earth Sciences, v. 94, p. 141–155, doi: 10.1016/j.jafrearsci.2013.06.008.

Estrade, G., Salvi, S., Béziat, D., and Williams-Jones, A.E., 2015, The origin of skarn-hosted rare-metal mineralization in the Ambohimirahavavy Alkaline Complex, Madagascar: Economic Geology, v. 110, p. 1485–1513, doi: 10.2113/econgeo.110.6.1485.

Estrade, G., Marquis, E., Smith, M., Goodenough, K., and Nason, P., 2019, REE concentration processes in ion adsorption deposits: Evidence from the Ambohimirahavavy Alkaline Complex in Madagascar: Ore Geology Reviews, v. 112, article 103027, doi: 10.1016/j.oregeorev.2019.103027.

European Commission, 2020, Critical materials for strategic technologies and sectors in the EU—a foresight study: European Union, Technical Report, doi: 10.2873/58081.

Falster, A.U., Simmons, W.B., Webber, K.L., and Boudreaux, A.P., 2018, Mineralogy and geochemistry of the Erongo sub-volcanic granite miarolitic-pegmatite complex, Erongo, Namibia: The Canadian Mineralogist, v. 56, p. 425–449, doi: 10.3749/canmin.1700090.

Féménias, O., Coussaert, N., Brassinnes, S., and Demaiffe, D., 2005, Emplacement processes and cooling history of layered cyclic unit II-7 from the Lovozero alkaline massif (Kola Peninsula, Russia): Lithos, v. 83, p. 371–393, doi: 10.1016/j.lithos.2005.03.012.

Feng, Y., and Samson, I.M., 2015, Replacement processes involving high field strength elements in the T zone, Thor Lake rare-metal deposit: The Canadian Mineralogist, v. 53, p. 31–60, doi: 10.3749/canmin.1400028.

Ferguson, J., 1964, Geology of the Ilímaussaq alkaline intrusion, South Greenland: Bulletin Grønlands Geologiske Undersøgelse, v. 39, 82 p.

Finch, A.A., McCreath, J.A., Reekie, C.D., Hutchison, W., Ismaila, A., Armour-Brown, A., Andersen, T., and Simonsen, S.L., 2019, From mantle to Motzfeldt: A genetic model for syenite-hosted Ta,Nb-mineralisation: Ore Geology Reviews, v. 107, p. 402–416, doi: 10.1016/j.oregeorev.2019.02.032.

Fitton, J.G., and Upton, B.G.J., 1987, Introduction: Geological Society, London, Special Publication 30, p. ix-xiv, doi: 10.1144/gsl.sp.1987.030.01.01.

Foley, S.F., and Fischer, T.P., 2017, An essential role for continental rifts and lithosphere in the deep carbon cycle: Nature Geoscience, v. 10, p. 897–902, doi: 10.1038/s41561-017-0002-7.

Frolov, A., 1971, Vertical zonation in deposition of ore, as in ultrabasic alkaline rocks and carbonatites: International Geology Review, v. 13, p. 685–695, doi: 10.1080/00206817109475486.

Furman, T., Nelson, W.R., and Elkins-Tanton, L.T., 2016, Evolution of the East African rift: Drip magmatism, lithospheric thinning and mafic volcanism: Geochimica et Cosmochimica Acta, v. 185, p. 418–434, doi: 10.1016/j.gca.2016.03.024.

García, A., Espinosa, R., Delgado, L., Casals, E., González, E., Puntes, V., Barata, C., Font, X., and Sánchez, A., 2011, Acute toxicity of cerium oxide, titanium oxide and iron oxide nanoparticles using standardized tests: Desalination, v. 269, p. 136–141, doi: 10.1016/j.desal.2010.10.052.

Garcia, M.O., Jorgenson, B.A., Mahoney, J.J., Ito, E., and Irving, A.J., 1993, An evaluation of temporal geochemical evolution of Loihi summit lavas: Results from Alvin submersible dives: Journal of Geophysical Research, v. 98, p. 537–550, doi: 10.1029/92JB01707.

Garson, M.S.S., 1965, Carbonatites in southern Malawi: Bulletin of the Geological Survey of Malawi, v. 15, p. 1–128.

Genge, M.J., Price, G., and Jones, A.P., 1995, Molecular dynamics simulations of $CaCO_3$ melts to mantle pressures and temperatures: Implications for carbonatite magmas: Earth and Planetary Science Letters, v. 131, p. 225–238, doi: 10.1016/0012-821X(95)00020-D.

Gerasimova, L., Nikolaev, A., Maslova, M., Shchukina, E., Samburov, G., Yakovenchuk, V., and Ivanyuk, G., 2018, Titanite ores of the Khibiny apatite-nepheline-deposits: Selective mining, processing and application for titanosilicate synthesis: Minerals, v. 8, article 446, doi: 10.3390/min8100446.

Gibson, C.E., Kelebek, S., and Aghamirian, M., 2015, Niobium oxide mineral flotation: A review of relevant literature and the current state of industrial operations: International Journal of Mineral Processing, v. 137, p. 82–97, doi: 10.1016/j.minpro.2015.02.005.

Giebel, R.J., Parsapoor, A., Walter, B.F., Braunger, S., Marks, M.A.W., Wenzel, T., and Markl, G., 2019, Evidence for magma-wall rock interaction in carbonatites from the Kaiserstuhl Volcanic Complex (southwest Germany): Journal of Petrology, v. 60, p. 1163–1194, doi: 10.1093/petrology/egz028.

Giehl, C., Marks, M., and Nowak, M., 2013, Phase relations and liquid lines of descent of an iron-rich peralkaline phonolitic melt: An experimental study: Contributions to Mineralogy and Petrology, v. 165, p. 283–304, doi: 10.1007/s00410-012-0809-6.

Goldfarb, R.J., and Groves, D.I., 2015, Orogenic gold: Common or evolving fluid and metal sources through time: Lithos, v. 233, p. 2–26, doi: 10.1016/j.lithos.2015.07.011.

Goodenough, K.M., Upton, B.G., and Ellam, R.M., 2000, Geochemical evolution of the Ivigtut granite, South Greenland: A fluorine-rich "A-type" intrusion: Lithos, v. 51, p. 205–221, doi: 10.1016/S0024-4937(99)00064-X.

Goodenough, K.M., Schilling, J., Jonsson, E., Kalvig, P., Charles, N., Tuduri, J., Deady, E.A., Sadeghi, M., Schiellerup, H., Müller, A., et al., 2016, Europe's rare earth element resource potential: An overview of REE metallogenetic provinces and their geodynamic setting: Ore Geology Reviews, v. 72, p. 838–856, doi: 10.1016/j.oregeorev.2015.09.019.

Goodenough, K.M., Wall, F., and Merriman, D., 2018, The rare earth elements: Demand, global resources, and challenges for resourcing future generations: Natural Resources Research, v. 27, p. 201–216, doi: 10.1007/s11053-017-9336-5.

Goodenough, K.M., Deady, E., Beard, C.D., Broom-Fendley, S., Elliott, H.A., van den Berg, F., and Ozturk, H., 2021, Carbonatites and alkaline igneous rocks in post-collisional settings: Storehouses of rare earth elements: Journal of Earth Science, v. 32, p. 1332–1358, doi: 10.1007/s12583-021-1500-5.

Grammatikopoulos, T., Mercer, W., and Gunning, C., 2013, Mineralogical characterisation using QEMSCAN of the Nechalacho heavy rare earth metal deposit, Northwest Territories, Canada: Canadian Metallurgical Quarterly, v. 52, p. 265–277, doi: 10.1179/1879139513Y.0000000090.

Greenland Minerals Ltd, 2015, Statement of identified mineral resources: The Ilímaussaq Complex (JORC-code 2012 compliant): Technical Report.

Grütter, H.S., Gurney, J.J., Menzies, A.H., and Winter, F., 2004, An updated classification scheme for mantle-derived garnet, for use by diamond explorers: Lithos, v. 77, p. 841–857, doi: 10.1016/j.lithos.2004.04.012.

Guo, D., and Liu, Y., 2019, Occurrence and geochemistry of bastnäsite in carbonatite-related REE deposits, Mianning-Dechang REE belt, Sichuan province, SW China: Ore Geology Reviews, v. 107, p. 266–282, doi: 10.1016/j.oregeorev.2019.02.028.

Guzmics, T., Mitchell, R.H., Szabó, C., Berkesi, M., Milke, R., and Ratter, K., 2012, Liquid immiscibility between silicate, carbonate and sulfide melts in melt inclusions hosted in co-precipitated minerals from Kerimasi

volcano (Tanzania): Evolution of carbonated nephelinitic magma: Contributions to Mineralogy and Petrology, v. 164, p. 101–122, doi: 10.1007/s00410-012-0728-6.

Guzmics, T., Berkesi, M., Bodnar, R.J., Fall, A., Bali, E., Milke, R., Vetlényi, E., and Szabó, C., 2019, Natrocarbonatites: A hidden product of three-phase immiscibility: Geology, v. 47, p. 527–530, doi: 10.1130/G46125.1.

Gysi, A.P., and Williams-Jones, A.E., 2013, Hydrothermal mobilization of pegmatite-hosted REE and Zr at Strange Lake, Canada: A reaction path model: Geochimica et Cosmochimica Acta, v. 122, p. 324–352, doi: 10.1016/j.gca.2013.08.031.

Haase, K.M., Beier, C., and Kemner, F., 2019, A comparison of the magmatic evolution of pacific intraplate volcanoes: Constraints on melting in mantle plumes: Frontiers in Earth Science, v. 6, p. 1–13, doi: 10.3389/feart.2018.00242.

Hagemann, S.G., Angerer, T., Duuring, P., Rosière, C.A., Figueiredo e Silva, R.C., Lobato, L., Hensler, A.S., and Walde, D.H.G., 2016, BIF-hosted iron mineral system: A review: Ore Geology Reviews, v. 76, p. 317–359, doi: 10.1016/j.oregeorev.2015.11.004.

Hagni, R.D., 1999, Mineralogy of beneficiation problems involving fluorspar concentrates from carbonatite-related fluorspar deposits: Mineralogy and Petrology, v. 67, p. 33–44, doi: 10.1007/BF01165114.

Harris, C., Marsh, J.S., and Milner, S.C., 1999, Petrology of the alkaline core of the Messum Igneous Complex, Namibia: Evidence for the progressively decreasing effect of crustal contamination: Journal of Petrology, v. 40, p. 1377– 1397, doi: 10.1093/petroj/40.9.1377.

Hedenquist, J.W., Arribas, A., and Gonzalez-Urien, E., 2000, Exploration for epithermal gold deposits: Reviews in Economic Geology, v. 13, p. 45–77.

Herzberg, C., Condie, K., and Korenaga, J., 2010, Thermal history of the Earth and its petrological expression: Earth and Planetary Science Letters, v. 292, p. 79–88, doi: 10.1016/j.epsl.2010.01.022.

Hodgkinson, J.H., and Smith, M.H., 2018, Climate change and sustainability as drivers for the next mining and metals boom: The need for climate-smart mining and recycling: Resources Policy, doi: 10.1016/j.resourpol.2018.05.016.

Honour, V.C., Goodenough, K.M., Shaw, R.A., Gabudianu, I., and Hirtopanu, P., 2018, REE mineralisation within the Ditrău Alkaline Complex, Romania: Interplay of magmatic and hydrothermal processes: Lithos, v. 314–315, p. 360– 381, doi: 10.1016/j.lithos.2018.05.029.

Hou, Z., Tian, S., Xie, Y., Yang, Z., Yuan, Z., Yin, S., Yi, L., Fei, H., Zou, T., Bai, G., and Li, X., 2009, The Himalayan Mianning-Dechang REE belt associated with carbonatite-alkaline complexes, eastern Indo-Asian collision zone, SW China: Ore Geology Reviews, v. 36, p. 65–89, doi: 10.1016/j.oregeorev.2009.03.001.

Hulett, S.R.W., Simonetti, A., Rasbury, E.T., and Hemming, N.G., 2016, Recycling of subducted crustal components into carbonatite melts revealed by boron isotopes: Nature Geoscience, v. 9, p. 904–908, doi: 10.1038/ngeo2831.

Humphreys, E.R., Bailey, K., Hawkesworth, C.J., Wall, F., Najorka, J., and Rankin, A.H., 2010, Aragonite in olivine from Calatrava, Spain: Evidence for mantle carbonatite melts from >100 km depth: Geology, v. 38, p. 911–914, doi: 10.1130/G31199.1.

Humphreys-Williams, E.R., and Zahirovic, S., 2021, Carbonatites and global tectonics: Elements, v. 17, no. 5, p. 339–344.

Hund, K., La Porta, D., Fabregas, T.P., Laing, T., and Drexhage, J., 2020, Minerals for climate action: The mineral intensity of the clean energy transition: World Bank Group, Technical Report.

Hunt, E.J., Finch, A.A., and Donaldson, C.H., 2017, Layering in peralkaline magmas, Ilímaussaq Complex, S Greenland: Lithos, 268–271, p. 1–15, doi: 10.1016/j.lithos.2016.10.023.

Huppert, H.E., and Sparks, R.S.J., 1988, Melting the roof of a chamber containing a hot, turbulently convecting fluid: Journal of Fluid Mechanics, v. 188, p. 107–131, doi: 10.1017/S0022112088000655.

Huston, D.L., Pehrsson, S., Eglington, B.M., and Zaw, K., 2010, The geology and metallogeny of volcanic-hosted massive sulfide deposits: Variations through geologic time and with tectonic setting: Economic Geology, v. 105, p. 571–591, doi: 10.2113/gsecongeo.105.3.571.

Huston, D.L., Maas, R., Cross, A., Hussey, K.J., Mernagh, T.P., Fraser, G., and Champion, D.C., 2016, The Nolans Bore rare-earth element-phosphorus-uranium mineral system: Geology, origin and postdepositional modifications: Mineralium Deposita, v. 51, p. 797–822, doi: 10.1007/s00126-015-0631-y.

Hutchison, W., Fusillo, R., Pyle, D.M., Mather, T.A., Blundy, J.D., Biggs, J., Yirgu, G., Cohen, B.E., Brooker, R.A., Barfod, D.N., and Calvert, A.T., 2016a, A pulse of mid-Pleistocene rift volcanism in Ethiopia at the dawn of modern humans: Nature Communications, v. 7, p. 1–12, doi: 10.1038/ncomms13192.

Hutchison, W., Pyle, D.M., Mather, T.A., Yirgu, G., Biggs, J., Cohen, B.E., Barfod, D.N., and Lewi, E., 2016b, The eruptive history and magmatic evolution of Aluto volcano: New insights into silicic peralkaline volcanism in the Ethiopian rift: Journal of Volcanology and Geothermal Research, v. 328, p. 9–33, doi: 10.1016/j.jvolgeores.2016.09.010.

Hutchison, W., Babiel, R.J., Finch, A.A., Marks, M.A.W., Markl, G., Boyce, A.J., Stüeken, E.E., Friis, H., Borst, A.M., and Horsburgh, N.J., 2019, Sulphur isotopes of alkaline magmas unlock long-term records of crustal recycling on Earth: Nature Communications, v. 10, p. 1–12, doi: 10.1038/s41467-019-12218-1.

Hutchison, W., Finch, A.A., and Boyce, A.J., 2020, The sulfur isotope evolution of magmatic-hydrothermal fluids: Insights into ore-forming processes: Geochimica et Cosmochimica Acta, v. 288, p. 176–198, doi: 10.1016/j.gca.2020.07.042.

Hutchison, W., Finch, A.A., Borst, A.M., Marks, M.A.W., Upton, B.G.J., Zerkle, A.L., Stüeken, E.E., and Boyce, A.J., 2021, Mantle sources and magma evolution in Europe's largest rare earth element belt (Gardar province, SW Greenland): New insights from sulfur isotopes: Earth and Planetary Science Letters, v. 568, article 117034, doi: 10.1016/j.epsl.2021.117034.

Hutton, D.H.W., 1988, Granite emplacement mechanisms and tectonic controls: Inferences from deformation studies: Transactions of the Royal Society of Edinburgh: Earth Sciences, v. 79, p. 245–255, doi: 10.1017/S0263593300014255.

Hutton, D.H.W., and Reavy, R.J., 1992, Strike-slip tectonics and granite petrogenesis: Tectonics, v. 11, p. 960–967.

Huw Davies, J., and von Blanckenburg, F., 1995, Slab breakoff: A model of lithosphere detachment and its test in the magmatism and deformation of collisional orogens: Earth and Planetary Science Letters, v. 129, p. 85–102, doi: 10.1016/0012-821X(94)00237-S.

Iacovino, K., Oppenheimer, C., Scaillet, B., and Kyle, P., 2016, Storage and evolution of mafic and intermediate alkaline magmas beneath Ross Island, Antarctica: Journal of Petrology, egv083, doi: 10.1093/petrology/egv083.

Jamaludin, H., and Lahiri-Dutt, K., 2017, Could Lynas make a difference in the global political economy of rare earth elements in future?: Resources Policy, v. 53, p. 267–273, doi: 10.1016/j.resourpol.2017.07.005.

Jaroni, M.S., Friedrich, B., and Letmathe, P., 2019, Economical feasibility of rare earth mining outside China: Minerals, v. 9, article 576, doi: 10.3390/min9100576.

John, T., Scambelluri, M., Frische, M., Barnes, J.D., and Bach, W., 2011, Dehydration of subducting serpentinite: Implications for halogen mobility in subduction zones and the deep halogen cycle: Earth and Planetary Science Letters, v. 308, p. 65–76, doi: 10.1016/j.epsl.2011.05.038.

Jones, A.P., 1984, Mafic silicates from the nepheline syenites of the Motzfeldt centre, South Greenland: Mineralogical Magazine, v. 48, p. 1–12, doi: 10.1180/minmag.1984.048.346.01.

Jordens, A., Cheng, Y.P., and Waters, K.E., 2013, A review of the beneficiation of rare earth element bearing minerals: Minerals Engineering, v. 41, p. 97–114, doi: 10.1016/j.mineng.2012.10.017.

Jowitt, S.M., Wong, V.N.L., Wilson, S.A., and Gore, O., 2017, Critical metals in the critical zone: Controls, resources and future prospectivity of regolith hosted rare earth elements: Australian Journal of Earth Sciences, v. 64, p. 1045–1054, doi: 10.1080/08120099.2017.1380701.

Jowitt, S.M., Werner, T.T., Weng, Z., and Mudd, G.M., 2018, Recycling of the rare earth elements: doi: 10.1016/j.cogsc.2018.02.008.

Kalashnikov, A.O., Konopleva, N.G., Pakhomovsky, Y.A., and Ivanyuk, G.Y., 2016a, Rare earth deposits of the Murmansk Region, Russia—a review: Economic Geology, v. 111, p. 1529–1559, doi: 10.2113/econgeo.111.7.1529.

Kalashnikov, A.O., Yakovenchuk, V.N., Pakhomovsky, Y.A., Bazai, A.V., Sokharev, V.A., Konopleva, N.G., Mikhailova, J.A., Goryainov, P.M., and Ivanyuk, G.Y., 2016b, Scandium of the Kovdor baddeleyite-apatite-magnetite deposit (Murmansk region, Russia): Mineralogy, spatial distribution, and potential resource: Ore Geology Reviews, v. 72, p. 532–537, doi: 10.1016/j.oregeorev.2015.08.017.

Kay, R.W., and Mahlburg Kay, S., 1993, Delamination and delamination magmatism: Tectonophysics, v. 219, p. 177–189, doi: 10.1016/0040-1951(93)90295-U.

Kerrick, D.M., and Connelly, J.A., 2001, Metamorphic devolatilization of subducted marine sediments and the transport of volatiles into the Earth's mantle: Nature, v. 411, p. 293–296, doi: 10.1038/35077056.

Khomyakov, A.P., and Sørensen, H., 2001, Zoning in steenstrupine-(Ce) from the Ilímaussaq Alkaline Complex, South Greenland: A review and discussion: Geology of Greenland Survey Bulletin, v. 190, p. 109–118.

Kieffer, B., Arndt, N., Lapierre, H., Bastien, F., Bosch, D., Pecher, A., Yirgu, G., Ayalew, D., Weis, D., Jerram, D.A., Keller, F., and Meugniot, C., 2004, Flood and shield basalts from Ethiopia: Magmas from the African Superswell: Journal of Petrology, v. 45, p. 793–834, doi: 10.1093/petrology/egg112.

Kinnaird, J.A., Nex, P.A.M., and Milani, L., 2016, Tin in Africa: Episodes, v. 39, p. 361–380, doi: 10.18814/epiiugs/2016/v39i2/95783.

Kinney, S.T., MacLennan, S.A., Keller, C.B., Schoene, B., Setera, J.B., VanTongeren, J.A., and Olsen, P.E., 2021, Zircon U-Pb geochronology constrains continental expression of Great Meteor Hotspot magmatism: Geophysical Research Letters, v. 48, e2020GL091390, doi: 10.1029/2020GL091390.

Knox-Robinson, C.M., and Wyborn, L.A., 1997, Towards a holistic exploration strategy: Using geographic information systems as a tool to enhance exploration: Australian Journal of Earth Sciences, v. 44, p. 453–463, doi: 10.1080/08120099708728326.

Kogarko, L., 2018, Chemical composition and petrogenetic implications of apatite in the Khibiny apatite-nepheline deposits (Kola Peninsula): Minerals, v. 8, article 532, doi: 10.3390/min8110532.

Köhler, J., Konnerup-Madsen, J., and Markl, G., 2008, Fluid geochemistry in the Ivigtut cryolite deposit, South Greenland: Lithos, v. 103, p. 369–392, doi: 10.1016/j.lithos.2007.10.005.

Köhler, J., Schönenberger, J., Upton, B., and Markl, G., 2009, Halogen and trace element chemistry in the Gardar province, South Greenland: Subduction related mantle metasomatism and fluid exsolution from alkalic melts: Lithos, v. 113, p. 731–747, doi: 10.1016/j.lithos.2009.07.004.

Konnerup-Madsen, J., and Rose-Hansen, J., 1984, Composition and significance of fluid inclusions in the Ilímaussaq peralkaline granite, South Greenland: Bulletin de Mineralogie, v. 107, p. 317–326, doi: 10.3406/bulmi.1984.7761.

Koptev, A., Calais, E., Burov, E., Leroy, S., and Gerya, T., 2015, Dual continental rift systems generated by plume-lithosphere interaction: Nature Geoscience, v. 8, p. 388–392, doi: 10.1038/ngeo2401.

Kovalenko, V.I., Tsaryeva, G.M., Goreglyad, A.V., Yarmolyuk, V.V., Troitsky, V.A., Hervig, R.L., and Farmer, G.L., 1995, The peralkaline granite-related Khaldzan-Buregtey rare metal (Zr, Nb, REE) deposit, western Mongolia: Economic Geology, v. 90, p. 530–547, doi: 10.2113/gsecongeo.90.3.530.

Kramm, U., and Kogarko, L.N., 1994, Nd and Sr isotope signatures of the Khibina and Lovozero agpaitic centres, Kola alkaline province, Russia: Lithos, v. 32, p. 225–242, doi: 10.1016/0024-4937(94)90041-8.

Krumrei, T.V., Villa, I.M., Marks, M.A., and Markl, G., 2006, A $^{40}Ar/^{39}Ar$ and U/Pb isotopic study of the Ilímaussaq Complex, South Greenland: Implications for the 40K decay constant and for the duration of magmatic activity in a peralkaline complex: Chemical Geology, v. 227, p. 258–273, doi: 10.1016/J.CHEMGEO.2005.10.004.

Krumrei, T.V., Pernicka, E., Kaliwoda, M., and Markl, G., 2007, Volatiles in a peralkaline system: Abiogenic hydrocarbons and F-Cl-Br systematics in the naujaite of the Ilímaussaq intrusion, South Greenland: Lithos, v. 95, p. 298–314, doi: 10.1016/j.lithos.2006.08.003.

Kulaksiz, S., and Bau, M., 2011, Rare earth elements in the Rhine River, Germany: First case of anthropogenic lanthanum as a dissolved microcontaminant in the hydrosphere: Environment International, v. 37, p. 973–979, doi: 10.1016/j.envint.2011.02.018.

Kursun, I., Terzi, M., and Ozdemir, O., 2019, Determination of surface chemistry and flotation properties of rare earth mineral allanite: Minerals Engineering, v. 132, p. 113–120, doi: 10.1016/j.mineng.2018.11.044.

Kynicky, J., Chakhmouradian, A.R., Xu, C., Krmicek, L., and Galiova, M., 2011, Distribution and evolution of zirconium mineralization in peralkaline granites and associated pegmatites of the Khan Bogd Complex, southern Mongolia: The Canadian Mineralogist, v. 49, p. 947–965, doi: 10.3749/canmin.49.4.947.

Larsen, L.M., 1976, Clinopyroxenes and coexisting mafic minerals from the alkaline Ilímaussaq intrusion, South Greenland: Journal of Petrology, v. 17, p. 258–290, doi: 10.1093/petrology/17.2.258.

Larsen, L.M., and Rex, D.C., 1992, A review of the 2500 Ma span of alkaline ultramafic, potassic and carbonatitic magmatism in West Greenland: Lithos, v. 28, p. 367–402, doi: 10.1016/0024-4937(92)90015-Q.

Larsen, L.M., and Sorensen, H., 1987, The Ilimaussaq intrusion—progressive crystallization and formation of layering in an agpaitic magma: Geological Society, London, Special Publication 30, p. 473–488, doi: 10.1144/GSL.SP.1987.030.01.23.

Lazareva, E.V., Zhmodik, S.M., Dobretsov, N.L., Tolstov, A.V., Shcherbov, B.L., Karmanov, N.S., Gerasimov, E.Y., and Bryanskaya, A.V., 2015, Main minerals of abnormally high-grade ores of the Tomtor deposit (Arctic Siberia): Russian Geology and Geophysics, v. 56, p 844–873, doi: 10.1016/j.rgg.2015.05.003.

Le Maitre, R.W., Streckeisen, A., Zanettin, B., Le Bas, M.J., Bonin, B., and Bateman, P., 2005, Igneous rocks: A classification and glossary of terms: Recommendations of the International Union of Geological Sciences Subcommission on the Systematics of Igneous Rocks: Cambridge University Press, 252 p.

Lenharo, S.L.R., Pollard, P.J., and Born, H., 2003, Petrology and textural evolution of granites associated with tin and rare-metals mineralization at the Pitinga mine, Amazonas, Brazil: Lithos, v. 66, p. 37–61, doi: 10.1016/S0024-4937(02)00201-3.

Li, M.Y.H., Zhao, W.W., and Zhou, M.F., 2017, Nature of parent rocks, mineralization styles and ore genesis of regolith-hosted REE deposits in South China: An integrated genetic model: Journal of Asian Earth Sciences, v. 148, p. 65–95, doi: 10.1016/j.jseaes.2017.08.004.

Li, M.Y.H., Zhou, M.F., and Williams-Jones, A.E., 2019, The genesis of regolith-hosted heavy rare earth element deposits: Insights from the world-class Zudong deposit in Jiangxi province, South China: Economic Geology, v. 114, p. 541–568, doi: 10.5382/econgeo.4642.

Li, M.Y.H., Zhou, M.F., and Williams-Jones, A.E., 2020, Controls on the dynamics of rare earth elements during subtropical hillslope processes and formation of regolith-hosted deposits: Economic Geology, v. 115, p. 1097–1118, doi: 10.5382/econgeo.4727.

Li, M.Y.H., Kwong, H.T., Williams-Jones, A.E., and Zhou, M.F., 2021, The thermodynamics of rare earth element liberation, mobilization and supergene enrichment during groundwater-regolith interaction: Geochimica et Cosmochimica Acta, doi: 10.1016/j.gca.2021.05.002.

Liu, Y., and Hou, Z., 2017, A synthesis of mineralization styles with an integrated genetic model of carbonatite-syenite-hosted REE deposits in the Cenozoic Mianning-Dechang REE metallogenic belt, the eastern Tibetan Plateau, southwestern China: Journal of Asian Earth Sciences, v. 137, p. 35–79, doi: 10.1016/j.jseaes.2017.01.010.

Liu, Y., Zhu, Z., Chen, C., Zhang, S., Sun, X., Yang, Z., and Liang, W., 2015, Geochemical and mineralogical characteristics of weathered ore in the Dalucao REE deposit, Mianning-Dechang REE Belt, western Sichuan province, southwestern China: Ore Geology Reviews, v. 71, p. 437–456, doi: 10.1016/j.oregeorev.2015.06.009.

Lund, K., 2008, Geometry of the Neoproterozoic and Paleozoic rift margin of western Laurentia: Implications for mineral deposit settings: Geosphere, v. 4, p. 429–444, doi: 10.1130/GES00121.1.

Macdonald, R., and Upton, B.G.J., 1993, The Proterozoic Gardar rift zone, South Greenland: Comparisons with the East African rift system: Geological Society, London, Special Publication 76, p. 427–442, doi: 10.1144/GSL.SP.1993.076.01.22.

Macdonald, R., Bagiński, B., and Upton, B., 2014, The volcano-pluton interface; the Longonot (Kenya) and Kûngnât (Greenland) peralkaline complexes: Lithos, v. 196–197, p. 232–241, doi: 10.1016/j.lithos.2014.03.009.

Macgregor, D., 2015, History of the development of the East African rift system: A series of interpreted maps through time: Journal of African Earth Sciences, v. 101, p. 232–252, doi: 10.1016/j.jafrearsci.2014.09.016.

Magee, C., Stevenson, C.T., Ebmeier, S.K., Keir, D., Hammond, J.O., Gottsmann, J.H., Whaler, K.A., Schofield, N., Jackson, C.A., Petronis, M.S., et al., 2018, Magma plumbing systems: A geophysical perspective: Journal of Petrology, v. 59, p. 1217–1251, doi: 10.1093/petrology/egy064.

Mahood, G.A., 1984, Pyroclastic rocks and calderas associated with strongly peralkaline magmatism: Journal of Geophysical Research: Solid Earth, v. 89, p. 8540–8552, doi: 10.1029/JB089iB10p08540.

Marion, C., Li, R., and Waters, K.E., 2020, A review of reagents applied to rare earth mineral flotation: Advances in Colloid and Interface Science, v. 279, article 102142, doi: 10.1016/j.cis.2020.102142.

Markl, G., Marks, M.A., Schwinn, G., and Sommer, H., 2001, Phase equilibrium constraints on intensive crystallization parameters of the Ilimaussaq Complex, South Greenland: Journal of Petrology, v. 42, p. 2231–2257, doi: 10.1093/petrology/42.12.2231.

Marks, M., and Markl, G., 2001, Fractionation and assimilation processes in the alkaline augite syenite unit of the Ilímaussaq intrusion, South Greenland, as deduced from phase equilibria: Journal of Petrology, v. 42, p. 1947–1969, doi: 10.1093/petrology/42.10.1947.

Marks, M.A.W., and Markl, G., 2015, The Ilímaussaq Alkaline Complex, South Greenland, *in* Charlier, B., Namur, O., Latypov, R., and Tegner, C., eds., Layered intrusions: Springer Geology, Dordrecht, p. 649–691, doi: 10.1007/978-94-017-9652-1_14.

——2017, A global review on agpaitic rocks: Earth-Science Reviews, v. 173, p. 229–258, doi: 10.1016/j.earscirev.2017.06.002.

Marks, M.A.W., Hettmann, K., Schilling, J., Frost, B.R., and Markl, G., 2011, The mineralogical diversity of alkaline igneous rocks: Critical factors for the transition from miaskitic to agpaitic phase assemblages: Journal of Petrology, v. 52, p. 439–455, doi: 10.1093/petrology/egq086.

Marr, R.A., Baker, D.R., and Williams-Jones, A.E., 1998, Chemical controls on the solubility of Zr-bearing phases in simplified peralkaline melts and application to the Strange Lake Intrusion, Quebec-Labrador: The Canadian Mineralogist, v. 36, p. 1001–1008.

Marschall, H.R., Dohmen, R., and Ludwig, T., 2013, Diffusion-induced fractionation of niobium and tantalum during continental crust formation: Earth and Planetary Science Letters, v. 375, p. 361–371, doi: 10.1016/j.epsl.2013.05.055.

Marsh, J.S., 1973, Relationships between transform directions and alkaline igneous rock lineaments in Africa and South America: Earth and Planetary Science Letters, v. 18, p. 317–323, doi: 10.1016/0012-821X(73)90070-8.

Märten, H., Kalka, H., Krause, J., Nicolai, J., Schubert, J., and Zauner, M.J., 2015, Advanced in-situ leaching technology for uranium: From innovative exploration to optimized recovery: FOG—Freiberg Online Geoscience, v. 39–42, p. 138–146.

Masotta, M., Mollo, S., Freda, C., Gaeta, M., and Moore, G., 2013, Clinopyroxene-liquid thermometers and barometers specific to alkaline differentiated magmas: Contributions to Mineralogy and Petrology, v. 166, p. 1545–1561, doi: 10.1007/s00410-013-0927-9.

Massuyeau, M., Gardés, E., Morizet, Y., and Gaillard, F., 2015, A model for the activity of silica along the carbonatite-kimberlite-mellilitite-basanite melt compositional joint: Chemical Geology, v. 418, p. 206–216, doi: 10.1016/j.chemgeo.2015.07.025.

McCafferty, A.E., Stoeser, D.B., and Van Gosen, B.S., 2014, Geophysical interpretation of U, Th, and rare earth element mineralization of the Bokan Mountain peralkaline granite complex, Prince of Wales Island, southeast Alaska: Interpretation, v. 2, p. SJ47-SJ63, doi: 10.1190/INT-2014-0010.1.

McCreath, J.A., Finch, A.A., Simonsen, S.L., Donaldson, C.H., and Armour-Brown, A., 2012, Independent ages of magmatic and hydrothermal activity in alkaline igneous rocks: The Motzfeldt centre, Gardar province, South Greenland: Contributions to Mineralogy and Petrology, v. 163, p. 967–982, doi: 10.1007/s00410-011-0709-1.

McCreath, J.A., Finch, A.A., Herd, D.A., and Armour-Brown, A., 2013, Geochemistry of pyrochlore minerals from the Motzfeldt center, South Greenland: The mineralogy of a syenite-hosted Ta, Nb deposit: American Mineralogist, v. 98, p. 426–438, doi: 10.2138/am.2013.4068.

McCuaig, T.C., and Hronsky, J.M.A., 2014, The mineral system concept: The key to exploration targeting: Society of Economic Geologists, Special Publication 18, p. 153–175.

McCuaig, T.C., Beresford, S., and Hronsky, J., 2010, Translating the mineral systems approach into an effective exploration targeting system: Ore Geology Reviews, v. 38, p. 128–138, doi: 10.1016/j.oregeorev.2010.05.008.

Méjean, P., Pinti, D.L., Kagoshima, T., Roulleau, E., Demarets, L., Poirier, A., Takahata, N., Sano, Y., and Larocque, M., 2020, Mantle helium in southern Quebec groundwater: A possible fossil record of the New England hotspot: Earth and Planetary Science Letters, v. 545, article 116352, doi: 10.1016/j.epsl.2020.116352.

Melluso, L., Cucciniello, C., Le Roex, A.P., and Morra, V., 2016, The geochemistry of primitive volcanic rocks of the Ankaratra Volcanic Complex, and source enrichment processes in the genesis of the Cenozoic magmatism in Madagascar: Geochimica et Cosmochimica Acta, v. 185, p. 435–452.

Mikhailova, J.A., Ivanyuk, G.Y., Kalashnikov, A.O., Pakhomovsky, Y.A., Bazai, A.V., and Yakovenchuk, V.N., 2019, Petrogenesis of the Eudialyte Complex of the Lovozero alkaline massif (Kola Peninsula, Russia): Minerals, v. 9, article 581, doi: 10.3390/min9100581.

Miller, R.M., 2008, The geology of Namibia, 3 volumes: Ministry of Mines and Energy, Geological Survey of Namibia, 1564 p.

Mitchell, R.H., 2015, Primary and secondary niobium mineral deposits associated with carbonatites: Ore Geology Reviews, v. 64, p. 626–641, doi: 10.1016/j.oregeorev.2014.03.010.

Mitchell, R.H., and Liferovich, R.P., 2006, Subsolidus deuteric/hydrothermal alteration of eudialyte in lujavrite from the Pilansberg Alkaline Complex, South Africa: Lithos, v. 91, p. 352–372, doi: 10.1016/j.lithos.2006.03.025.

Moldoveanu, G.A., and Papangelakis, V.G., 2016, An overview of rare-earth recovery by ion-exchange leaching from ion-adsorption clays of various origins: Mineralogical Magazine, v. 80, p. 63–76, doi: 10.1180/minmag.2016.080.051.

Möller, V., and Williams-Jones, A.E., 2016a, Petrogenesis of the Nechalacho layered suite, Canada: Magmatic evolution of a REE-Nb–rich nepheline syenite intrusion: Journal of Petrology, v. 57, p. 229–276, doi: 10.1093/petrology/egw003.

——2016b, Stable and radiogenic isotope constraints on the magmatic and hydrothermal evolution of the Nechalacho Layered Suite, northwest Canada: Chemical Geology, v. 440, p. 248–274, doi: 10.1016/j.chemgeo.2016.07.010.

——2017, Magmatic and hydrothermal controls on the mineralogy of the Basal zone, Nechalacho REE-Nb-Zr deposit, Canada: Economic Geology, v. 112, p. 1823–1856, doi: 10.5382/econgeo.2017.4531.

——2018, A hyperspectral study (V-NIRSWIR) of the Nechalacho REE-Nb-Zr deposit, Canada: Journal of Geochemical Exploration, v. 188, p. 194–215, doi: 10.1016/j.gexplo.2018.01.011.

Morgenstern, R., Turnbull, R.E., Hill, M., Smillie, R., and Strong, D.T., 2017, The search for rare earth elements in New Zealand: A mineral systems and data discovery approach: Australasian Institute for Mining and Metallurgy (AusIMM) New Zealand Branch Conference, Christchurch, New Zealand, 2017, Proceedings, p. 174–183.

Müller-Lorch, D., Marks, M.A.W., and Markl, G., 2007, Na and K distribution in agpaitic pegmatites: Lithos, v. 95, p. 315–330, doi: 10.1016/j.lithos.2006. 08.004.

Mumford, T.R., 2013, Petrology of the Blatchford Lake Intrusive Suite, Northwest Territories, Canada: Ph.D. thesis, Ottawa, Carleton University, 240 p.

Mumford, T.R., Cousens, B.L., and Hanley, J., 2014, Constraints on the relationships between Paleoproterozoic intrusions and dyke swarms, East Arm of Great Slave Lake, N.W.T., Canada: Canadian Journal of Earth Sciences, v. 51, p. 419–438, doi: 10.1139/cjes-2013-0124.

Mutele, L., Billay, A., and Hunt, J.P., 2017, Knowledge-driven prospectivity mapping for granite-related polymetallic Sn-F-(REE) mineralization, Bushveld Igneous Complex, South Africa: Natural Resources Research, v. 26, p. 535–552, doi: 10.1007/s11053-017-9325-8.

Neave, D.A., Black, M., Riley, T.R., Gibson, S.A., Ferrier, G., Wall, F., and Broom-Fendley, S., 2016, On the feasibility of imaging carbonatite-hosted rare earth element deposits using remote sensing: Economic Geology, v. 111, p. 641–665, doi: 10.2113/econgeo.111.3.641.

Néron, A., Bédard, L.P., and Gaboury, D., 2018, The Saint-Honoré carbonatite REE zone, Québec, Canada: Combined magmatic and hydrothermal processes: Minerals, v. 8, doi: 10.3390/min8090397.

Neumann, R., and Medeiros, E.B., 2015, Comprehensive mineralogical and technological characterisation of the Araxá (SE Brazil) Complex REE (Nb-P) ore, and the fate of its processing: International Journal of Mineral Processing, v. 144, p. 1–10, doi: 10.1016/j.minpro.2015.08.009.

Nisbet, H., Migdisov, A.A., Williams-Jones, A.E., Xu, H., van Hinsberg, V.J., and Roback, R., 2019, Challenging the thorium-immobility paradigm: Scientific Reports, v. 9, p. 8–13, doi: 10.1038/s41598-019-53571-x.

Nyalugwe, V.N., Abdelsalam, M.G., Atekwana, E.A., Katumwehe, A., Mickus, K., Salima, J., Njinju, E.A., and Emishaw, L., 2019, Lithospheric structure beneath the Cretaceous Chilwa alkaline province (CAP) in southern Malawi and northeastern Mozambique: Journal of Geophysical Research: Solid Earth, v. 124, p. 12,224–12,240, doi: 10.1029/2019JB018430.

O'Brien, H., Heilimo, E., and Heino, P., 2015, The Archean Siilinjärvi Carbonatite Complex, *in* Maier, W.D., Lahtinen, R., and O'Brien, H., eds., Mineral deposits of Finland: Elsevier, p. 327–343, doi: 10.1016/B978-0-12-410438-9.00013-3.

O'Brien, T.M., and van der Pluijm, B.A., 2012, Timing of Iapetus Ocean rifting from Ar geochronology of pseudotachylytes in the St. Lawrence rift system of southern Quebec: Geology, v. 40, p. 443–446, doi: 10.1130/G32691.1.

Oreskes, N., and Einaudi, M.T., 1990, Origin of rare earth element-enriched hematite breccias at the Olympic Dam Cu-U-Au-Ag deposit, Roxby Downs, South Australia: Economic Geology, v. 85, p. 1–28, doi: 10.2113/gsecongeo.85.1.1.

Pagano, G., Guida, M., Tommasi, F., and Oral, R., 2015, Health effects and toxicity mechanisms of rare earth elements—knowledge gaps and research prospects: Ecotoxicology and Environmental Safety, v. 115, p. 40–48, doi: 10.1016/j.ecoenv.2015.01.030.

Pell, R., Wall, F., Yan, X., Li, J., and Zeng, X., 2019, Mineral processing simulation based-environmental life cycle assessment for rare earth project development: A case study on the Songwe Hill project: Journal of Environmental Management, v. 249, article 109353, doi: 10.1016/j.jenvman.2019.109353.

Pell, R., Tijsseling, L., Goodenough, K., Wall, F., Dehaine, Q., Grant, A., Deak, D., Yan, X., and Whattoff, P., 2021, Towards sustainable extraction of technology materials through integrated approaches: Nature Reviews Earth and Environment, doi: 10.1038/s43017-021-00211-6.

Percival, J.A., Sanborn-Barrie, M., Skulski, T., Stott, G.M., Helmstaedt, H., and White, D.J., 2006, Tectonic evolution of the western Superior province from NATMAP and lithoprobe studies: Canadian Journal of Earth Sciences, v. 43, p. 1085–1117.

Petford, N., Cruden, A.R., McCaffrey, K.J., and Vigneresse, J.L., 2000, Granite magma formation, transport and emplacement in the Earth's crust: Nature, v. 408, p. 669–673, doi: 10.1038/35047000.

Phua, K.L., and Velu, S.S., 2012, Lynas Corporation's rare earth extraction plant in Gebeng, Malaysia: A case report on the ongoing saga of people power versus state-backed corporate power: Journal of Environmental Engineering and Ecological Science, 5 p., doi: 10.7243/2050-1323-1-2.

Pilet, S., Baker, M.B., and Stolper, E.M., 2008, Metasomatized lithosphere and the origin of alkaline lavas: Science, v. 320, 916–919, doi: 10.1126/science.1156563.

Pilet, S., Ulmer, P., and Villiger, S., 2010, Liquid line of descent of a basanitic liquid at 1.5 Gpa: Constraints on the formation of metasomatic veins: Contributions to Mineralogy and Petrology, v. 159, p. 621–643, doi: 10.1007/s00410-009-0445-y.

Pirajno, F., 2010, Intracontinental strike-slip faults, associated magmatism, mineral systems and mantle dynamics: Examples from NW China and Altay-Sayan (Siberia): Journal of Geodynamics, v. 50, p. 325–346, doi: 10.1016/j.jog.2010.01.018.

——2015, Intracontinental anorogenic alkaline magmatism and carbonatites, associated mineral systems and the mantle plume connection: Gondwana Research, v. 27, p. 1181–1216, doi: 10.1016/J.GR.2014.09.008.

Plank, T., 2013, The chemical composition of subducting sediments, *in* Rudnick, R.L., ed., Treatise on geochemistry, v. 4, 2nd ed.: Elsevier, p. 607–629, doi: 10.1016/B978-0-08-095975-7.00319-3.

Putirka, K.D., 2008, Thermometers and barometers for volcanic systems: Reviews in Mineralogy and Geochemistry, v. 69, p. 61–120, doi: 10.2138/rmg.2008.69.3.

Putnis, A., 1992, An introduction to mineral sciences: Cambridge, Cambridge University Press, doi: 10.1017/CBO9781139170383.

Qiu, K., Yu, H., Wu, M., Geng, J., Ge, X., Gou, Z., and Taylor, R.D., 2019, Discrete Zr and REE mineralization of the Baerzhe rare-metal deposit, China: American Mineralogist, v. 104, p. 1487–1502, doi: 10.2138/am-2019-6890.

Quest Rare Minerals Ltd., 2017, Updated mineral resource estimate for the Strange Lake property, Quebec, Canada: NI 43-101 Technical Report, www.sedar.com.

Ram Resources, 2012, Maiden inferred resource of 340 million tonnes for Aries project (JORC-code 2004 compliant): Technical Report.

Ratschbacher, B.C., Marks, M.A.W., Bons, P.D., Wenzel, T., and Markl, G., 2015, Emplacement and geochemical evolution of highly evolved syenites investigated by a combined structural and geochemical field study: The lujavrites of the Ilímaussaq Complex, SW Greenland: Lithos, v. 231, p. 62–76, doi: 10.1016/j.lithos.2015.06.004.

Riedel, S., Jacobs, J., and Jokat, W., 2013, Interpretation of new regional aeromagnetic data over Dronning Maud Land (East Antarctica): Tectonophysics, v. 585, p. 161–171, doi: 10.1016/j.tecto.2012.10.011.

Riishuus, M.S., Peate, D.W., Tegner, C., Wilson, J.R., and Brooks, C.K., 2008, Petrogenesis of cogenetic silica-oversaturated and -undersaturated syenites by periodic recharge in a crustally contaminated magma chamber: The Kangerlussuaq intrusion, East Greenland: Journal of Petrology, v. 49, p. 493–522, doi: 10.1093/petrology/egm090.

Rim, K.T., Koo, K.H., and Park, J.S., 2013, Toxicological evaluations of rare earths and their health impacts to workers: A literature review: doi: 10.5491/SHAW.2013.4.1.12.

Roberts, D.E., and Hudson, G.R., 1983, The Olympic Dam copper-uranium-gold deposit, Roxby Downs, South Australia: Economic Geology, v. 78, p. 799–822, doi: 10.2113/gsecongeo.78.5.799.

Robertson, E.A.M., Biggs, J., Cashman, K.V., Floyd, M.A., and Vye-Brown, C., 2016, Influence of regional tectonics and pre-existing structures on the formation of elliptical calderas in the Kenyan rift: Geological Society, London, Special Publication 420, p. 43–67, doi: 10.1144/SP420.12.

Romano, P., Andújar, J., Scaillet, B., Romengo, N., di Carlo, I., and Rotolo, S.G., 2018, Phase equilibria of Pantelleria trachytes (Italy): Constraints on pre-eruptive conditions and on the metaluminous to peralkaline transition in silicic magmas: Journal of Petrology, v. 59, p. 559–588, doi: 10.1093/petrology/egy037.

Rooney, T.O., 2017, The Cenozoic magmatism of East-Africa: Part I—flood basalts and pulsed magmatism: Lithos, v. 286, p. 264–301, doi: 10.1016/j.lithos.2017.05.014.

——2020a, The Cenozoic magmatism of East Africa: Part IV—the terminal stages of rifting preserved in the northern East African rift system: Lithos, v. 360, article 105381, doi: 10.1016/j.lithos.2020.105381.

——2020b, The Cenozoic magmatism of East Africa: Part V—magma sources and processes in the East African rift: Lithos, v. 360, article 105296.

Rosatelli, G., Wall, F., and Stoppa, F., 2007, Calcio-carbonatite melts and metasomatism in the mantle beneath Mt. Vulture (Southern Italy): Lithos, v. 99, p. 229–248, doi: 10.1016/j.lithos.2007.05.011.

Roulleau, E., and Stevenson, R., 2013, Geochemical and isotopic (Nd-Sr-Hf-Pb) evidence for a lithospheric mantle source in the formation of the alkaline Monteregian province (Quebec): Canadian Journal of Earth Sciences, v. 50, p. 650–666, doi: 10.1139/cjes-2012-0145.

Rukhlov, A.S., and Bell, K., 2010, Geochronology of carbonatites from the Canadian and Baltic shields, and the Canadian Cordillera: Clues to mantle evolution: Mineralogy and Petrology, v. 98, p. 11–54, doi: 10.1007/s00710-009-0054-5.

Salvi, S., and Williams-Jones, A.E., 1996, The role of hydrothermal processes in concentrating high-field strength elements in the Strange Lake Peralkaline Complex, northeastern Canada: Geochimica et Cosmochimica Acta, v. 60, p. 1917–1932, doi: 10.1016/0016-7037(96)00071-3.

——2006, Alteration, HFSE mineralisation and hydrocarbon formation in peralkaline igneous systems: Insights from the Strange Lake pluton, Canada: Lithos, v. 91, p. 19–34, doi: 10.1016/j.lithos.2006.03.040.

Samrock, F., Grayver, A.V., Eysteinsson, H., and Saar, M.O., 2018, Magnetotelluric image of transcrustal magmatic system beneath the Tulu Moye geothermal prospect in the Ethiopian rift: Geophysical Research Letters, v. 45, p. 12,847–12,855, doi: 10.1029/2018GL080333.

Sanematsu, K., and Watanabe, Y., 2016, Characteristics and genesis of ion adsorption-type rare earth element deposits: Reviews in Economic Geology, v. 18, p. 55–79.

Saria, E., Calais, E., Stamps, D.S., Delvaux, D., and Hartnady, C.J.H., 2014, Present-day kinematics of the East African rift: Journal of Geophysical Research: Solid Earth, v. 119, p. 1–17, doi: 10.1002/2013JB010901.

Sasada, T., Hiyagon, H., Bell, K., and Ebihara, M., 1997, Mantle-derived noble gases in carbonatites: Geochimica et Cosmochimica Acta, v. 61, p. 4219–4228, doi: 10.1016/S0016-7037(97)00202-0.

Schmidt, M., and Poli, S., 2014, Devolatilization during subduction, *in* Rudnick, R.L., ed., Treatise on geochemistry, v. 4: The crust, 2nd ed.: Elsevier, p. 669–701.

Schmidt, M.W., and Weidendorfer, D., 2018, Carbonatites in oceanic hotspots: Geology, v. 46, p. 435–438, doi: 10.1130/G39621.1.

Schmitt, A.K., Emmermann, R., Trumbull, R.B., Bühn, B., and Henjes-Kunst, F., 2000, Petrogenesis and $^{40}Ar/^{39}Ar$ geochronology of the Brandberg Complex, Namibia: Evidence for a major mantle contribution in metaluminous and peralkaline granites: Journal of Petrology, v. 41, p. 1207– 1239, doi: 10.1093/petrology/41.8.1207.

Schmitt, A.K., Trumbull, R.B., Dulski, P., and Emmermann, R., 2002, Zr-Nb-REE mineralization in peralkaline granites from the Amis Complex, Brandberg (Namibia): Evidence for magmatic pre-enrichment from melt inclusions: Economic Geology, v. 97, p. 399–413, doi: 10.2113/gsecongeo.97.2.399.

Schorscher, H.D., and Shea, M.E., 1992, The regional geology of the Poços de Caldas Alkaline Complex: Mineralogy and geochemistry of selected nepheline syenites and phonolites: Journal of Geochemical Exploration, v. 45, p. 25–51.

Schulze, D., 2003, A classification scheme for mantle-derived garnets in kimberlite: A tool for investigating the mantle and exploring for diamonds: Lithos, v. 71, p. 195–213, doi: 10.1016/s0024-4937(03)00113-0.

Şengör, A.M.C., and Natal'in, B.A., 2001, Rifts of the world: Geological Society of America, Special Paper 352, p. 389–482.

Shives, R.B.K., 2015, Using gamma ray spectrometry to find rare metals: British Columbia Geological Survey, Paper 2015-3, p. 199–209.

Siegel, K., Vasyukova, O.V., and Williams-Jones, A.E., 2018, Magmatic evolution and controls on rare metal-enrichment of the Strange Lake A-type

peralkaline granitic pluton, Québec-Labrador: Lithos, v. 308–309, p. 34–52, doi: 10.1016/j.lithos.2018.03.003.
Siegfried, P., Wall, F., and Moore, K., 2018, In search of the forgotten rare earth: Geoscientist, v. 28, p. 10–15, doi: 10.1144/geosci2018-021.
Sillitoe, R.H., 2010, Porphyry copper systems: Economic Geology, v. 105, p. 3–41, doi: 10.2113/gsecongeo.105.1.3.
Simandl, G.J., 2015, Carbonatites and related exploration targets: British Columbia Geological Survey, Paper 2015-3, p. 31–37.
Simandl, G.J., and Paradis, S., 2018, Carbonatites: Related ore deposits, resources, footprint, and exploration methods: Applied Earth Science, doi: 10.1080/25726838.2018.1516935.
Sjöqvist, A.S., Cornell, D.H., Andersen, T., Christensson, U.I., and Berg, J.T., 2017, Magmatic age of rare-earth element and zirconium mineralisation at the Norra Kärr Alkaline Complex, southern Sweden, determined by U-Pb and Lu-Hf isotope analyses of metasomatic zircon and eudialyte: Lithos, v. 294–295, p. 73–86, doi: 10.1016/j.lithos.2017.09.023.
Sjöqvist, A.S., Zack, T., Honn, D.K., and Baxter, E.F., 2020, Modification of a rare-earth element deposit by low-temperature partial melting during metamorphic overprinting: Norra Kärr Alkaline Complex, southern Sweden: Chemical Geology, v. 545, article 119640, doi: 10.1016/j.chemgeo.2020.119640.
Smith, E.M., Shirey, S.B., Richardson, S.H., Nestola, F., Bullock, E.S., Wang, J., and Wang, W., 2018, Blue boron-bearing diamonds from Earth's lower mantle: Nature, v. 560, p. 84–87, doi: 10.1038/s41586-018-0334-5.
Smith, M.P., Moore, K., Kavecsánszki, D., Finch, A.A., Kynicky, J., and Wall, F., 2016, From mantle to critical zone: A review of large and giant sized deposits of the rare earth elements: Geoscience Frontiers, v. 7, p. 315– 334, doi: 10.1016/j.gsf.2015.12.006.
Smythe, D.M., Lombard, A., and Coetzee, L.L., 2013, Rare earth element deportment studies utilising QEMSCAN technology: Minerals Engineering, v. 52, p. 52–61, doi: 10.1016/j.mineng.2013.03.010.
Sokół, K., Finch, A.A., Hutchison, W., Cloutier, J., Borst, A.M., and Humphreys, M.C.S., 2022, Quantifying metasomatic high-field-strength and rare-earth element transport from alkaline magmas: Geology, v. 50, p. 305–310, doi: 10.1130/G49471.1.
Song, W., Xu, C., Smith, M.P., Chakhmouradian, A.R., Brenna, M., Kynický, J., Chen, W., Yang, Y., Deng, M., and Tang, H., 2018, Genesis of the world's largest rare earth element deposit, Bayan Obo, China: Protracted mineralization evolution over ~1 b.y.: Geology, v. 46, p. 323–326, doi: 10.1130/G39801.1.
Sørensen, H., 1969, Rhythmic igneous layering in peralkaline intrusions: An essay review on Ilímaussaq (Greenland) and Lovozero (Kola, USSR): Lithos, v. 2, p. 261–283, doi: 10.1016/S0024-4937(69)80034-4.
——1970, Internal structures and geological setting of the three agpaitic intrusions, Khibina and Lovozero of the Kola peninsula and Ilimaussaq, South Greenland: The Canadian Mineralogist, v. 10, p. 299–334.
——1974, The alkaline rocks: London, Wiley, 622 p.
——1992, Agpaitic nepheline syenites: A potential source of rare elements: Applied Geochemistry, v. 7, p. 417–427, doi: 10.1016/0883-2927(92)90003-L.
——2006, Ilímaussaq Alkaline Complex, South Greenland: An overview of 200 years of research and an outlook: Museum Tusculanum Press, 74 p.
Sørensen, H., and Larsen, L.M., 2001, The hyper-agpaitic stage in the evolution of the Ilímaussaq Alkaline Complex, South Greenland: Geology of Greenland Survey Bulletin, v. 190, p. 83–94.
Sørensen, H., Bohse, H., and Bailey, J.C., 2006, The origin and mode of emplacement of lujavrites in the Ilímaussaq Alkaline Complex, South Greenland: Lithos, v. 91, p. 286–300, doi: 10.1016/j.lithos.2006.03.021.
Sørensen, H., Bailey, J.C., and Rose-Hansen, J., 2011, The emplacement and crystallization of the U-Th-REE–rich agpaitic and hyperagpaitic lujavrites at Kvanefjeld, Ilímaussaq Alkaline Complex, South Greenland: Bulletin of the Geological Society of Denmark, v. 59, p. 69–92.
Spandler, C., and Morris, C., 2016, Geology and genesis of the Toongi rare metal (Zr, Hf, Nb, Ta, Y and REE) deposit, NSW, Australia, and implications for rare metal mineralization in peralkaline igneous rocks: Contributions to Mineralogy and Petrology, v. 171, article 104, doi: 10.1007/s00410-016-1316-y.
Spandler, C., and Pirard, C., 2013, Element recycling from subducting slabs to arc crust: A review: Lithos, v. 170–171, p. 208–223, doi: 10.1016/j.lithos.2013.02.016.
Speiser, A., Smith, K., and Wall, F., 2019, Environmental impact of mines in alkaline rocks and carbonatites: Deliverable 6.2 for the HiTech Alk-Carb project, 62 p.
Spera, F.J., 1984, Carbon dioxide in petrogenesis III: Role of volatiles in the ascent of alkaline magma with special reference to xenolith-bearing mafic lavas: Contributions to Mineralogy and Petrology, v. 88, p. 217–232.
Stark, T., Silin, I., and Wotruba, H., 2017, Mineral processing of eudialyte ore from Norra Kärr: Journal of Sustainable Metallurgy, v. 3, p. 32–38, doi: 10.1007/s40831-016-0073-5.
Steenfelt, A., 1991, High-technology metals in alkaline and carbonatitic rocks in Greenland: Recognition and exploration: Journal of Geochemical Exploration, v. 40, p. 263–279, doi: 10.1016/0375-6742(91)90042-S.
——2012, Rare earth elements in Greenland: Known and new targets identified and characterised by regional stream sediment data: Geochemistry: Exploration, Environment, Analysis, v. 12, p. 313–326, doi: 10.1144/geochem2011-113.
Stephenson, D., and Upton, B.G.J., 1982, Ferromagnesian silicates in a differentiated Alkaline Complex: Kûngnât Fjeld, South Greenland: Mineralogical Magazine, v. 46, p. 283–300, doi: 10.1180/minmag.1982.046.340.02.
Stern, R.J., 2020, The Mesoproterozoic single-lid tectonic episode: Prelude to modern plate tectonics: GSA Today, v. 30, p. 4–10, doi: 10.1130/GSATG480A.1.
Stevenson, R., Upton, B.G., and Steenfelt, A., 1997, Crust-mantle interaction in the evolution of the Ilímaussaq Complex, South Greenland: Nd isotopic studies: Lithos, v. 40, p. 189–202, doi: 10.1016/S0024-4937(97)00025-X.
Stockmann, Karlsson, A., Lewerentz, A., Thomsen, T., Kokfelt, T., Tollefsen, E., Sturkell, E., and Lundqvist, L., 2018, New Rb-Sr and zircon U-Pb dating of the Grønnedal-Íka Igenous Complex, SW Greenland: Geological Society of Denmark and Technical University of Denmark, Nordic Geological Winter Meeting, 33rd, Copenhagen, January 10–12, 2018, Proceedings.
Suli, L.M., Ibrahim, W.H.W., Aziz, B.A., Deraman, M.R., and Ismail, N.A., 2017, A review of rare earth mineral processing technology: Chemical Engineering Research Bulletin, v. 19, p. 20–35, doi: 10.3329/cerb.v19i0.33773.
Sylvester, P.J., 1989, Post-collisional alkaline granites: The Journal of Geology, v. 97, p. 261–280, doi: 10.1086/629302.
Takehara, L., Silveira, F.V., and Santos, R.V., 2016, Potentiality of rare earth elements in Brazil, *in* Borges De Lima, I., and Leal Filho, W.B.T.R.E.I., eds., Rare earths industry: Boston, Elsevier, p. 57–72, doi: 10.1016/B978-0-12-802328-0.00004-8.
Tappe, S., Romer, R.L., Stracke, A., Steenfelt, A., Smart, K.A., Muehlenbachs, K., and Torsvik, T.H., 2017, Sources and mobility of carbonate melts beneath cratons, with implications for deep carbon cycling, metasomatism and rift initiation: Earth and Planetary Science Letters, v. 466, p. 152–167, doi: 10.1016/j.epsl.2017.03.011.
Timofeev, A., Migdisov, A., and Williams-Jones, A., 2015, An experimental study of the solubility and speciation of niobium in fluoride-bearing aqueous solutions at elevated temperature: Geochimica et Cosmochimica Acta, v. 158, p. 103–111, doi: 10.1016/J.GCA.2015.02.015.
Timofeev, A., Migdisov, A.A., Williams-Jones, A.E., Roback, R., Nelson, A.T., and Xu, H., 2018, Uranium transport in acidic brines under reducing conditions: Nature Communications, v. 9, article 1469, doi: 10.1038/s41467-018-03564-7.
Tolstikhin, I.N., Kamensky, I.L., Marty, B., Nivin, V.A., Vetrin, V.R., Balaganskaya, E.G., Ikorsky, S.V., Gannibal, M.A., Weiss, D., Verhulst, A., and Demaiffe, D., 2002, Rare gas isotopes and parent trace elements in ultrabasic-alkaline-carbonatite complexes, Kola Peninsula: Identification of lower mantle plume component: Geochimica et Cosmochimica Acta, v. 66, p. 881–901, doi: 10.1016/S0016-7037(01)00807-9.
Tremblay, A., Roden-Tice, M.K., Brandt, J.A., and Megan, T.W., 2013, Mesozoic fault reactivation along the St. Lawrence rift system, eastern Canada: Thermochronologic evidence from apatite fission-track dating: GSA Bulletin, v. 125, p. 794–810, doi: 10.1130/B30703.1.
Trumbull, R.B., Bühn, B., Romer, R.L., and Volker, F., 2003, The petrology of basanite-tephrite intrusions in the Erongo Complex and implications for a plume origin of Cretaceous alkaline complexes in Namibia: Journal of Petrology, v. 44, p. 93–112, doi: 10.1093/petrology/44.1.93.
Tukiainen, T., 1988, Niobium-tantalum mineralisation in the Motzfeldt centre of the Igaliko nepheline syenite complex, South Greenland, *in* Mineral deposits within the European community: Berlin Heidelberg, Springer, p. 230–246, doi: 10.1007/978-3-642-51858-4_13.
Tukiainen, T., Bradshaw, C., and Emeleus, C.H., 1984, Geological and radiometric mapping of the Motzfeldt centre of the Igaliko Complex, South Greenland: Groenlands Geologiske Undersoegelse, Rapport 120, p. 78–83.
Ulbrich, H.H., Vlach, S.R.F., Demaiffe, D., and Ulbrich, M.N.C., 2005, Structure and origin of the Poços de Caldas alkaline massif, SE Brazil, *in* Comin-Chiaramonti, P., and Gomes, C.d.B., eds., Mesozoic to Cenozoic

alkaline magmatism in the Brazilian platform: Sao Paulo, Editora da Universidade de Sao Paulo, p. 367–418.
Upton, B.G.J., 2013, Tectono-magmatic evolution of the younger Gardar southern rift, South Greenland: Geological Survey of Denmark and Greenland, Bulletin 29, 124 p.
Upton, B.G.J., and Emeleus, C.H., 1987, Mid-Proterozoic alkaline magmatism in southern Greenland: The Gardar province: Geological Society, London, Special Publication 30, p. 449–471.
Upton, B.G.J., Emeleus, C.H., Heaman, L.M., Goodenough, K.M., and Finch, A.A., 2003, Magmatism of the mid-Proterozoic Gardar province, South Greenland: Chronology, petrogenesis and geological setting: Lithos, v. 68, p. 43–65, doi: 10.1016/S0024-4937(03)00030-6.
Upton, B.G.J., Macdonald, R., Odling, N., Rämö, O.T., and Bagiński, B., 2013, Kûngnât, revisited. A review of five decades of research into an alkaline complex in South Greenland, with new trace-element and Nd isotopic data: Mineralogical Magazine, v. 77, p. 523–550, doi: 10.1180/minmag.2013.077.4.11.
U.S. Geological Survey, 2019, Mineral commodity summaries: doi: 10.3133/70202434.
Vaccarezza, V., and Anderson, C., 2020, An overview of beneficiation and hydrometallurgical techniques on eudialyte group minerals: Mining, Metallurgy and Exploration, v. 37, p. 39–50, doi: 10.1007/s42461-019-00132-5.
van de Ven, M.A.J., Borst, A.M., Davies, G.R., Hunt, E.J., and Finch, A.A., 2019, Hydrothermal alteration of eudialyte-hosted critical metal deposits: Fluid source and implications for deposit grade: Minerals, v. 9, article 422, doi: 10.3390/min9070422.
Vasyukova, O., and Williams-Jones, A., 2014, Fluoride-silicate melt immiscibility and its role in REE ore formation: Evidence from the Strange Lake rare metal deposit, Québec-Labrador, Canada: Geochimica et Cosmochimica Acta, v. 139, p. 110–130, doi: 10.1016/j.gca.2014.04.031.
——2016, The evolution of immiscible silicate and fluoride melts: Implications for REE ore-genesis: Geochimica et Cosmochimica Acta, v. 172, p. 205–224, doi: 10.1016/j.gca.2015.09.018.
——2019a, Tracing the evolution of a fertile REE granite by modelling amphibole-melt partitioning, the Strange Lake story: Chemical Geology, doi: 10.1016/j.chemgeo.2019.03.030.
——2019b, Closed system fluid-mineral-mediated trace element behaviour in peralkaline rare metal pegmatites: Evidence from Strange Lake: Chemical Geology, v. 505, p. 86–99, doi: 10.1016/j.chemgeo.2018.12.023.
——2020, Partial melting, fractional crystallisation, liquid immiscibility and hydrothermal mobilisation—a "recipe" for the formation of economic A-type granite-hosted HFSE deposits: Lithos, v. 356–357, article 105300, doi: 10.1016/j.lithos.2019.105300.
Vasyukova, O., Williams-Jones, A., and Blamey, N., 2016, Fluid evolution in the Strange Lake granitic pluton, Canada: Implications for HFSE mobilisation: Chemical Geology, v. 444, p. 83–100, doi: 10.1016/j.chemgeo.2016.10.009.
Veksler, I.V., 2004, Liquid immiscibility and its role at the magmatic-hydrothermal transition: A summary of experimental studies: Chemical Geology, v. 210, p. 7–31, doi: 10.1016/j.chemgeo.2004.06.002.
Veksler, I.V., Dorfman, A.M., Dulski, P., Kamenetsky, V.S., Danyushevsky, L.V., Jeffries, T., and Dingwell, D.B., 2012, Partitioning of elements between silicate melt and immiscible fluoride, chloride, carbonate, phosphate and sulfate melts, with implications to the origin of natrocarbonatite: Geochimica et Cosmochimica Acta, v. 79, p. 20–40, doi: 10.1016/j.gca.2011.11.035.
Verplanck, P.L., Van Gosen, B.S., Seal, R.R., an McCafferty, A.E., 2014, A deposit model for carbonatite and peralkaline intrusion-related rare earth element deposits: U.S. Geological Survey, Scientific Investigations Report 2010-5070, 58 p., doi: 10.3133/sir20105070J.
Verplanck, P.L., Mariano, A.N., and Mariano, A., Jr., 2016, Rare earth element ore geology of carbonatites: Reviews in Economic Geology, v. 18, p. 5–32.
Voice, P.J., Kowalewski, M., and Eriksson, K.A., 2011, Quantifying the timing and rate of crustal evolution: Global compilation of radiometrically dated detrital zircon grains: The Journal of Geology, v. 119, p. 109–126, doi: 10.1086/658295.
Voßenkaul, D., Birich, A., Müller, N., Stoltz, N., and Friedrich, B., 2017, Hydrometallurgical processing of eudialyte bearing concentrates to recover rare earth elements via low-temperature dry digestion to prevent the silica gel formation: Journal of Sustainable Metallurgy, v. 3, p. 79–89, doi: 10.1007/s40831-016-0084-2.
Wall, F., 2013, Rare earth elements, *in* Gunn, G., ed., Critical metals handbook: Oxford, Wiley, p. 312–339, doi: 10.1002/9781118755341.ch13.
Wall, F., and Zaitsev, A.N., 2004, Rare earth minerals in Kola carbonatites, *in* Wall, F., and Zaitsev, A.N., eds., Phoscorites and carbonatites from mantle to mine: The key example of the Kola alkaline province: London, Mineralogical Society, p. 341–373, doi: 10.1180/mss.10.10.
Wall, F., Williams, C.T., Woolley, A.R., and Stanley, C.J., 1999, Pyrochlore in niobium ore deposits: Mineral Deposits: Processes to Processing, Society for Geology Applied to Mineral Deposits (SGA) Biennial Meeting, 5th, and International Association on the Genesis of Ore Deposits (IAGOD) Quadrennial Symposium, 10th, London, 1999, Proceedings, p. 687–690.
Wall, F., Rollat, A., and Pell, R.S., 2017, Responsible sourcing of critical metals: Elements, v. 13, p. 313–318, doi: 10.2138/gselements.13.5.313.
Walter, B.F., Parsapoor, A., Braunger, S., Marks, M.A., Wenzel, T., Martin, M., and Markl, G., 2018, Pyrochlore as a monitor for magmatic and hydrothermal processes in carbonatites from the Kaiserstuhl Volcanic Complex (SW Germany): Chemical Geology, v. 498, p. 1–16, doi: 10.1016/j.chemgeo.2018.08.008.
Walter, B.F., Giebel, R.J., Steele-MacInnis, M., Marks, M.A.W., Kolb, J., and Markl, G., 2021, Fluids associated with carbonatitic magmatism: A critical review and implications for carbonatite magma ascent: Earth-Science Reviews, v. 215, article 103509, doi: 10.1016/j.earscirev.2021.103509.
Wang, Z.Y., Fan, H.R., Zhou, L., Yang, K.F., and She, H.D., 2020, Carbonatite-related REE deposits: An overview: Minerals, v. 10, p. 1–26, doi: 10.3390/min10110965.
Weller, O.M., Copley, A., Miller, W.G.R., Palin, R.M., and Dyck, B., 2019, The relationship between mantle potential temperature and oceanic lithosphere buoyancy: Earth and Planetary Science Letters, v. 518, p. 86–99, doi: 10.1016/j.epsl.2019.05.005.
Weller, O.M., Mottram, C.M., St-Onge, M.R., Möller, C., Strachan, R., Rivers, T., and Copley, A., 2021, The metamorphic and magmatic record of collisional orogens: Nature Reviews Earth and Environment, v. 2, p. 781–799, doi: 10.1038/s43017-021-00218-z.
Weng, Z., Jowitt, S.M., Mudd, G.M., and Haque, N., 2015, A detailed assessment of global rare earth element resources: Opportunities and challenges: Economic Geology, v. 110, p. 1925–1952, doi: 10.2113/econgeo.110.8.1925.
White, W.M., 2015, Probing the earth's deep interior through geochemistry: Geochemical Perspectives, v. 4, p. 95–251, doi: 10.7185/geochempersp.4.2.
Wiesmaier, S., Troll, V.R., Carracedo, J.C., Ellam, R.M., Bindeman, I., and Wolff, J.A., 2012, Bimodality of lavas in the Teide-Pico Viejo succession in Tenerife—the role of crustal melting in the origin of recent phonolites: Journal of Petrology, v. 53, p. 2465–2495, doi: 10.1093/petrology/egs056.
Willbold, M., and Stracke, A., 2006, Trace element composition of mantle end-members: Implications for recycling of oceanic and upper and lower continental crust: Geochemistry Geophysics Geosystems, v. 7, p. 1–30, doi: 10.1029/2005GC001005.
——2010, Formation of enriched mantle components by recycling of upper and lower continental crust: Chemical Geology, v. 276, p. 188–197, doi: 10.1016/j.chemgeo.2010.06.005.
Williams-Jones, A.E., and Vasyukova, O.V., 2018, The economic geology of scandium, the runt of the rare earth element litter: Economic Geology, v. 113, p. 973–988, doi: 10.5382/econgeo.2018.4579.
Williamson, B.J., Herrington, R.J., and Morris, A., 2016, Porphyry copper enrichment linked to excess aluminium in plagioclase: Nature Geoscience, v. 9, p. 237–241, doi: 10.1038/ngeo2651.
Wolff, J.A., Forni, F., Ellis, B.S., and Szymanowski, D., 2020, Europium and barium enrichments in compositionally zoned felsic tuffs: A smoking gun for the origin of chemical and physical gradients by cumulate melting: Earth and Planetary Science Letters, v. 540, article 116251, doi: 10.1016/j.epsl.2020.116251.
Woolley, A.R., 2003, Igneous silicate rocks associated with carbonatites: Their diversity, relative abundances and implications for carbonatite genesis: Periodico di Mineralogia, v. 72, p. 9–17.
——2019, Alkaline rocks and carbonatites of the world, part 4: Antarctica, Asia and Europe (excluding the former USSR), Australasia and Oceanic Islands: London, Geological Society, 562 p.
Woolley, A.R., and Bailey, D.K., 2012, The crucial role of lithospheric structure in the generation and release of carbonatites: Geological evidence: Mineralogical Magazine, v. 76, p. 259–270, doi: 10.1180/minmag.2012.076.2.02.
Woolley, A.R., and Kjarsgaard, B.A., 2008, Carbonatite occurrences of the world: Map and database: Geological Survey of Canada, Open File 5796, 28 p., 1 sheet, CD-ROM.
Wu, M., Samson, I.M., Qiu, K., and Zhang, D., 2021, Concentration mechanisms of rare earth element-Nb-Zr-Be mineralization in the Baerzhe

deposit, Northeast China: Insights from textural and chemical features of amphibole and rare metal minerals: Economic Geology, v. 116, p. 651–679, doi: 10.5382/econgeo.4789.

Xu, C., Kynický, J., Smith, M.P., Kopriva, A., Brtnický, M., Urubek, T., Yang, Y., Zhao, Z., He, C., and Song, W., 2017, Origin of heavy rare earth mineralization in South China: Nature Communications, v. 8, article 7, doi: 10.1038/ncomms14598.

Yang, L., and van Hinsberg, V.J., 2019, Liquid immiscibility in the CaF 2-granite system and trace element partitioning between the immiscible liquids: Chemical Geology, v. 511, p. 28–41, doi: 10.1016/j.chemgeo.2019.02.017.

Yang, M., Liang, X., Ma, L., Huang, J., He, H., and Zhu, J., 2019, Adsorption of REEs on kaolinite and halloysite: A link to the REE distribution on clays in the weathering crust of granite: Chemical Geology, v. 525, p. 210–217, doi: 10.1016/j.chemgeo.2019.07.024.

Yang, W.B., Niu, H.C., Shan, Q., Sun, W.D., Zhang, H., Li, N.B., Jiang, Y.H., and Yu, X.Y., 2014, Geochemistry of magmatic and hydrothermal zircon from the highly evolved Baerzhe alkaline granite: Implications for Zr-REE-Nb mineralization: Mineralium Deposita, v. 49, p. 451–470, doi: 10.1007/s00126-013-0504-1.

Yang, X.J., Lin, A., Li, X.L., Wu, Y., Zhou, W., and Chen, Z., 2013, China's ion-adsorption rare earth resources, mining consequences and preservation: Environmental Development, v. 8, p. 131–136, doi: 10.1016/j.envdev.2013.03.006.

Zakharov, V.I., Maiorov, D.V., Alishkin, A.R., and Matveev, V.A., 2011, Causes of insufficient recovery of zirconium during acidic processing of Lovozero eudialyte concentrate: Russian Journal of Non-Ferrous Metals, v. 52, p. 423–428, doi: 10.3103/S1067821211050129.

Zheng, X., Liu, Y., and Zhang, L., 2021, The role of sulfate-, alkali-, and halogen-rich fluids in mobilization and mineralization of rare earth elements: Insights from bulk fluid compositions in the Mianning-Dechang carbonatite-related REE belt, southwestern China: Lithos, v. 386, article 106008, doi: 10.1016/j.lithos.2021.106008.

Charles D. Beard is a research associate in economic geology at the University of Cambridge, UK. He studied for his M.Sci. degree at the University of Bristol, UK, and the University of British Columbia, Canada, and for his Ph.D. degree at McGill University, Canada. He and his collaborators combine field, experimental, and theoretical studies to investigate the scale, longevity, and connectivity of magmatic-hydrothermal mineral systems. He is especially interested in critical metals deposits, links between geodynamics and mineralization, and the mineral compositional record of magmatic-hydrothermal system evolution.